

**STUDIES OF THE CHEMICAL MECHANISMS OF FLAVOENZYMES**

A Dissertation

by

PABLO SOBRADO

Submitted to the Office of Graduate Studies of  
Texas A&M University  
in partial fulfillment of the requirements for the degree of

DOCTOR OF PHILOSOPHY

August 2003

Major Subject: Biochemistry

# STUDIES OF THE CHEMICAL MECHANISMS OF FLAVOENZYMES

A Dissertation

by

PABLO SOBRADO

Submitted to Texas A&M University  
in partial fulfillment of the requirements  
for the degree of

DOCTOR OF PHILOSOPHY

Approved as to style and content by:

---

Paul F. Fitzpatrick  
(Chair of Committee)

---

James C. Hu  
(Member)

---

Arthur E. Johnson  
(Member)

---

Gregory D. Reinhart  
(Member)

---

Gregory D. Reinhart  
(Head of Department)

August 2003

Major Subject: Biochemistry

**ABSTRACT**

Studies of the Chemical Mechanisms of Flavoenzymes. (August 2003)

Pablo Sobrado, B.S., Merrimack College

Chair of Advisory Committee: Dr. Paul F. Fitzpatrick

Flavocytochrome  $b_2$  catalyzes the oxidation of lactate to pyruvate. Primary deuterium and solvent kinetic isotope effects have been used to determine the relative timing of cleavage of the lactate OH and CH bonds by the wild type enzyme, a mutant protein lacking the heme domain, and the D282N enzyme. The  $^D V_{\max}$  and  $^D(V/K_{\text{lactate}})$  values are both 3.0, 3.6 and 4.5 for the wild type enzyme, flavin domain and D282N enzymes, respectively. The  $^{D_2^0} V_{\max}$  values are 1.38, 1.18, and 0.98 for the wild type enzyme, the flavin domain, and the D282N enzyme; the respective  $^{D_2^0}(V/K_{\text{lactate}})$  values are 0.9, 0.44, and 1.0. The  $^D k_{\text{red}}$  value is 5.4 for the wild type enzyme and 3.5 for the flavin domain, whereas the  $^{D_2^0} k_{\text{red}}$  is 1.0 for both enzymes. The  $V/K_{\text{lactate}}$  value for the flavin domain increases 2-fold at moderate concentrations of glycerol. The data are consistent with the lactate hydroxyl proton not being in flight in the transition state for CH bond cleavage and there being an internal equilibrium prior to CH bond cleavage which is sensitive to solution conditions. Removal of the hydroxyl proton may occur in this pre-equilibrium. Tryptophan 2-monooxygenase catalyzes the oxidative decarboxylation of tryptophan to indoleacetamide, carbon dioxide and water. Sequence alignments identified this enzyme as a member of the L-amino acid oxidase family. The tyrosine and arginine residues in L-amino acid oxidase that bind the carboxylate of o-aminobenzoate are conserved and correspond to Tyr413 and Arg98 in tryptophan 2-monooxygenase. Mutation and characterization of the Y413A, Y413F, R98K and R98A

enzymes indicate that these residues are in the active site and interact with the substrate. Deletion of the OH group of Tyr413 increases the  $K_d$  for the substrate and makes CH bond cleavage totally rate limiting. The pH  $V/K_{trp}$  rate profile for the Tyr413 mutant enzymes shows that this residue must be protonated for activity. For both the R98A and R98K enzymes flavin reduction is rate limiting. The  $V_{max}$  and  $V/K_{trp}$  pH profiles indicate that the unprotonated form of the substrate is the active form for activity.

## DEDICATION

This dissertation is dedicated  
to the memory of my twin brother,  
Cristián Sobrado Castro

## ACKNOWLEDGMENTS

I would like to thank my advisor, Dr. Paul F. Fitzpatrick, for his guidance and patience over the course of this work. I would like to thank the members of my committee, Dr. Art Johnson, Dr. Jim Hu, and Dr. Gregory Reinhart. I also would like to thank my friends, Peter McCormick, Matthew Champion, Eugene Shakirov and Dr. Leonardo Marino for their help and support.

I would like to thank my aunt, Dr. Janet Krefting, for her unconditional support. Lastly, I thank my brother, Jose I. Sobrado, for inspiring me to become a better person and my wife, Alejandra, for her love and support.

## TABLE OF CONTENTS

	Page
ABSTRACT .....	iii
DEDICATION .....	v
ACKNOWLEDGMENTS.....	vi
TABLE OF CONTENTS .....	vii
LIST OF FIGURES.....	x
LIST OF TABLES .....	xiii
ABBREVIATIONS.....	xvi
CHAPTER	
I INTRODUCTION .....	1
II PROBING THE RELATIVE TIMING OF HYDROGEN ABSTRACTION STEPS IN THE FLAVOCYTOCHROME B <sub>2</sub> REACTION WITH PRIMARY AND SOLVENT DEUTERIUM ISOTOPE EFFECTS AND MUTANT ENZYMES .....	13
Introduction .....	13
Experimental Procedures.....	16
Results .....	22
Discussion .....	35
III ROLE OF TYR254 IN THE REACTION CATALYZED BY FLAVOCYTOCHROME B <sub>2</sub> .....	41
Introduction .....	41

CHAPTER	Page
Experimental Procedures.....	43
Results .....	45
Discussion .....	55
 IV CHARACTERIZATION OF THIOLACTATE AS SUBSTRATE FOR FLAVOCYTOCHROME B <sub>2</sub> .....	   59
Introduction .....	59
Experimental Procedures.....	59
Results .....	61
Discussion .....	67
 V ANALYSIS OF THE ROLES OF AMINO ACID RESIDUES IN THE FLAVOPROTEIN TRYPTOPHAN 2-MONOOXYGENASE MODIFIED BY 2-OXO-3-PENTINOATE: CHARACTERIZATION OF HIS338, CYS339, AND CYS511 MUTANT ENZYMES .....	     69
Introduction .....	69
Experimental Procedures.....	70
Results .....	73
Discussion .....	76
 VI TYROSINE 413 IN TRYPTOPHAN 2-MONOOXYGENASE, A MEMBER OF THE L-AMINO ACID OXIDASE FAMILY, IS IMPORTANT FOR CATALYSIS AND PROPER CONFORMATION OF THE ENZYME-INTERMEDIATE COMPLEX.....	     88
Introduction .....	88



CHAPTER	Page
Experimental Procedures.....	91
Results .....	95
Discussion .....	104
VII ARG98 IS IMPORTANT FOR SUBSTRATE BINDING AND TRANSITION STATE STABILIZATION IN THE REACTION CATALYZED BY TRYPTOPHAN 2-MONOOXYGENASE .....	113
Introduction .....	113
Experimental Procedures.....	117
Results .....	121
Discussion .....	127
VIII SUMMARY .....	136
REFERENCES.....	138
VITA .....	145

## LIST OF FIGURES

FIGURE		Page
1	Spectra of oxidized, semiquinone and fully reduced FAD in tryptophan 2-monooxygenase from <i>P. savastanoi</i> .....	2
2	Proposed active site for the family of $\alpha$ -hydroxy acid oxidases .....	7
3	pL dependence of wild-type and mutant flavocytochromes b <sub>2</sub> .....	26
4	Proton inventories for wild-type flavocytochrome b <sub>2</sub> (O) and the flavin domain(●) .....	32
5	Effects of viscosity on the steady state kinetic parameters for wild-type flavocytochrome b <sub>2</sub> (●) and the flavin domain (O).....	33
6	pH dependence of wild-type and Y254F flavocytochromes b <sub>2</sub> .....	52
7	Effects of viscosity on the steady state kinetic parameters for wild-type flavocytochrome b <sub>2</sub> (●) and the Y254F enzyme (O).....	53
8	Rate of heme reduction for the Y254F enzyme as a function of lactate concentration .....	54
9	Ratio of the activities of D282N and wild-type enzymes with thiolactate and lactate .....	68

FIGURE	Page
10	Alignment of <i>P. savastanoi</i> tryptophan monooxygenase and <i>C. rhodostoma</i> L-amino acid oxidase..... 86
11	Modeling of tryptophan monooxygenase using the L-amino acid oxidase structure ..... 87
12	Active site of L-amino acid oxidase with aminobenzoate (AB) bound showing the interactions with Arg90 and Tyr372 ..... 90
13	Amino acid sequence alignment of <i>P. savastanoi</i> tryptophan 2-monooxygenase and <i>C. rhodostoma</i> L-amino acid oxidase ..... 97
14	Results of phenylalanine scanning mutagenesis of TMO ..... 98
15	Spectral changes during reduction of TMO by tryptophan..... 102
16	$V/K_{trp}$ pH dependence of the wild-type (●), Y413A (■) and Y413F (▲) enzymes..... 106
17	A) Amino acid sequence alignment of <i>P. savastanoi</i> tryptophan 2-monooxygenase with the FAD binding domain of <i>C. rhodostoma</i> L-amino acid oxidase The alignment was generated with the program PSI-Blast using the amino acid sequence of TMO as a probe. The numbering for LAAO is that used in reference (27). B) Sequence of putative FAD binding domain of tryptophan 2-monooxygenases. The GxGxxG motif of the putative nucleotide binding region and the GG motif of the family of L-amino oxidases are indicated (103)..... 115
18	Active site of <i>Calloselasma rhodostoma</i> L-amino acid oxidase with aminobenzoate (AB) bound showing the interactions with Arg90 and Tyr372 ..... 116

FIGURE		Page
19	Spectral changes during reduction of wild-type and Arg98 mutant enzymes by tryptophan .....	125
20	$V/K_{\text{trp}}$ (A) and $V_{\text{max}}$ (B) pH dependence of the wild-type (O), R98K ( $\Delta$ ) and R98A ( $\blacksquare$ ) enzymes.wild-type (O), R98K ( $\Delta$ ) and R98A ( $\blacksquare$ ) enzymes.....	129

**LIST OF TABLES**

TABLE		Page
1	Steady State Kinetic Parameters and Primary Isotope Effects on the Oxidation of Lactate by Wild-type and Mutant Flavocytochromes b <sub>2</sub> .....	24
2	pK <sub>a</sub> Values for Wild-type and Mutant Flavocytochromes b <sub>2</sub> .....	25
3	Solvent Isotope Effects on the Oxidation of Lactate by Wild-type and Mutant Flavocytochromes b <sub>2</sub> .....	29
4	Rapid Reaction Kinetic Parameters for the Oxidation of Lactate by Wild-type and Mutant Flavocytochromes b <sub>2</sub> .....	30
5	Steady State Kinetic Parameters and Primary Isotope Effects on the Oxidation of Lactate by Wild-type and Y254F Flavocytochromes b <sub>2</sub> .....	47
6	Primary and Solvent Kinetic Isotope Effects on the Oxidation of Lactate by Wild-type and Y254F Mutant Flavocytochrome b <sub>2</sub> .....	48
7	pK <sub>a</sub> Values for Wild-type and Y254F Enzymes .....	49
8	Rapid Reaction Kinetic Parameters for the Oxidation of Lactate by Wild-type and Y254F Flavocytochromes b <sub>2</sub> .....	50
9	Wild-type Flavocytochrome b <sub>2</sub> Steady-State Kinetic Parameters for Cytochrome c .....	63

TABLE	Page
10	Steady-State Kinetic Parameters for the Oxidation of Lactate and Thiolactate by Wild-type and the Mutant D282N Flavocytochromes $b_2$ ..... 64
11	Rapid Reaction Kinetic Parameters for the Oxidation of Lactate and Thiolactate by Wild-type Flavocytochrome $b_2$ measured at 438 nm ..... 65
12	Rapid Reaction Kinetic Parameters for the Oxidation of Lactate and Thiolactate by Wild-type and the Mutant D282N Flavocytochromes $b_2$ Measured at 550 nm..... 66
13	Steady State Kinetic Parameters of Tryptophan Monooxygenase Mutant Proteins..... 77
14	Primary Deuterium Isotope Effects for Tryptophan Monooxygenase Mutant Proteins ..... 79
15	Calculated Intrinsic Rate Constants for C511S Tryptophan Monooxygenase..... 81
16	Steady State Kinetic Parameters for Wild-type and Mutant Tryptophan 2-Monooxygenases..... 101
17	Rapid Reaction Kinetic Parameters for Wild-type and Y413A Tryptophan 2-Monooxygenases ..... 103
18	$pK_a$ Values for Wild-type and Tyr413 Mutant Tryptophan 2-Monooxygenases..... 105
19	Differences in Binding Energies and Activation Energies Between Wild-type and Tyr413 Mutant Tryptophan 2-Monooxygenases..... 108

TABLE		Page
20	Intrinsic Rate Constants for Wild-type and Try413 Mutant Tryptophan 2-Monooxygenases .....	112
21	Steady State Kinetic Parameters for Wild-type and Arg98 Mutant Enzymes.....	123
22	Rapid Reaction Kinetic Parameters for Tryptophan 2-Monooxygenase Enzymes .....	126
23	pK <sub>a</sub> Values for Wild-type and Mutant Tryptophan 2-Monooxygenases.....	128
24	Differences in Binding Energies and Activation Energies Between Wild-type and Mutants Tryptophan 2-Monooxygenases.....	131
25	Intrinsic Rate Constants for Wild-type and Mutant Tryptophan 2-Monooxygenases .....	132

## ABBREVIATIONS

Flb<sub>2</sub>, flavocytochrome b<sub>2</sub>; TMO, tryptophan 2-monooxygenase; LAAO, L-amino acid oxidase; LB, Luria-Bertani; FAD, flavin adenine dinucleotide; FMN, flavin mononucleotide; Tris, tris(hydroxymethyl)aminomethane; ACES, N-(2-acetamido)-2-aminoethanesulfonic acid; EDTA, ethylenediaminetetraacetate.



## CHAPTER I

### INTRODUCTION

Enzymes that contain FAD and FMN as cofactors are involved in a wide range of chemical reactions, including electron transfer and dehydrogenation reactions, signal transduction, regulation of biological clocks, photosynthesis, and DNA repair (1). The chemical versatility of flavoenzymes arises from the ability of the reduced isoalloxazine ring to be oxidized in two or single electron steps. The study of the chemical mechanism of flavoproteins enjoys the benefit of the drastic differences in the absorbance spectra of the different electronic states of the flavin in the reduced, semiquinone and oxidized states (Figure 1). The oxidation of stable CH bonds catalyzed by flavoenzymes has been studied for many years. There are several families of flavoenzymes that catalyze the oxidation of CH bonds adjacent to either nitrogen or oxygen. The most studied are the amino acid oxidases and monooxygenases,  $\alpha$ -hydroxy-acid oxidases, amine oxidases and alcohol oxidases (2, 3). All of these enzymes catalyze a dehydrogenation reaction in which a CH bond is cleaved with concomitant transfer of two electrons to the flavin cofactor (Scheme 1).

---

This dissertation follows the style and format of *Biochemistry*.

Scheme 1

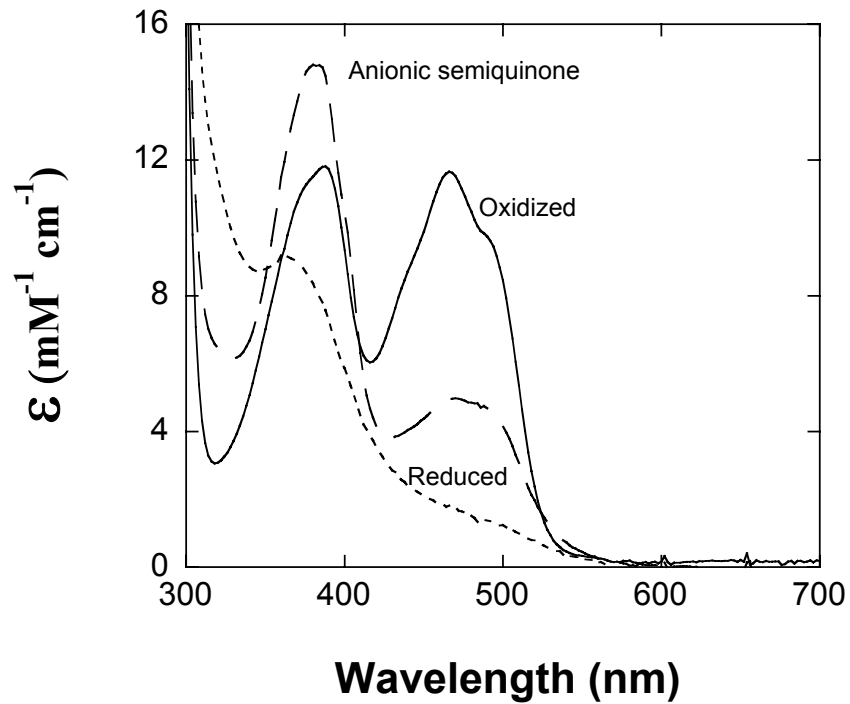
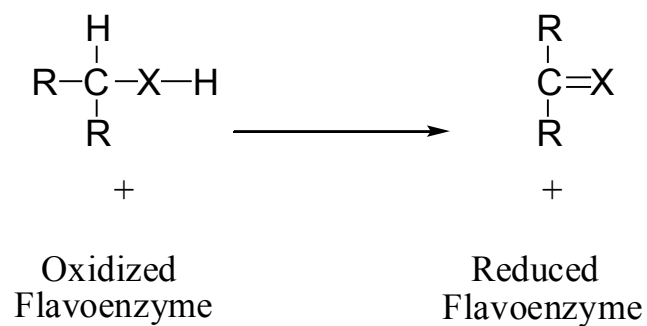
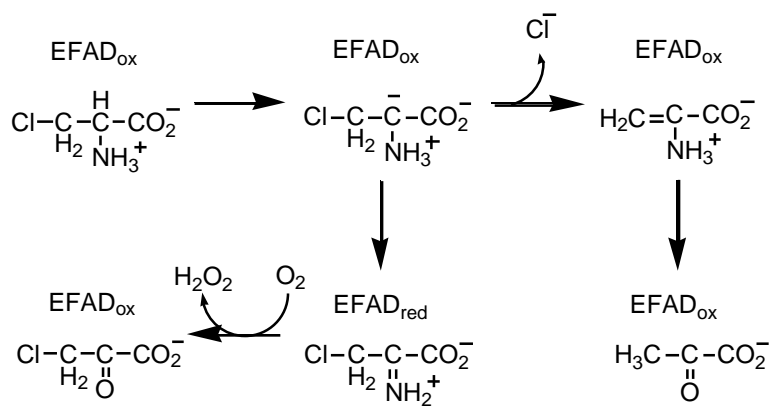


FIGURE 1. Spectra of oxidized, semiquinone and fully reduced FAD in tryptophan 2-monooxygenase from *P. savastanoi*.

The kinetic mechanisms of flavoenzymes that catalyze dehydrogenation reactions can be divided into two half-reactions. In the reductive half-reaction the substrate CH bond is broken and the flavin is reduced. In the oxidative half-reaction the reduced enzyme is oxidized either by molecular oxygen or another electron acceptor. The initial studies of CH bond cleavage in flavoproteins were done with the enzyme D-amino acid oxidase. DAAO catalyzes the conversion of  $\alpha$ -chloro-alanine to chloropyruvate and to pyruvate (4). A kinetic isotope effect was observed when the  $\alpha$ -hydrogen of  $\alpha$ -chloro-alanine was substituted with deuterium, but the product distribution remained the same. This is consistent with the formation of a common precursor for both chloropyruvate and pyruvate. The precursor was proposed to be a carbanion as shown in Scheme 2.

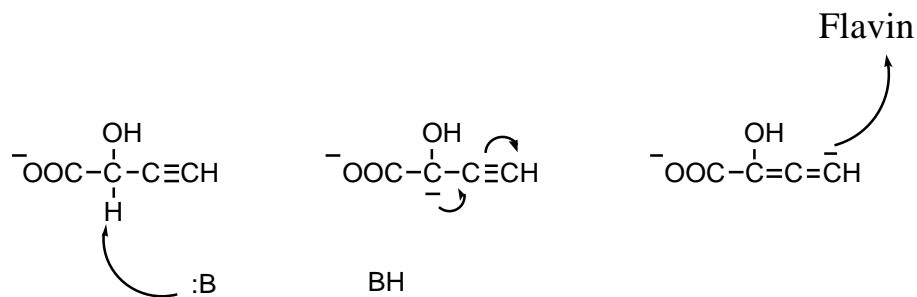
Scheme 2



With the enzyme flavocytochrome  $b_2$  (Flb<sub>2</sub>) similar experiments with bromopyruvate were carried out in the wild-type and mutant enzymes, and as with DAAO formation of bromopyruvate and pyruvate were observed (5). Thus, a carbanion mechanism was also proposed for Flb<sub>2</sub> and other members of the  $\alpha$ -hydroxy acid

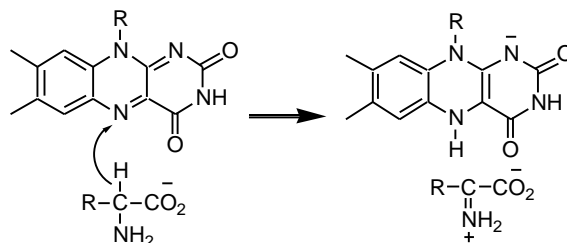
dehydrogenases. Other experimental evidence that supported a carbanion mechanism came from the inactivation of several flavoprotein hydrogenases by 2-hydroxy-3-butyrate (6, 7). In the reaction proposed for inactivation, the  $\alpha$ -proton from the acetylenic acid is abstracted; this is followed by rearrangement to form an allene which reacts with the flavin to produce a flavin adduct (Scheme 3)(8).

Scheme 3



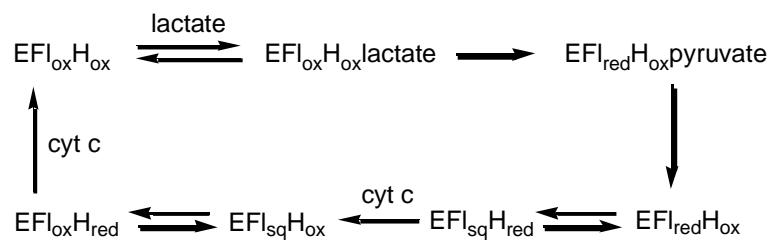
The validity of the carbanion mechanism in DAAO was questioned when the three dimensional structure of this enzyme was solved (9). In the active site of DAAO there is no active site base to abstract the proton at the alpha position as required in a carbanion mechanism. It was proposed that DAAO instead catalyzes the oxidation of D-amino acids via a hydride transfer mechanism (9). Experimental evidence for hydride transfer mechanism came from  $^{15}\text{N}$  isotope effects. The  $^{15}(\text{V/K})$  value with D-serine is 0.997, a value consistent with the direct formation of the imino acid from an unprotonated amino acid (10). Thus, a hydride transfer mechanism involving the unprotonated form of the substrate was proposed for DAAO (Scheme 4).

Scheme 4



Since the carbanion mechanism proposed for the  $\alpha$ -hydroxy acid oxidases was based on the results on DAAO, the validity of this mechanism for these enzymes is questionable. This family of enzymes is composed of flavocytochrome  $b_2$ , glycolate oxidase, lactate oxidase, mandelate dehydrogenase, lactate monooxygenase and long chain hydroxy acid oxidase (11). The enzyme flavocytochrome  $b_2$  (Flb $_2$ ) has been one of the most studied member of this family. Flb $_2$  catalyzes the conversion of lactate to pyruvate. The enzyme contains tightly bound FMN and heme  $b_2$  cofactors. During catalytic turnover the electrons are transferred from lactate to the FMN to the heme and then to cytochrome  $c$  *in vivo* (Scheme 5)(12, 13).

Scheme 5



The crystal structure with pyruvate bound in the active site has been solved at 2.4 Å resolution (14)(Figure 2). In the active site the carboxylate of pyruvate is bound by Arg376 and Tyr143. Mutation of Arg376 to lysine abolishes all detectable activity (15),

while mutation of Tyr143 decreases the  $V/K$  value for lactate several fold (16). His373 has been proposed to be the active site base (14). Consistent with this proposal mutation of His373 to glutamine decreases the rate of lactate oxidation by at least  $10^5$  (17). Asp282 is proposed to orient His373 in the correct position for proton abstraction. Mutation of Asp282 to asparagine decreases the  $V_{\max}$  and  $V/K_{\text{lactate}}$  values two orders of magnitude (18). These residues are conserved in all members of this family (Figure 2)(19-23).

Modeling studies were done to predict the position of the hydroxyl group of lactate in the active site of Flb<sub>2</sub> (24). It was found that lactate can be placed in two orientations. In one (Scheme 6, path a), the  $\alpha$ -proton of lactate is closest to His373 and the hydroxyl proton is close to Tyr254. In the second (Scheme 6, path b), lactate is oriented such that the hydroxyl proton is closest to His373. These two possible binding modes make different mechanistic predictions. Abstraction of the substrate  $\alpha$ -proton by His373 would form a carbanion. Alternatively, abstraction of the hydroxyl proton by His373 would be consistent with direct hydride transfer of the  $\alpha$ -hydrogen to the FMN as a hydride (Scheme 6, path b)(24).

The flavoenzyme L-amino acid oxidase (LAAO) catalyzes the oxidation of L-amino acids to the corresponding keto acids (25). The most studied LAAOs are those from snake venom (26). The three dimensional structure of *Calloselasma rhodostoma* LAAO complex with the competitive inhibitor aminobenzoate has been recently solved at 2.0 Å resolution (27). The expression of recombinant LAAO has not been reported; thus the role of active site residues in these enzymes has been unexplored.

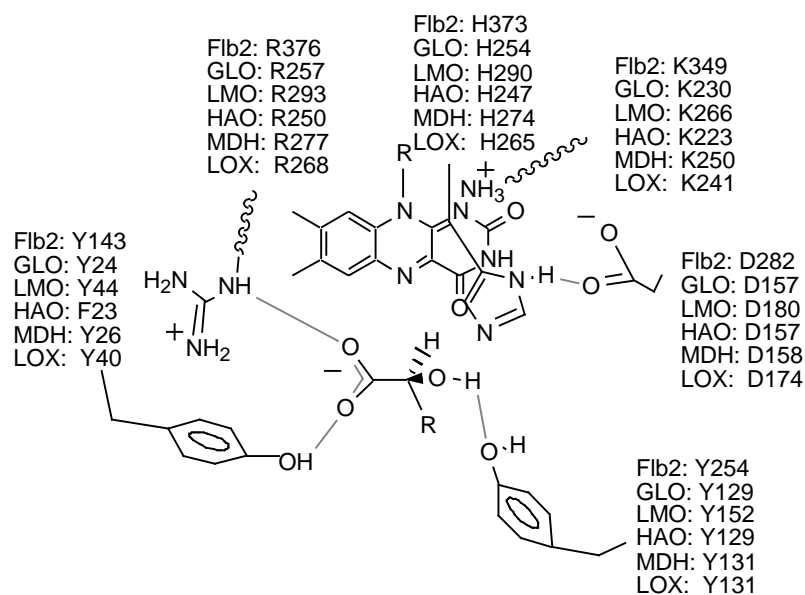
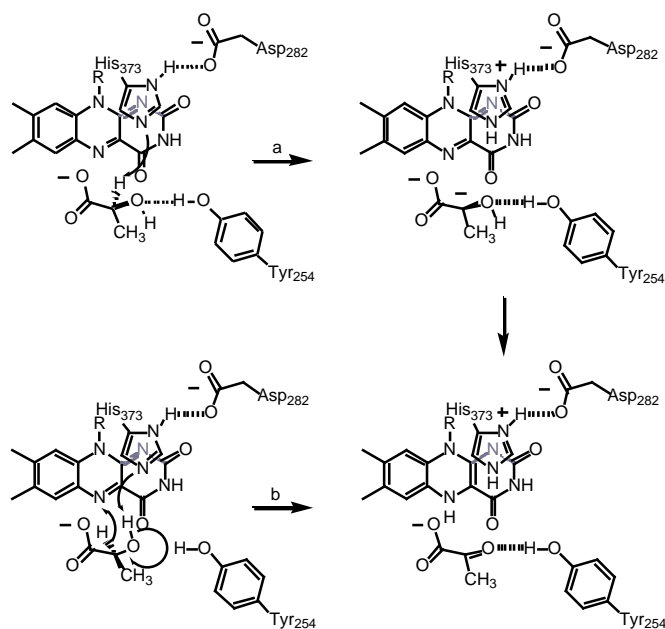


FIGURE 2. Proposed active site for the family of  $\alpha$ -hydroxy acid oxidases. The conserved residues in flavocytochrome  $b_2$  (Flb2), glycolate oxidase (GLO), lactate monooxygenase (LMO), long chain hydroxy acid oxidase (HAO), mandalate dehydrogenase (MDH), and lactate oxidase (LOX) are shown.

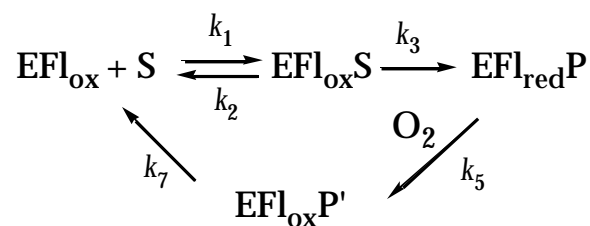
Scheme 6



The flavoenzyme tryptophan 2-monooxygenase (TMO) catalyzes the oxidative decarboxylation of L-tryptophan to indoleacetamide and water (28). The kinetic mechanism with tryptophan has been determined (29). In the reductive half reaction the oxidized enzyme forms a complex with the substrate and oxidation occurs to form reduced enzyme and imino acid, in the oxidative half reaction the imino-acid enzyme complex react with molecular oxygen forming oxidized enzyme and product (Scheme 7)(29). TMO is one of four flavoenzymes that catalyze the oxidative decarboxylation of amino acids; the other three are L-phenylalanine oxidase (30), L-arginine 2-monooxygenase (31) and L-lysine 2-monooxygenase (32). There is no three dimensional structure for any of these enzymes. This limits the mechanistic information that can be obtained from site directed mutants of active site residues.

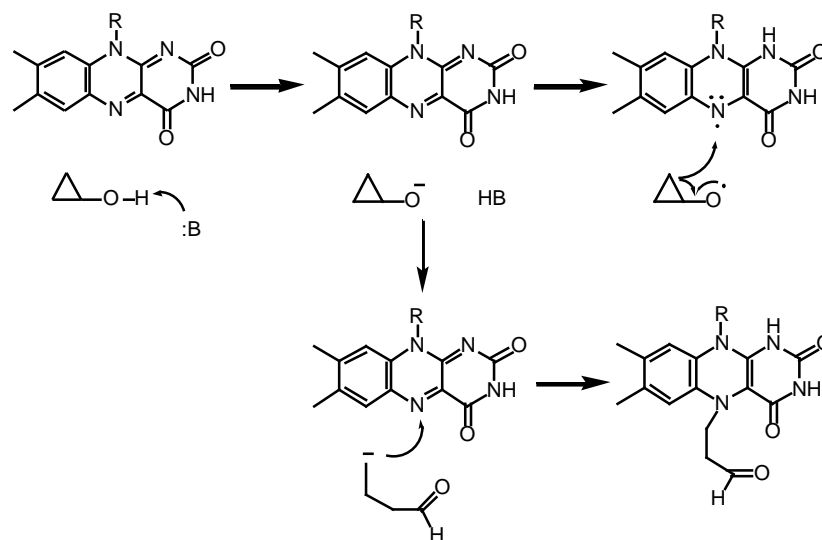


Scheme 7



Glucose oxidase, cholesterol oxidase and methanol oxidase are the best known samples of flavoenzymes that catalyze alcohol oxidation. The mechanism of these flavoenzymes has been studied with substrate analogues that contain cyclopropyl groups and by kinetic isotope effects. Methanol oxidase does not turn over cyclopropanol; instead the enzyme is inactivated (33). The inactivated enzyme contains a covalent adduct between the flavin and the ring opened inhibitor. Proposed mechanisms involve the inactivation by an ionic species or by a radical species following ring opening (Scheme 8). Cholesterol oxidase is inactivated by 2,3-cyclopropanol-5-cholestan-3-ol in a similar fashion (34). In support of a radical mechanism of inactivation of methanol oxidase by cyclopropanol, when the native FAD is substituted by 5-deaza-FAD no adduct is formed (33). Cyclopropyl methanol, which should form a carbon radical does not inactivate methanol oxidase, questioning the validity of the proposed radical in methanol oxidase. In addition, mutation of His 447 in cholesterol oxidase, the residue proposed to be the active site base, decreases the rate of inactivation by 2,3-cyclopropanol-5-cholestan-3-ol 10-fold to the rate of nonenzymatic ring opening providing evidence for inactivation not involving a radical intermediate.

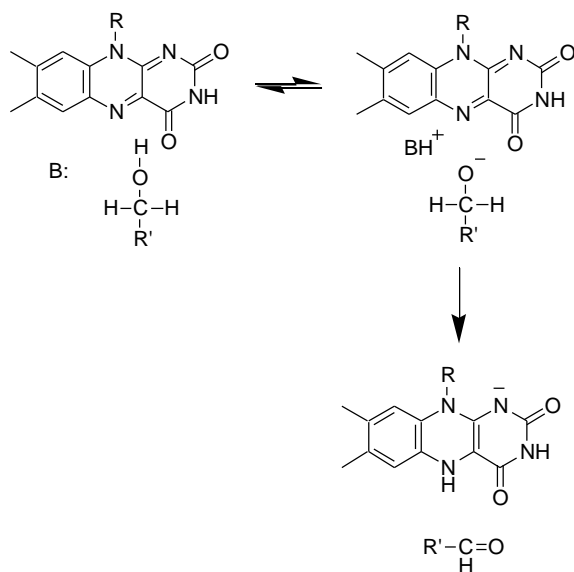
Scheme 8



The chemical mechanism of methanol oxidase from *Hansenula polymorpha* has been studied with substituted alcohols and kinetic isotope effects (35). Based on a solvent isotope of 2 and a primary deuterium isotope effect close to unity on the  $V/K$  with benzyl alcohol, it was concluded that OH bond cleavage did not occur in the same step as CH bond cleavage. Further experiments with substituted alcohols add to the conclusion that the reaction occurs via hydride transfer following OH bond cleavage (Scheme 9) (35). Similarly to the mechanism of alcohol oxidation, the mechanism of amine oxidation by monoamine oxidases A and B has been probed with inhibitors containing cyclopropyl groups. The results from these experiments were analyzed in support of a mechanism that involves a single electron transfer from the amine nitrogen to the oxidized flavin, producing an aminium cation radical and flavin semiquinone (36) (Scheme 10). The subsequent abstraction of the  $\beta$ -hydrogen could happen either by direct transfer of the hydrogen to the flavin or by formation of a carbon radical. This

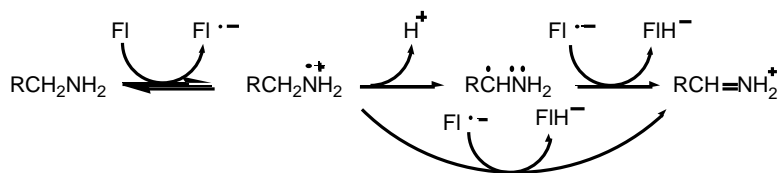
mechanism has been questioned since no flavin semiquinone is observed during rapid reaction experiments (37).

Scheme 9



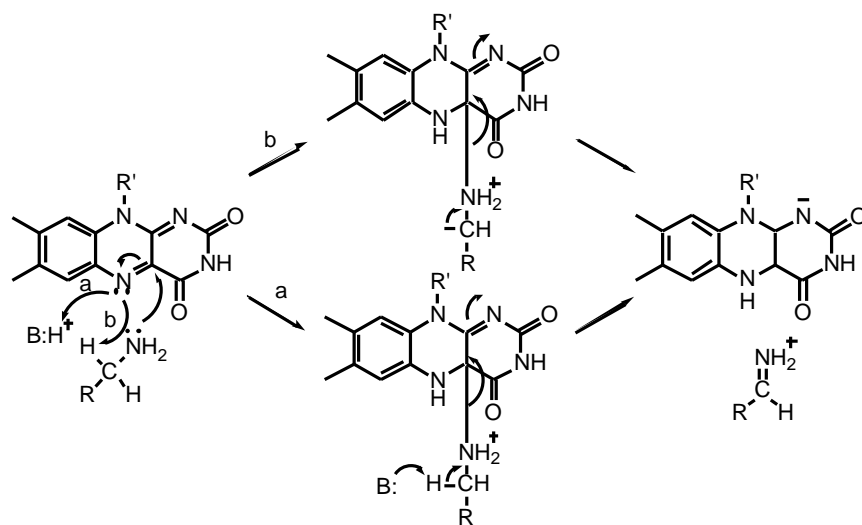
Studies in MAO A with substituted para-benzylamines resulted in large  $k_{\text{cat}}$  values supporting abstraction of the  $\alpha$ -CH proton. A polar nucleophilic mechanism which involves a 4a-flavin adduct, with the flavin N5 acting as the base, was proposed instead

Scheme 10



(Scheme 11a). This is a modification of a polar nucleophilic mechanism previously proposed for MAO A (Scheme 11 b) (38). The polar nucleophilic mechanism has been questioned since the formation of the flavin adduct is not observed, even though  $\alpha$ -CH bond cleavage is rate limiting (37).

Scheme 11



## CHAPTER II

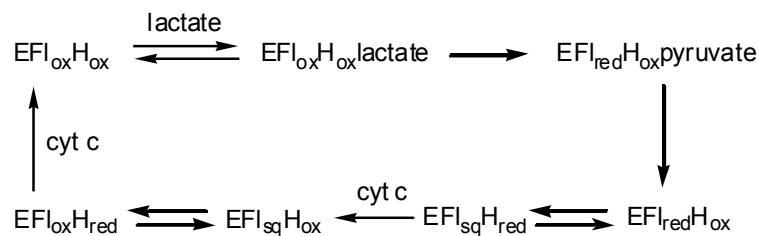
### PROBING THE RELATIVE TIMING OF HYDROGEN ABSTRACTION STEPS IN THE FLAVOCYTOCHROME b<sub>2</sub> REACTION WITH PRIMARY AND SOLVENT DEUTERIUM ISOTOPE EFFECTS AND MUTANT ENZYMES

#### INTRODUCTION

Flavocytochrome b<sub>2</sub> from *Saccharomyces cerevisiae* catalyzes the oxidation of L-lactate to pyruvate. The enzyme is a member of a family of homologous flavoenzymes catalyzing similar oxidations of  $\alpha$ -hydroxy acids to keto acids; this family includes the enzymes glycolate oxidase, lactate monooxygenase, lactate oxidase, mandelate dehydrogenase, and 2-hydroxyacid oxidase (39-42). Each of the identical 57,500 M<sub>r</sub> subunits in the tetrameric flavocytochrome b<sub>2</sub> contains a heme b<sub>2</sub> and an FMN (43). In the course of the reaction, a hydride equivalent is first transferred from L-lactate to the FMN; this is followed by two single electron transfers to the heme and then to a final acceptor (Scheme 12) (44-46). The final electron acceptor *in vivo* is cytochrome c, but this can be replaced by a variety of acceptors *in vitro*.

The crystal structure of the enzyme with pyruvate bound has been determined (14, 47), allowing identification of potential catalytic residues (14, 48, 49). The carboxylate of pyruvate is bound by Arg376 and Tyr143, suggesting similar roles for these residues in the binding of the  $\alpha$ -hydroxy acid substrate. In support of this, mutation of Arg376 to lysine decreases the activity by at least three orders of magnitude (50), while mutation of Tyr143 decreases the V/K value for lactate by several fold (16). Lactate can be placed into the active site in place of pyruvate in two alternative

Scheme 12

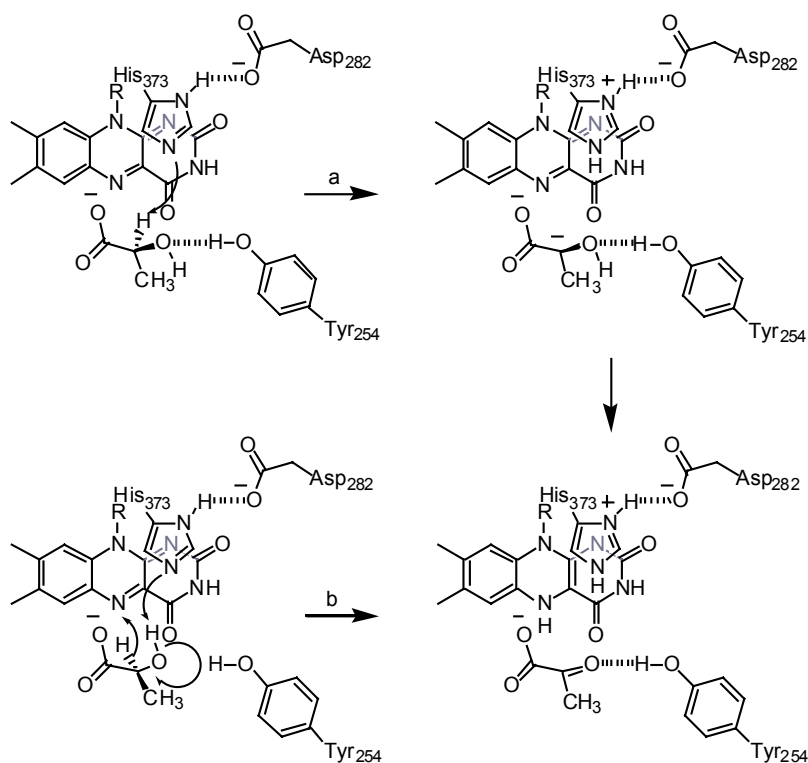


orientations (24). In one (Scheme 13, path a), the  $\alpha$  proton of lactate is closest to His373 and the hydroxyl proton is close to Tyr254. In the second (Scheme 13, path b), lactate is oriented such that the hydroxyl proton is closest to His373. Mutation of His373 to glutamine decreases the rate of lactate oxidation by at least  $10^5$  (17), consistent with a role for this residue as an active site base. The two possible orientations of lactate make different mechanistic predictions (Scheme 13). Abstraction of the substrate  $\alpha$ -hydrogen by His373 would form a carbanion. Alternatively, abstraction of the hydroxyl hydrogen by this residue would be consistent with direct transfer of the  $\alpha$ -hydrogen to the FMN as a hydride. Experimental studies of flavocytochrome  $b_2$  and the other members of this flavoenzyme family have been interpreted as favoring either a carbanion mechanism (51) or a hydride transfer mechanism (52, 53).

The oxidation of lactate to pyruvate requires removal of both the hydrogen bound to the  $\alpha$ -carbon and the hydroxyl proton. The relative timing of these bond cleavages differs in the two mechanisms of Scheme 13. If the reaction proceeds via a carbanion intermediate, the  $\alpha$ -proton would be abstracted first, with cleavage of the oxygen-hydrogen bond occurring in a subsequent step. In contrast, the bond cleavages could be concerted in a hydride transfer mechanism. In the work described herein, primary deuterium and solvent kinetic isotope effects have been used to probe the order of bond cleavage in the flavocytochrome  $b_2$  reaction to provide further insight into the

mechanism. In addition to experiments with wild-type enzyme, the analyses were carried out with a mutant protein lacking the heme domain, to eliminate effects due to electron transfer between the cofactors, and with the active site mutant D282N, a protein for which chemical steps appear to be rate-limiting (18). Scheme 13 presents the proposed mechanisms for lactate dehydrogenation by flavocytochrome  $b_2$ : a, carbanion mechanism, in which His373 abstracts the alpha proton from lactate to form a

Scheme 13



carbanion. This intermediate reacts with the FMN, producing reduced flavin and pyruvate. b, hydride transfer mechanism in which His 373 abstracts the hydroxyl proton as the alpha proton is transferred as a hydride directly to the FMN in a concerted manner. The scheme was adapted from references (24) and (16).

## EXPERIMENTAL PROCEDURES

*Materials.* Sodium L-[2-<sup>2</sup>H]lactate (98%) and deuterium oxide (99.9%) were purchased from Cambridge Isotope Co., Andover, MA. L-Lactate and D,L-lactate were from Sigma Chemical Corporation (St. Louis, MO). Hydroxyapatite was from BioRad laboratories, Hercules, CA. All other reagents were of the highest purity commercially available.

*DNA Manipulation.* Custom oligonucleotides were synthesized on an Applied Biosystems Model 380B DNA synthesizer by the Gene Technology Laboratory of Texas A&M. Restriction endonucleases were from New England Biolabs Inc. *Pfu* DNA polymerase was obtained from Stratagene USA. Plasmids were purified using kits from Qiagen Inc. The plasmid pDSb<sub>2</sub> (50), which contains the coding region for wild-type flavocytochrome b<sub>2</sub>, and a plasmid coding for flavocytochrome b<sub>2</sub> D282N were generous gifts from Dr. Florence Lederer.

The DNA fragment coding for mature flavocytochrome b<sub>2</sub> was removed from pDSb<sub>2</sub> by digestion with *EcoRI* and *HindIII*, and placed by ligation into pET21d which had been digested with *EcoRI* and *HindIII*. This construct was called pEFCB3. Site-directed mutagenesis (54) with the oligonucleotide 5'-AGCGGGCGAAATCTTTTGTATCCATGGCCAGTTTCGGCTCGTTGTC-3' was used to introduce a new *NcoI* restriction site into pEFCB3 so that the ATG of the restriction site coincided with the codon for methionine 6 of the mature enzyme. The resulting plasmid, pEFCB4, was digested with *NcoI* and incubated with T4 DNA ligase. The plasmid found to have lost the sequence between the *NcoI* site of pET21b and the newly introduced *NcoI* site (pEFCB5) was utilized for expression of the wild-type enzyme.



Flavocytochrome b<sub>2</sub> lacking the amino terminal 100 amino acid residues comprising the heme domain was constructed by incorporating an additional *NcoI* recognition site at position 300 of the gene in pEFCB5 using the QuikChange protocol (Stratagene) with the oligonucleotides 5'GCTCCTGGTGA AACCATGGAAGATATCGC'3 and 5'GCGATATCTTCCATGGTTTCACCAGGAGC'3. The resulting mutagenesis mixture was used to transform XL1-Blue cells. Mutated plasmids were detected by electrophoretic analysis of restriction digests of plasmids, using *NcoI* and *HindIII*. A plasmid containing the additional *NcoI* site (pEFCB6) was digested with *NcoI* and then ligated with T4 DNA ligase. This ligation mixture was used to transform XL1-Blue cells. Resulting colonies were screened for the correct construct using the polymerase chain reaction. Isolated colonies were picked, duplicated on a second agar plate, and the remaining cells dispersed in 100 µl of 10 mM Tris-Cl, pH 8.0. The samples were boiled for 5 minutes, chilled on ice, and centrifuged for 5 minutes. The supernatants were used as templates for a PCR reaction, using Taq polymerase from Stratagene USA and oligonucleotide primers that flanked the entire flavocytochrome b<sub>2</sub> gene. Colonies yielding products with a flavocytochrome b<sub>2</sub> gene 300 bp shorter than the wild-type gene were selected for plasmid isolation and DNA sequencing. A plasmid containing the truncated coding region, pEFCBΔheme, was introduced into competent *E. coli* BL21(DE3) cells. Small cultures were stored as 10% glycerol stocks at -80 °C.

*Cells Strains and Growth.* Cells from permanent stocks containing the appropriate plasmid were streaked on LB agar plates containing 100 µg/mL ampicillin; a single colony was used to inoculate a 50 mL liquid culture. After incubation of the latter overnight at 37 °C, 10 mL was used to inoculate a 1 L culture of LB broth containing 100 µg/mL ampicillin. When the A<sub>600</sub> value of the culture reached 0.8, isopropyl-β-D-

thioglucanopyranoside was added to a final concentration of 500  $\mu\text{M}$ . Incubation was continued for 6 hr, at which time cells were harvested by centrifugation for 1 hr at 5000 x g.

*Enzyme Purification.* For purification of the wild-type enzyme, cell pellets were resuspended in 10 mM Tris-HCl, 10 mM EDTA, 0.2 mg/ml lysozyme, 20 mM D,L-lactate, 1 mM phenylmethylsulfonyl fluoride, pH 7.5, at 4 °C, using 10 ml/g. The cell suspension was stirred for 1 hr at 4 °C, then centrifuged at 12,000 x g for 1 hr at 4 °C. The resulting supernatant was brought to 30% saturation with ammonium sulfate, followed by centrifugation at 10,000 x g for 30 min. This supernatant was brought to 70% saturation with ammonium sulfate. The pellet produced by centrifugation was resuspended in 100 ml of 10 mM potassium phosphate, 1 mM EDTA, 20 mM D,L-lactate, pH 7.5, and loaded on to a hydroxyapatite column previously equilibrated with the same buffer. The enzyme was eluted with a linear gradient from 10 mM to 300 mM potassium phosphate. Purification of the flavin domain was done as described by Balme et al. (55). The D282N enzyme was purified as described by Gondry et al. (56). Enzyme concentrations were determined using an  $\epsilon_{423}$  value of 183  $\text{mM}^{-1}\text{cm}^{-1}$  and an  $\epsilon_{413}$  value of 129.5  $\text{mM}^{-1}\text{cm}^{-1}$  for the reduced and oxidized full length enzymes, respectively (12), and an  $\epsilon_{453}$  value of 11.1  $\text{mM}^{-1}\text{cm}^{-1}$  for the flavin domain (57). Purified enzymes were stored in 100 mM potassium phosphate, 1 mM EDTA, 20 mM D,L-lactate, pH 7.5, at -70 °C.

To remove the lactate used for storage, the day of use an aliquot was precipitated with 70% ammonium sulfate in 100 mM potassium phosphate, 1 mM EDTA, pH 7.5, at 4 °C. The pellet obtained by centrifugation at 15,000 x g for 5 min was resuspended in 100 mM potassium phosphate, 1 mM EDTA, pH 7.5. This procedure was repeated twice. The final enzyme concentration was about 3  $\mu\text{M}$ . This treatment also resulted in

oxidation of the cofactors. For stopped-flow experiments, enzyme was passed through a Sephadex G-25 column in 100 mM potassium phosphate, 1 mM EDTA, pH 7.5, to remove the lactate.

*Enzyme Assays.* Initial rate assays were performed in 100 mM potassium phosphate, 1 mM EDTA, 1 mM potassium ferricyanide, pH 7.5, 25 °C, with varied concentrations of L-lactate or L-[2-<sup>2</sup>H]lactate, following the decrease in absorbance at 420 nm, and using an  $\epsilon_{420}$  value for ferricyanide of  $1.04 \text{ mM}^{-1}\text{cm}^{-1}$ . For the flavin domain, 3 mM potassium ferricyanide was used. The steady state kinetic parameters given in Table 1 for the flavin domain were obtained by varying the concentrations of both potassium ferricyanide and L-lactate. Concentrations of lactate were determined by end point assay with wild-type flavocytochrome b<sub>2</sub>.

For pH studies, the buffer was 50 mM Bis-Tris at pH 5.5-7.0, 150 mM HEPES at pH 7.0-8.5, and 50 mM ethanolamine at pH 8.5-10.0. All assays were done in the presence of 1 mM potassium ferricyanide at 25 °C. pD profiles were done in the same buffers made up using 99.9% deuterium oxide and adjusting the pD with DCl and NaOD as needed, adding 0.4 to the value indicated by the pH meter (58). Steady state kinetic solvent isotope effects and proton inventories were carried out in 100 mM phosphate, 1 mM EDTA, pH 7.5 or pD 8.0, with 1 mM potassium ferricyanide for the wild-type and D282N enzymes and 3 mM for the flavin domain at 25 °C. For the proton inventory experiments, the desired atom fraction of D<sub>2</sub>O was achieved by combining appropriate volumes of assay components made up in H<sub>2</sub>O or D<sub>2</sub>O. Assays were initiated by the addition of 5  $\mu\text{l}$  of enzyme in H<sub>2</sub>O into a final volume of 1 ml.

The effects of viscosity on steady state kinetic parameters were measured in 100 mM potassium phosphate, 1 mM EDTA, pH 7.5, 25 °C, using 1 mM potassium ferricyanide for wild-type enzyme and 3 mM for the flavin domain. The values for the

relative viscosities of glycerol-containing solutions were taken from Weast (59) and adjusted for 25 °C.

For rapid reaction analyses, flavin reduction was monitored on an Applied Photophysics SX.18MV stopped-flow spectrophotometer. Enzyme in 100 mM potassium phosphate, 1 mM EDTA, pH 7.5, was mixed with an equal volume of the same buffer containing varied concentrations of lactate at 25 °C. The reaction of the wild-type enzyme was monitored at 438 nm, a heme isosbestic point, while that of the flavin domain was monitored at 452 nm (55). To determine solvent isotope effects, enzyme in aqueous buffer was mixed with an equal volume of lactate in D<sub>2</sub>O-containing buffer.

*Data Analysis.* Kinetic data were fit to equations 1-8 using the programs Kaleidagraph (Adelbeck Software, Reading, PA), KinetAsyst (IntelliKinetics, State College, PA) or Igor (Wavemetrics, Lake Oswego, OR). Initial rate data when only one substrate was varied were fit to the Michaelis-Menten equation. When both lactate and ferricyanide were varied, the data were fit to equation 1. Primary deuterium and solvent isotope effects were calculated using equations 2-4. Equation 2 is for separate isotope effects on the  $V_{\max}$  and  $V/K_{\text{lactate}}$  values; equation 3 is for an isotope effect on the  $V_{\max}$  value only; equation 4 is for an isotope effect on the  $V/K_{\text{lactate}}$  value only. In each,  $F_i$  is the fraction of heavy atom substitution in the substrate,  $E_v$  is the isotope effect on the  $V_{\max}$  value minus 1, and  $E_{vK}$  is the isotope effect on the  $V/K_{\text{lactate}}$  value minus 1. The pH profiles were obtained by fitting the  $V_{\max}$  and  $V/K_{\text{lactate}}$  values obtained at each pH to equation 5; here,  $K_1$  and  $K_2$  are the dissociation constants of the ionizable groups, and  $C$  is the pH independent value of the specific kinetic parameter. Proton inventory data were fit to equation 6, where  $n$  is the atom fraction of D<sub>2</sub>O,  ${}^n k$  is the solvent isotope effect at that D<sub>2</sub>O content, and  ${}^{\text{D}_2\text{O}} k$  is the solvent isotope effect in 100% D<sub>2</sub>O. Stopped-flow

traces were fit to equation 7 which describes a biphasic exponential decay;  $\lambda_1$  and  $\lambda_2$  are first order rate constants,  $t$  is time, and  $A_a$ ,  $A_b$ , and  $A_c$  are the absorbances of species A, B, and C. The lactate concentration dependence of the rapid phase, which corresponds to flavin reduction, was analyzed using equation 8 (45); here  $k_{obs}$  is the observed rate of reduction of the flavin,  $k_{red}$  is the limiting rate of reduction at saturating substrate concentration, and  $K_d$  is the concentration of substrate at which the rate of reduction is one-half the maximum value. To calculate isotope effects on rapid reaction kinetic parameters, the observed rates of reduction were fit to equation 2, using the  $k_{obs}$  values in place of initial rates.

$$v = \frac{VAB}{K_aB + K_bA + AB} \quad (1)$$

$$v = \frac{VA}{K_m(1 + F_i(E_{vk})) + A(1 + F_i(E_v))} \quad (2)$$

$$v = \frac{VA}{K_m + A(1 + F_i(E_v))} \quad (3)$$

$$v = \frac{VA}{K_m(1 + F_i(E_{vk})) + A} \quad (4)$$

$$\log Y = \log \frac{C}{1 + \frac{H}{K_1} + \frac{K_2}{H}} \quad (5)$$

$$1/{}^n k = 1 - n + (n/{}^{D2O}k_1) \quad (6)$$

$$A_{total} = (A_a - A_c) e^{\lambda_1 t} + \frac{\lambda_1(A_b - A_c)}{\lambda_1 - \lambda_2} (e^{-\lambda_2 t} - e^{-\lambda_1 t}) + A_c \quad (7)$$

$$k_{obs} = \frac{k_{red}A}{K_d + A} \quad (8)$$

## RESULTS

*Wild-type Flavocytochrome b<sub>2</sub>*. As a measure of the extent to which the  $V_{\max}$  and  $V/K_{\text{lactate}}$  values reflect the rate of the cleavage of the carbon-hydrogen bond of lactate, primary kinetic isotope effects were determined with 2-<sup>2</sup>H-lactate. Ferricyanide was used as the electron acceptor in these analyses because the oxidative half reaction becomes partially rate-limiting when cytochrome c is used (16). The concentration of ferricyanide was kept at least 50-fold higher than its  $K_M$  value to ensure that reduction was irreversible in the steady state. For the mechanism of Scheme 12, the  $V/K_{\text{lactate}}$  value includes the rates of steps for the reaction of free enzyme and lactate to form the reduced enzyme-pyruvate complex. The  $^D V_{\max}$  and  $^D(V/K_{\text{lactate}})$  values for wild-type flavocytochrome b<sub>2</sub> are close to 3 at pH 7.5 (Table 1). The primary isotope effects are independent of pH; at pH 5.2, the  $^D V_{\max}$  and  $^D(V/K_{\text{lactate}})$  values are  $3.0 \pm 0.2$  and  $3.0 \pm 0.4$ , respectively, while at pH 9.2 the values are  $2.9 \pm 0.2$  and  $3.0 \pm 0.5$ . The values are within the range of values previously determined under slightly different conditions (16, 24, 45).

Solvent isotope effects were determined to probe the timing of steps involving solvent exchangeable protons, such as the cleavage of the lactate oxygen-hydrogen bond. As a necessary step in the measurement of solvent isotope effects on the flavocytochrome b<sub>2</sub> reaction, the pH dependences of the  $V_{\max}$  and  $V/K_{\text{lactate}}$  values for the wild-type enzyme were determined over the accessible pH range. The  $V/K_{\text{lactate}}$  pH profile of wild-type flavocytochrome b<sub>2</sub> is bell-shaped, consistent with the involvement of two ionizable groups in the free enzyme (Figure 3A). One group with a  $pK_a$  value of  $5.4 \pm 0.1$  must be unprotonated and one with a  $pK_a$  value of  $8.7 \pm 0.1$  must be protonated for activity. The  $V_{\max}$  pH profile is also bell-shaped, reflecting apparent  $pK_a$  values of  $5.0 \pm 0.2$  and  $9.4 \pm 0.1$  for the groups which must be unprotonated and protonated for

catalysis, respectively (Figure 3B). These values are in good agreement with previously published values obtained under different conditions (60, 61).

When the pH dependence is carried out in D<sub>2</sub>O, all of the pK<sub>a</sub> values in the V<sub>max</sub> and V/ K<sub>lactate</sub> profiles are shifted upward, as expected (Figure 3 and Table 2). These analyses show that the V<sub>max</sub> and V/ K<sub>lactate</sub> values are independent of pL at pH 7.5 and pD 8.0. Therefore, we chose pH 7.5 and pD 8.0 to measure the solvent isotope effects. With the wild-type enzyme, there is a normal effect on the V<sub>max</sub> value of  $1.38 \pm 0.07$  and a slightly inverse effect on the V/ K<sub>lactate</sub> value of  $0.90 \pm 0.04$  (Table 3). Similar values with slightly lower precision could be calculated from the complete pL dependences. Two approaches were taken to determine if the solvent isotope effects with the wild-type enzyme were on the step in which the lactate carbon-hydrogen bond is cleaved. In the first, the solvent isotope effects were measured with 2-<sup>2</sup>H-lactate under the conditions used with the nondeuterated substrate. This gave values for <sup>D2O</sup>(V/K<sub>lactate</sub>)<sub>D</sub> of  $0.87 \pm 0.1$  and for (<sup>D2O</sup>V)<sub>D</sub> of  $1.1 \pm 0.03$ . The decrease in the magnitude of the <sup>D2O</sup>V value with deuterated lactate is consistent with the solvent isotope effect on this parameter arising from a different step than that generating the primary isotope effect (62). The magnitudes of the <sup>D2O</sup>(V/K<sub>lactate</sub>) values are too small to draw conclusions.

Table 1. Steady State Kinetic Parameters and Primary Isotope Effects on the Oxidation of Lactate by Wild-type and Mutant Flavocytochromes b<sub>2</sub>\*

Enzyme	V s <sup>-1</sup>	V/ K <sub>lactate</sub> mM <sup>-1</sup> s <sup>-1</sup>	K <sub>lactate</sub> mM	<sup>D</sup> V	<sup>D</sup> (V/K)
Wild-type	372 ± 12	2300 ± 215	0.16 ± 0.02	2.9 ± 0.1	3.0 ± 0.3
Flavin Domain	200 ± 7	543 ± 32	0.36 ± 0.03	3.7 ± 0.3	3.5 ± 0.2
D282N	2.2 ± 0.1	15 ± 1	0.15 ± 0.02	4.9 ± 0.3	4.3 ± 1.1

\*Conditions: 100 mM potassium phosphate, 1 mM EDTA, and 1 mM ferricyanide for the wild-type and D282N enzymes and 3 mM ferricyanide for the flavin domain, pH 7.5, 25°C.



Table 2. pK<sub>a</sub> Values for Wild-type and Mutant Flavocytochromes b<sub>2</sub>\*

Enzyme	Parameter	Solvent	pK <sub>a</sub>	pK <sub>a</sub>
Wild-type	V	H <sub>2</sub> O	5.0 ± 0.2	9.4 ± 0.1
	V	D <sub>2</sub> O	5.3 ± 0.1	10.4 ± 0.1
	V/ K <sub>lactate</sub>	H <sub>2</sub> O	5.4 ± 0.1	8.7 ± 0.1
	V/ K <sub>lactate</sub>	D <sub>2</sub> O	5.8 ± 0.2	9.4 ± 0.2
Flavin Domain	V	H <sub>2</sub> O	6.2 ± 0.2	8.5 ± 0.2
	V/ K <sub>lactate</sub>	H <sub>2</sub> O	5.5 ± 0.3	8.4 ± 0.2
D282N	V	H <sub>2</sub> O	5.9 ± 0.1	10.2 ± 0.1

\*Conditions: 150 mM HEPES, 50 mM Bis-Tris, 50 mM ethanolamine, 1 mM or 3 mM ferricyanide, pH 5.5-10.0, 25°C.

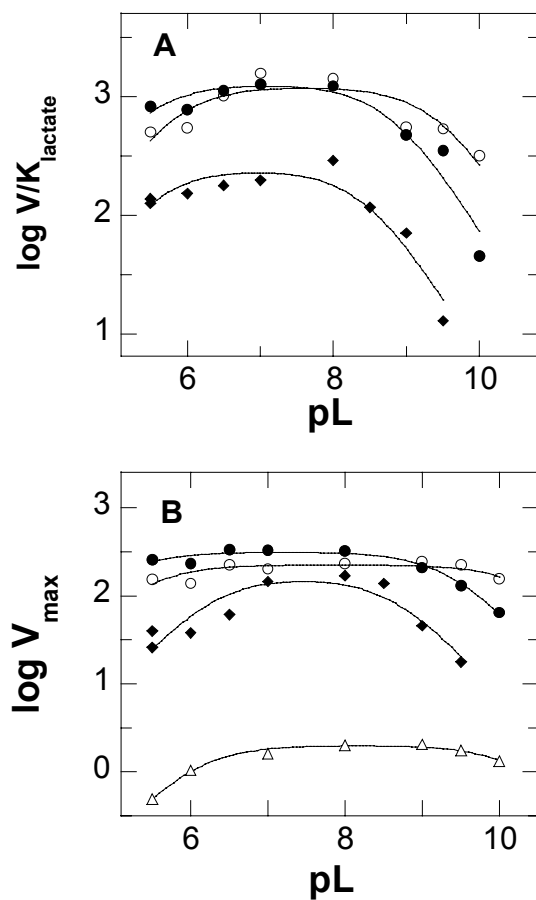


FIGURE 3. pL dependence of wild-type and mutant flavocytochromes b<sub>2</sub>. Initial rates were determined with ferricyanide as the electron acceptor as described in Experimental Procedures. Panel A shows the  $V/K_{\text{lactate}}$  profile in H<sub>2</sub>O for the wild-type (●) and flavin domain (◆) enzymes and in D<sub>2</sub>O for the wild-type enzyme (○). Panel B shows the  $V_{\text{max}}$  profile in H<sub>2</sub>O for the wild-type (●), the D282N (△), and flavin domain (◆) enzymes, and in D<sub>2</sub>O for the wild-type enzyme (○). The lines are fits of the data to equation 5.

As an alternative approach, isotope effects were determined for the rate of reduction of the flavin by lactate using a stopped-flow spectrophotometer. When lactate is mixed with flavocytochrome  $b_2$  in the absence of an electron acceptor, complete reduction of the FMN occurs in an apparently irreversible first-order process. Direct measurements of FMN reduction eliminates contributions from subsequent electron transfer steps between FMN and heme  $b_2$  and between heme  $b_2$  and ferricyanide. In this experiment the wild-type enzyme showed a  $D_{k_{\text{red}}}$  of 5.4 (Table 4). The solvent isotope effect on the rate of reduction was measured by mixing enzyme in aqueous buffer with an equal volume of lactate in  $D_2O$  in the stopped-flow spectrophotometer. No significant solvent isotope effect on the limiting rate of reduction of the flavin could be detected (Table 4).

*Isolated Flavin Domain.* The lack of a solvent isotope effect on the rate of flavin reduction suggests that the solvent isotope effect on the  $V_{\text{max}}$  value for the wild-type enzyme occurs on a step after flavin reduction. As a test of this hypothesis, isotope effects were determined with a mutant protein lacking the heme domain, an enzyme previously described by Balme et al. (55). While the ability of this enzyme to utilize cytochrome  $c$  as an electron acceptor is nearly eliminated by the truncation, the effects on kinetic parameters with ferricyanide as electron acceptor are much less. The  $V/K_{\text{lactate}}$  and  $V_{\text{max}}$  values decrease severalfold, and there is an increase in the value of the primary isotope effects on these parameters (Table 1), in agreement with the previous characterization (55). The pH dependence of steady state kinetic parameters was also determined with this mutant protein. The  $V/K_{\text{lactate}}$  pH profile for the flavin domain is indistinguishable from that of the wild-type enzyme (Figure 3A and Table 2). This was expected since catalytic steps involved in  $V/K_{\text{lactate}}$  should not require the heme domain.

The  $V_{\max}$  profile is still bell-shaped, but the  $pK_a$  values are shifted inwards compared to those of the wild-type enzyme (Figure 3B and Table 2).

Solvent isotope effects were determined with the flavin domain at pH 7.5 and pD 8. The data were fit best by assuming isotope effects on both the  $V/K_{\text{lactate}}$  and  $V_{\max}$  values (Table 3). The solvent isotope effect on the  $V_{\max}$  value is normal and smaller than that seen with the wild-type enzyme, consistent with most of the effect with the latter being due to steps in the oxidative half reaction. Surprisingly, there was a relatively large inverse effect on the  $V/K_{\text{lactate}}$  value. The solvent isotope effect on the limiting rate of reduction of the flavin by lactate was also determined directly by stopped-flow methods. As was the case with the wild-type enzyme, there was no significant solvent isotope effect on this parameter (Table 4). A large inverse effect was seen on the apparent second order rate constant for reduction; this parameter should be equivalent to the steady state  $V/K_{\text{lactate}}$ .

*Proton Inventories.* Proton inventories, in which kinetic parameters are determined in mixtures of  $H_2O$  and  $D_2O$ , can often provide insight into the origin of solvent isotope effects (58). Consequently, such analyses were done with wild-type flavocytochrome  $b_2$  and the isolated flavin domain. With both enzymes, the  $V_{\max}$  proton inventory shows a linear dependence of the solvent isotope effect on the fraction of  $D_2O$  (Figure 4A), although the small magnitude of the effect with the flavin domain precludes ruling out more complex behavior. The  $V/K_{\text{lactate}}$  proton inventories for both enzymes are also linear, although inverse (Figure 4B).

Table 3. Solvent Isotope Effects on the Oxidation of Lactate by Wild-type and Mutant Flavocytochromes b<sub>2</sub>\*

Enzyme	$D_2O(V/K_{\text{lactate}})$	$D_2OV$	Equation	$\chi^2$
Wild-type	0.90 ± 0.04	1.38 ± 0.07	2	236
		1.35 ± 0.03	3	265
		1.52 ± 0.34	4	3185
Flavin domain	0.44 ± 0.05	1.18 ± 0.05	2	1784
		0.93 ± 0.08	3	10333
		0.55 ± 0.06	4	3416
D282N	1.06 ± 0.14	0.97 ± 0.04	2	0.099
		0.98 ± 0.04	3	0.101
		1.00 ± 0.16	4	0.104

\* Conditions: 100 mM potassium phosphate, 1 mM EDTA, 1 or 3 mM ferricyanide, pH 7.5 or pD 8.0, 25°C.

Table 4. Rapid Reaction Kinetic Parameters for the Oxidation of Lactate by Wild-type and Mutant Flavocytochromes b<sub>2</sub>\*

Enzyme	$k_{\text{red}}$ $\text{s}^{-1}$	$k_{\text{red}}/K_{\text{lactate}}$ $\text{mM}^{-1} \text{s}^{-1}$	$K_{\text{lactate}}$ $\text{mM}$	$^D k_{\text{red}}$	$^{D_2O} k_{\text{red}}^a$	$^{D_2O} k_{\text{red}}/K_{\text{lactate}}^a$
Wild-type	$520 \pm 19$	$1100 \pm 78$	$0.47 \pm 0.05$	$5.4 \pm 0.4$	$1.0 \pm 0.10$	$1.1 \pm 0.2$
Flavin	$227 \pm 6$	$785 \pm 64$	$0.30 \pm 0.02$	$3.5 \pm 0.2$	$1.02 \pm 0.02$	$0.6 \pm 0.1$
Domain						

\*Conditions: 100 mM potassium phosphate, 1 mM EDTA, pH 7.5 or pD 8.0, 25°C.

<sup>a</sup>Calculated assuming a linear dependence of the isotope effect on the mole fraction of D<sub>2</sub>O.

*Viscosity Effects.* Small solvent isotope effects can arise because the viscosity of D<sub>2</sub>O is greater than that of H<sub>2</sub>O by 23% at 25 °C (63). This will decrease the rate of diffusion-limited steps such as substrate association and product dissociation. The effects of viscosity on the  $V_{\max}$  and  $V/K_{\text{lactate}}$  values of the wild-type enzyme and the flavin domain were determined with glycerol as the viscogen. The  $V_{\max}$  values for both enzymes decreased slightly as the viscosity of the medium increased. A plot of the normalized increase in the  $V_{\max}$  value as a function of the normalized increase in viscosity allows calculation of the extent to which diffusion limits the  $V_{\max}$  value. As shown in Figure 5A, the slope of the line for wild-type flavocytochrome b<sub>2</sub> is  $0.32 \pm 0.03$ , while that for the flavin domain  $0.15 \pm 0.02$ . Thus, a viscosity-sensitive step such as product release partially limits the  $V_{\max}$  value for both wild-type flavocytochrome b<sub>2</sub> and the isolated flavin domain.

The effects of viscosity on the  $V/K_{\text{lactate}}$  values are more complex with both enzymes. The  $V/K_{\text{lactate}}$  for the wild-type enzyme increases slightly with increasing concentrations of glycerol (Figure 5B). The flavin domain is activated up to twofold by moderate concentrations of glycerol (10-20%) (Figure 5B).

*Characterization of D282N Flavocytochrome b<sub>2</sub>.* The primary isotope effects on the  $V/K_{\text{lactate}}$  and  $V_{\max}$  values for wild-type flavocytochrome b<sub>2</sub> and the flavin domain could be decreased from the intrinsic values on the chemical step by contributions to these kinetic parameters from steps other than that in which the lactate CH bond is cleaved. One approach to minimizing this problem is to utilize substrates for which the chemistry is slowed, so that catalysis becomes more rate limiting. An alternative approach is to use modified enzymes in which the rate of the chemical step of interest has been decreased. In the active site of flavocytochrome b<sub>2</sub>, His373 is appropriately

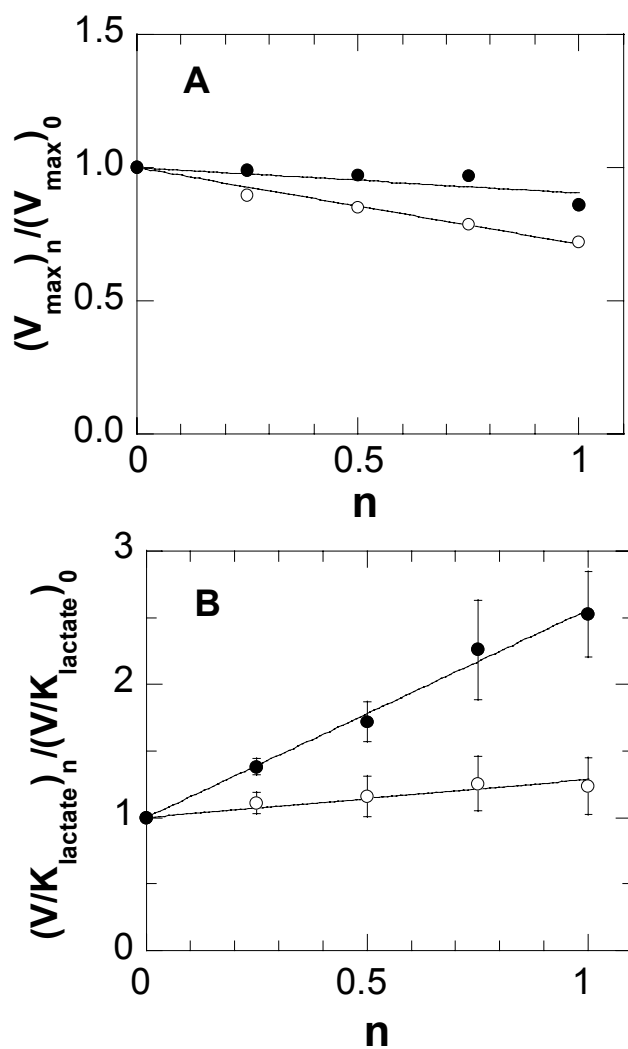


FIGURE 4. Proton inventories for wild-type flavocytochrome b<sub>2</sub> (O) and the flavin domain (●). The observed isotope effects on the  $V_{\max}$  (A) and  $V/K_{\text{lactate}}$  (B) values are plotted as a function of the mole fraction of D<sub>2</sub>O. The lines are fits of the data to equation 6.



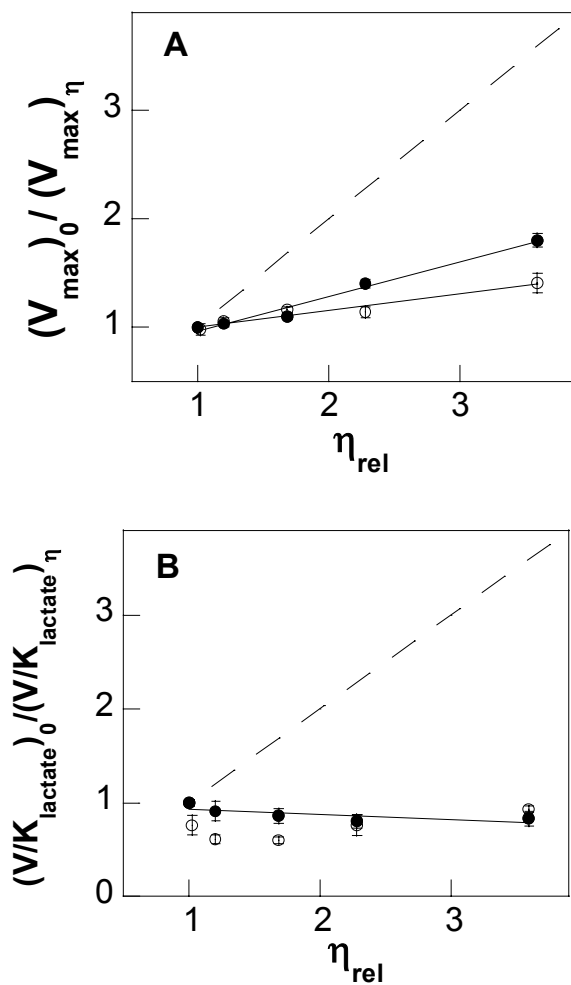


FIGURE 5. Effects of viscosity on the steady state kinetic parameters for wild-type flavocytochrome  $b_2$  (●) and the flavin domain (○). Panel A shows the effect on the  $V_{max}$  value and panel B the effect on the  $V/K_{lactate}$  value when the viscosity is increased with glycerol. The dashed line has a slope of one and indicates the expected results for a fully diffusion limited reaction.

placed to act as an active site base (48). However, mutagenesis of His373 to glutamine results in an enzyme with no detectable activity (17), ruling out this mutant for further analyses. The side chain of Asp282 is appropriately placed for an electrostatic interaction with the imidazole ring of His373 (14), and disruption of this interaction by mutagenesis of Asp282 has been reported to decrease both the  $V_{\max}$  and  $V/K_{\text{lactate}}$  values by 70-100 fold (18). Consequently, the D282N enzyme was selected as a protein in which the rate of the CH bond cleavage step was likely to be significantly decreased, simplifying interpretation of isotope effects.

In agreement with the previous work (18), we found that the D282N mutation decreases both the  $V_{\max}$  and the  $V/K_{\text{lactate}}$  values by about two orders of magnitude (Table 1). The primary isotope effects on both kinetic parameters also increase, consistent with cleavage of the lactate CH bond becoming rate-limiting. The  $V_{\max}$  pH profile for the D282N enzyme shows a bell-shaped curve with two ionizable groups (Figure 3B). The  $\text{pK}_a$  values are shifted upwards compared to the wild-type enzyme (Table 2). The  $V/K_{\text{lactate}}$  pH profile was not determined due to the low activity of this enzyme. It was not possible to follow the flavin reduction by rapid reaction methods, as noted previously, due to electron transfer between the redox centers in the different subunits reoxidizing the flavin more rapidly than it is reduced by lactate (18).

Solvent isotope effects on the  $V_{\max}$  and  $V/K_{\text{lactate}}$  values were determined with the D282N enzyme under the conditions used for the wild-type enzyme, pH 7.5 and pD 8.0. Neither isotope effect was significantly different from one, although the precision of the  $^{D20}V/K_{\text{lactate}}$  value was not as good due to the low activity of this enzyme (Table 3). Thus, with a mutant in which CH bond cleavage is rate limiting, there is no evidence for an exchangeable proton in flight in the transition state for cleavage of the lactate CH bond.

## DISCUSSION

Despite a great deal of mechanistic and structural analysis, the mechanism by which flavoproteins oxidize  $\alpha$ -hydroxy acids to the corresponding keto acids remains controversial. The majority of the data are readily accommodated by removal of the  $\alpha$ -hydrogen as a proton to form a carbanion (51). The various members of this family have been shown to varying extents to catalyze halide elimination from  $\beta$ -substituted substrates and to be inactivated by acetylenic substrate analogs. In addition, flavocytochrome  $b_2$  will catalyze transfer of tritium from 2- $^3\text{H}$ -lactate to 3-Br- and 3-Cl-pyruvate, forming both labeled pyruvate and the respective labeled lactate; this reaction has been interpreted in favor of partitioning of a carbanion intermediate (64). The homologous active sites of these enzymes contain a conserved histidine residue properly placed to abstract a proton from the substrate (11, 65). In all cases mutagenesis of this histidine decreases the rate of substrate oxidation by 3-5 orders of magnitude, consistent with a role as an active site base. However, neither the mechanistic nor the structural data provide unambiguous support for a carbanion mechanism. Halide elimination can be accommodated by nucleophilic displacement of the halide by a hydride from the N(5) position of the reduced flavin. If the exchange of this proton with solvent is hindered, the transhydrogenation reaction can be similarly rationalized. Inactivation by acetylenic compounds could involve attack of an active site nucleophile on the enzyme bound product. A structure is not available for a member of this family with substrate bound due to the chemical reactivity of such a complex. Instead, structures with bound keto acid product have been used to model the enzyme- substrate complex. The results of such modeling studies are ambiguous, in that the hydroxy acid can be modeled with the conserved histidine near either the  $\alpha$ -proton or the hydroxyl proton (24). The former orientation is consistent with formation of a carbanion, while the latter is more

suggestive of transfer of the  $\alpha$ -hydrogen as a hydride. The dramatic effects of mutagenesis of this residue are consistent with either role.

The experiments described here were designed to address the mechanism of lactate oxidation by flavocytochrome  $b_2$  by focusing on the relative timing of the cleavage of the lactate CH and OH bonds. Primary deuterium kinetic isotope effects provide a probe of the status of the CH bond, while solvent isotope effects can be used to probe the status of the OH bond. With wild-type flavocytochrome  $b_2$ , both the  $^D V$  and  $^D V / K_{\text{lactate}}$  values are about 3, establishing that cleavage of the lactate CH bond is at least partially rate limiting for both the reductive half-reaction and for overall turnover. The solvent isotope effect on the  $V_{\text{max}}$  value could arise from any of the first order steps in Scheme 12. The decrease in the  $^{D_2O} V$  value when 2- $^2\text{H}$ -lactate is the substrate is consistent with the solvent isotope effect arising from a separate step than the primary deuterium isotope effect. The rapid reaction kinetic parameters confirm this conclusion in a more direct fashion. The limiting rate of reduction of the flavin, which should be a direct measure of  $k_3$  in Scheme 12, shows a larger primary isotope effect of the magnitude expected for the intrinsic effect, but no solvent isotope effect. These data are consistent with no change in the OH bond order in the transition state for CH bond cleavage in the wild-type enzyme.

If the solvent isotope effect on the  $V_{\text{max}}$  value for the wild-type enzyme does not arise from lactate oxidation, it must be due to subsequent steps in the oxidative half reaction. The data are consistent with several steps contributing to the  $^{D_2O} V$  value. Part of the effect is due to the increased viscosity of  $\text{D}_2\text{O}$  compared to  $\text{H}_2\text{O}$ . The  $V_{\text{max}}$  value for the wild-type enzyme is about 30% limited by viscosity. This effect could be due to product release steps or conformational changes. The viscosity contribution to the

solvent isotope effect can be calculated to be about 1.09, with the remainder of the effect due to other steps in the oxidation of the reduced enzyme by ferricyanide.

The behavior of the isolated flavin domain confirms the conclusions drawn from the wild-type enzyme. In this case the reduced enzyme reacts directly with the oxidant, without first transferring the electrons to the heme  $b_2$ . Again there is no significant solvent isotope effect on the limiting rate of flavin reduction by lactate. Both the solvent isotope effect and the effect of viscosity on the  $V_{\max}$  value for the flavin domain are attenuated from the wild-type value. This is readily explained by the loss of contributions from steps in the oxidative half-reaction.

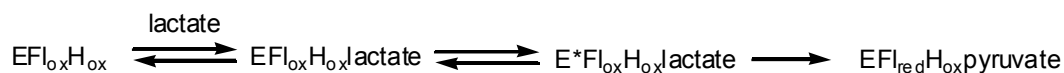
The analyses of both the wild-type enzyme and the flavin domain required the use of rapid reaction kinetics to measure the isotope effects on lactate oxidation without interference from other steps. An alternative approach is to utilize mutant proteins in which the rate of lactate oxidation is decreased sufficiently that CH bond cleavage is fully rate limiting for turnover. His373 is appropriately placed in the active site of flavocytochrome  $b_2$  to act as a base during catalysis (24). Mutagenesis of His373 decreases turnover by at least five orders of magnitude (17), eliminating mutation of this residue from consideration. However, mutagenesis of Asp282, which interacts with His373, has the desired effect, decreasing both the  $V_{\max}$  and the  $V/K_{\text{lactate}}$  values by two orders of magnitude and increasing the isotope effects on these parameters to the values seen in the reductive half reaction of the wild-type enzyme (16).

The properties of the D282N enzyme are consistent with a sufficient decrease in the rate of lactate CH bond cleavage that this step becomes fully rate limiting. There is no solvent isotope effect on the  $V_{\max}$  value for this enzyme, confirming the conclusion drawn from the wild-type enzyme and the flavin domain that there is no change in the bond order of the lactate OH bond in the transition state for CH bond cleavage. These

results confirm the critical role of His373 as an active site base and illustrate the utility of using appropriately mutated enzymes to make chemical steps in enzyme-catalyzed reactions manifest.

While the isotope effects on the  $V_{\max}$  values of the wild-type and mutant enzymes are consistent with the expectations of the carbanion mechanism shown in Scheme 13, the effects on the  $V/K_{\text{lactate}}$  values establish that the situation is more complex. With wild-type flavocytochrome  $b_2$  there is a small but significant inverse solvent isotope effect on the  $V/K_{\text{lactate}}$  value. This increases markedly in the flavin domain. In addition, the  $V/K_{\text{lactate}}$  value for the flavin domain shows an unusual increase in activity in the presence of low concentrations of glycerol. A reasonable explanation for these results is that there is an internal equilibrium after formation of the enzyme-lactate complex but before CH bond cleavage, as shown in Scheme 14. This equilibrium is shifted by the presence of either glycerol or  $D_2O$ . Both of these solvents affect the stability of proteins favorably, and in both cases the effect has been attributed to changes in solvation (66, 67). Thus, it is reasonable that they could have similar effects on conformational equilibria. Other possible explanations for inverse solvent isotope effects are the presence of a thiol or metal-bound water; both of these possibilities can be ruled out for flavocytochrome  $b_2$ . The NAD malic enzyme from *Ascaris suum* provides a previous example in which an inverse solvent isotope effect could be reproduced by the addition of glycerol; this result was similarly attributed to an effect on enzyme conformation (68). Indeed, the results described here for flavocytochrome  $b_2$  reinforce the recommendation of Karsten et al. (68) that an evaluation of viscosity effects is prudent for all solvent isotope effects studies.

## Scheme 14



The solvent inventories for the  $V/K_{\text{lactate}}$  values are consistent with a single exchangeable proton being responsible for the inverse solvent isotope effect. If the inverse effect is due to a change in a conformational equilibrium, an effect due to multiple protons is often expected (63). The precision of the  $V/K_{\text{lactate}}$  values is such that a small degree of curvature can not be ruled out. Moreover, the possibility must be considered that the apparent linearity arises from compensating isotope effects, with an inverse effect on enzyme conformation being opposed by a normal kinetic effect on OH bond cleavage. A previous study of the *Bacillus* lactate dehydrogenase provides a useful comparison with the present results with flavocytochrome  $b_2$ , since both enzymes catalyze the interconversion of lactate and pyruvate. The pyridine nucleotide-dependent lactate dehydrogenase would be expected to utilize a hydride transfer mechanism. With the *Bacillus* enzyme, in the direction of pyruvate reduction the primary deuterium isotope effect on the  $V/K_{\text{NADH}}$  value is 5.5, while the solvent isotope effect on the same kinetic parameter is unity or slightly inverse (69). Xie et al. concluded that the simplest explanation for these results is that OH bond cleavage and hydride transfer do not occur in the same step. However, they pointed out that the data could not rule out a normal isotope effect from OH bond cleavage which is opposed by a multi-proton effect arising from an enzyme conformational change. The same possibility must be considered in the case of flavocytochrome  $b_2$ .

In summary, the data presented here with flavocytochrome  $b_2$  support the conclusion that there is no solvent isotope effect on the step in catalysis in which the

lactate CH bond is cleaved. This is based on both the results of rapid kinetic analyses and the results with a mutant in which carbon-hydrogen bond cleavage is fully rate-limiting. A reasonable conclusion from these data is that the hydroxyl proton of lactate is not in flight in the transition state for cleavage of the lactate carbon-hydrogen bond. This is fully consistent with the predictions of a carbanion mechanism for this enzyme. However, the data cannot rule out an alternative mechanism in which the hydroxyl proton is removed in an equilibrium coupled to an enzyme conformational change which occurs prior to cleavage of the carbon-hydrogen bond by hydride transfer.



## CHAPTER III

### ROLE OF TYR254 IN THE REACTION CATALYZED BY FLAVOCYTOCHROME B<sub>2</sub>

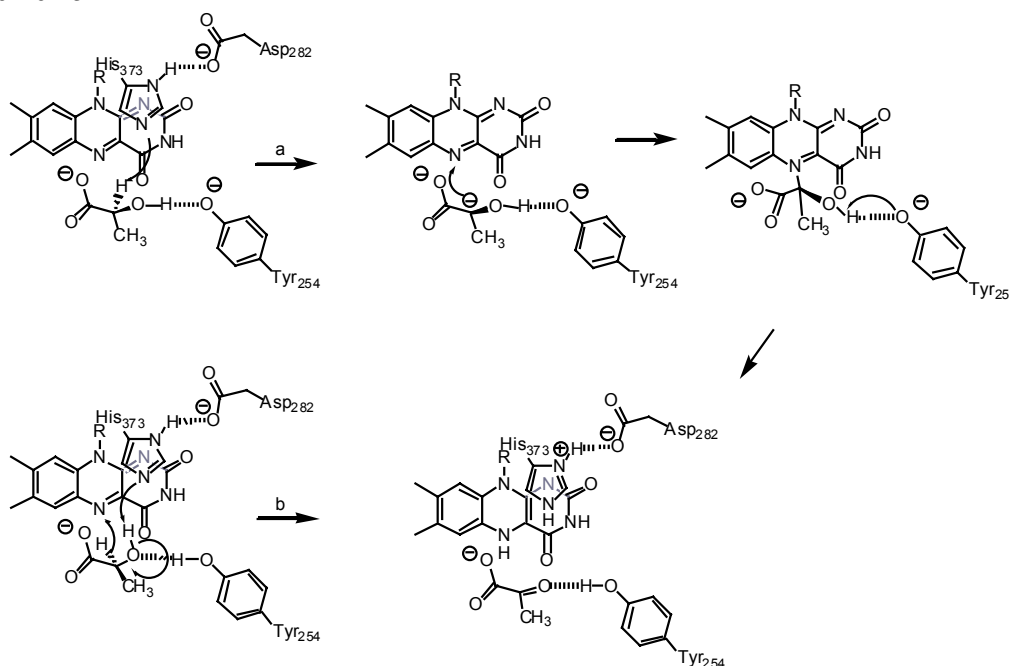
#### INTRODUCTION

The enzyme flavocytochrome b<sub>2</sub> from the yeast *Saccharomyces cerevisiae* catalyzes the oxidation of L-lactate to pyruvate. The enzyme is composed of four identical subunits each containing an FMN and a heme b<sub>2</sub> cofactor (47). The catalytic cycle begins with the oxidation of lactate and the transfer of a hydride equivalent to the FMN cofactor. After FMN reduction, a series of single electron transfer steps takes place between the flavin and the heme, until the electrons reach the final acceptor, cytochrome *c in vivo* (12). The structure of the wild-type native enzyme complexed with pyruvate has been solved at a resolution of 2.4 Å (14).

The chemical mechanism of CH bond cleavage by Flb<sub>2</sub> has been the subject of intense investigation with conflicting results. There are several reports that support a carbanion mechanism for proton abstraction (45, 48), while others support a hydride transfer mechanism (9, 70). Since there is no crystal structure with lactate in the active site, the conformation of bound substrate has been modeled by replacing pyruvate with lactate (24). In the active site, the lactate hydroxyl can be positioned to hydrogen bond to either His373 or Tyr254 (Scheme 15). If the lactate hydroxyl is hydrogen bonding with Tyr254, the  $\alpha$  hydrogen points towards His373, which would abstract the proton to form the carbanion intermediate; Tyr254 is proposed to facilitate electron transfer by deprotonating the substrate hydroxyl (Scheme 15 a) (24). In the alternative position the hydroxyl hydrogen points towards His373. This residue would abstract the hydroxyl

proton as the hydride is transferred to the FMN in a concerted mechanism (Scheme 15 b) (13, 24).

Scheme 15



Scheme 15 presents the proposed mechanisms for lactate dehydrogenation by flavocytochrome  $b_2$ : a, carbanion mechanism, in which His373 abstracts the alpha proton from lactate to form a carbanion and Tyr254 hydrogen bonds with the OH group; b, concerted hydride transfer mechanism in which His 373 abstracts the hydroxyl proton as the alpha proton is transferred as a hydride directly to the FMN.

In the two chemical mechanisms for Flb<sub>2</sub>, Tyr254 would play a role in binding to the hydroxyl proton in the Michaelis complex (Scheme 15). The Y254F enzyme has been constructed and partially characterized and the crystal structure has been solved (24, 71, 72). The phenyl ring of the Y254F enzyme is in the same position as the phenol group in the wild-type enzyme, while pyruvate is found in a slightly different conformation. The resolution was only at 2.9 Å, making analysis for mechanistic

interpretation speculative. The mutant enzyme shows a decrease in the  $V_{\max}$  and  $V/K_{\text{lactate}}$  values of around 50 fold, and an increase in the  $^D V_{\max}$  and  $^D(V/K_{\text{lactate}})$  values to 5 compared to 3 in the wild type enzyme. Interestingly, there is no effect on the binding of lactate or the binding of several competitive inhibitors. Based on the observed effects on catalysis it was concluded that Tyr254 plays a role in transition state stabilization (24). These reports failed to explain the discrepancy between the proposed role in binding and the lack of effect on the  $K_d$  for lactate in the mutant enzyme. More importantly, the specific role in transition state stabilization attributed to Tyr254 is not described. In this work, an alternative mechanism is described that is consistent with the experimental data.

## EXPERIMENTAL PROCEDURES

*Materials.* Sodium L-[2- $^2\text{H}$ ]-lactate (98%) and deuterium oxide (99.9%) were purchased from Cambridge Isotope Co., Andover, MA. Lithium L-Lactate and D,L-lactate were from Sigma Chemical Corporation (St. Louis, MO). Restriction endonucleases were from New England Biolabs Inc. *Pfu* DNA polymerase was obtained from Stratagene USA. Hydroxyapatite was from BioRad laboratories (Hercules, CA). All other reagents were of the highest purity commercially available.

*DNA Manipulation.* The mutagenesis of Tyr254 to phenylalanine was performed following the QuikChange protocol (Stratagene). The sense primer used was 5'CAATGGTACCAACTATTTIGTTAACTCTG'3. The primers were purchased from the Gene Technology Laboratory at Texas A&M. Plasmids were purified using kits from Qiagen Inc. The coding region was sequenced to ensure that no unwanted mutations were incorporated during the polymerase chain reaction.

*Cell Growth and Enzyme Purification.* Cells were grown and enzymes were purified following published protocols (70).

*Enzyme Assays.* Initial rate assays were performed in 100 mM potassium phosphate, 1 mM EDTA, 1 mM potassium ferricyanide, pH 7.5, 25 °C, with varied concentrations of L-lactate or L-[2-<sup>2</sup>H]-lactate, by following the decrease in absorbance at 420 nm and using an  $\epsilon_{420}$  value for ferricyanide of 1.04 mM<sup>-1</sup>cm<sup>-1</sup>. Concentrations of lactate were determined by end point assays with wild type flavocytochrome b<sub>2</sub>.

For pH studies, the buffer was 50 mM Bis-Tris at pH 5.5-7.0, 150 mM HEPES at pH 7.0-8.5, and 50 mM ethanolamine at pH 8.5-10.0. All assays were done in the presence of 1 mM potassium ferricyanide at 25 °C. Solvent isotope effects were done in the same buffers made up using 99.9% deuterium oxide and adjusting the pD with DCl and NaOD as needed, adding 0.4 to the value indicated by the pH meter (58). Steady state kinetic solvent isotope effects were determined in 100 mM phosphate, 1 mM EDTA, pH 7.5 or pD 8.0, with 1 mM potassium ferricyanide. For rapid reaction analyses, heme reduction was monitored at 557 nm on an Applied Photophysics SX.18MV stopped-flow spectrophotometer. Enzyme in 100 mM potassium phosphate, 1 mM EDTA, pH 7.5, was mixed with an equal volume of the same buffer containing varied concentrations of lactate at 25 °C.

*Data Analysis.* The data was analyzed using the programs Kaleidagraph (Adelbeck Software, Reading, PA), KinetAsyst (IntelliKinetics, State College, PA) or Igor (Wavemetrics, Lake Oswego, OR). Initial rate data were fit to the Michaelis-Menten equation. Primary deuterium and solvent isotope effects were calculated using equation 2, which describes separate isotope effects for the  $V_{\max}$  and  $V/K_{\text{lactate}}$  values.  $F_i$  is the fraction of heavy atom substitution in the substrate,  $E_V$  is the isotope effect on the  $V_{\max}$  value minus 1, and  $E_{VK}$  is the isotope effect on the  $V/K_{\text{lactate}}$  value minus 1. The pH

profiles were obtained by fitting the  $V_{\max}$  and  $V/K_{\text{lactate}}$  values obtained at each pH to equation 5; here,  $K_1$  and  $K_2$  are the dissociation constants of the ionizable groups, and  $C$  is the pH independent value of the specific kinetic parameter. Stopped-flow traces were fit to equation 8 which describes a biphasic exponential decay;  $\lambda_1$  and  $\lambda_2$  are the first order rate constants for each phase;  $A_1$  and  $A_2$  are the absorbance of each species at time  $t$  and  $A_{\infty}$  is the final absorbance. The rate of the rapid phase, at different concentration of tryptophan was analyzed using equation 8, here  $k_{\text{red}}$  is the maximum rate of flavin reduction and  $K_d$  is the apparent dissociation constant for the substrate.

$$v = \frac{VA}{K_m(1 + F_i(E_{vk})) + A(1 + F_i(E_v))} \quad (2)$$

$$\log Y = \log \frac{C}{1 + \frac{H}{K_1} + \frac{K_2}{H}} \quad (5)$$

$$A = A_{\infty} + A_1 e^{-\lambda_1 t} + A_2 e^{-\lambda_2 t} \quad (9)$$

$$k_{\text{obs}} = \frac{k_{\text{red}}A}{K_d + A} \quad (8)$$

## RESULTS

*Steady State Kinetic Parameters.* The effect of removal of the hydroxyl group of Tyr254 was measured under steady state conditions with ferricyanide as the final electron acceptor. The  $V_{\max}$  value decreased 40 fold while the  $V/K_{\text{lactate}}$  value decreased close to 60 fold compared to wild-type values (Table 5). The  $K_m$  for lactate remains unchanged for the Y254F enzyme. These values are consistent with previously reported data (24, 72). The changes in the steady state kinetic parameters clearly indicate that the hydroxyl group of Tyr254 is important for enzymatic activity. For the wild-type enzyme

the  $^D V_{\max}$  and  $^D(V/K_{\text{lactate}})$  values are close to 3, consistent with CH cleavage being partially rate limiting. Removal of the hydroxyl group at position 254 makes this step more rate limiting as indicated by the increase in the  $^D V_{\max}$  and  $^D(V/K_{\text{lactate}})$  values to around 5 (Table 6). These values are close to the intrinsic isotope effect value of 5.4 for the wild-type enzyme (70).

*Solvent Isotope Effects.* In the wild-type enzyme, the  $^{D_2O}(V/K_{\text{lactate}})$  value is slightly inverse with a value of 0.90 while the  $^{D_2O}V_{\max}$  value is 1.38 (70). For the Y254F enzyme the  $^{D_2O}V_{\max}$  increases and the  $^{D_2O}(V/K_{\text{lactate}})$  becomes slightly normal (Table 6). These results indicate that OH bond cleavage is not rate limiting on  $V/K_{\text{lactate}}$  while a solvent sensitive step is partially rate limiting on  $V_{\max}$ . The solvent isotope effect on the wild-type enzyme was previously determined to be on a step after CH bond cleavage (70). Solvent isotope effects were also measured using L-2- $^2\text{H}$ -lactate. For the wild-type enzyme the  $^{D_2O}V_{\max}$  decreases with the deuterated substrate. For the Y245F enzyme the larger  $^{D_2O}V_{\max}$  value also decreases with deuterated substrate

*pH Profiles.* The effects of pH on the  $V_{\max}$  and  $V/K_{\text{lactate}}$  values for the Y254F enzyme were determined. The  $V/K_{\text{lactate}}$  pH profile for the Y254F enzyme is bell-shaped consistent with two ionizable groups in the free enzyme (Figure 6). One group needs to be protonated for activity with a  $\text{pK}_a$  value of 8.9, and another group needs to be unprotonated for activity with a  $\text{pK}_a$  value of 5.2. The  $V_{\max}$  pH rate profile for this mutant enzyme is also bell-shaped, consistent with two ionizable groups being important for catalysis; one group with a  $\text{pK}_a$  value of 10 must be protonated for activity, and the other group with a  $\text{pK}_a$  value of 5.2 needs to be unprotonated. The  $\text{pK}_a$  values are very similar to the values for the wild-type enzyme (Table 7 and Figure 6) (70, 73).

Table 5. Steady State Kinetic Parameters and Primary Isotope Effects on the Oxidation of Lactate by Wild-type and Y254F Flavocytochromes b<sub>2</sub>\*

Enzyme	V, s <sup>-1</sup>	V/ K <sub>lactate</sub> mM <sup>-1</sup> s <sup>-1</sup>	K <sub>lactate</sub> mM
wild-type <sup>a</sup>	372 ± 12	2300 ± 215	0.16 ± 0.02
Y254F	11 ± 0.4	44 ± 5	0.25 ± 0.03

\*Conditions: 100 mM potassium phosphate, 1 mM EDTA, and 1 mM ferricyanide pH

7.5, 25°C.

<sup>a</sup> From reference (70).

Table 6. Primary and Solvent Kinetic Isotope Effects on the Oxidation of Lactate by Wild-type and Y254F Mutant Flavocytochrome b<sub>2</sub>\*

Enzyme	wild-type <sup>a</sup>	Y254F
<sup>D</sup> V	2.9 ± 0.1	5.6 ± 0.3
<sup>D</sup> (V/K)	3.0 ± 0.3	4.2 ± 0.6
<sup>D</sup> <sub>2</sub> O V	1.38 ± 0.07	1.70 ± 0.07
<sup>D</sup> <sub>2</sub> O (V/K)	0.90 ± 0.04	1.2 ± 0.1
<sup>D</sup> <sub>2</sub> O V <sub>D</sub>	1.1 ± 0.03	1.38 ± 0.06
<sup>D</sup> <sub>2</sub> O (V/K) <sub>D</sub>	0.87 ± 0.1	1.33 ± 0.3

\*Conditions: 100 mM potassium phosphate, 1 mM EDTA, and 1 mM ferricyanide, pH 7.5 or pD 8.0, 25°C.

<sup>a</sup> From reference (70).



Table 7. pK<sub>a</sub> Values for Wild-type and Y254F Enzymes\*

Enzyme	Parameter	pK <sub>1</sub>	pK <sub>2</sub>
wild-type <sup>a</sup>	V <sub>max</sub>	5.6 ± 0.1	9.4 ± 0.1
	V/K <sub>lactate</sub>	5.8 ± 0.1	8.9 ± 0.1
Y254F	V <sub>max</sub>	5.2 ± 0.2	10.0 ± 0.1
	V/K <sub>lactate</sub>	5.2 ± 0.2	8.9 ± 0.1

\*Conditions: 100 mM potassium phosphate, 1 mM EDTA, and 1 mM ferricyanide, pH 7.5, 25°C.

<sup>a</sup> From reference (70).

Table 8. Rapid Reaction Kinetic Parameters for the Oxidation of Lactate by Wild-type and Y254F Flavocytochromes  $b_2$ \*

Enzyme	$k_{\text{red}}, \text{s}^{-1}$	$k_{\text{red}}/K_{\text{lactate}}, \text{mM}^{-1} \text{s}^{-1}$	$K_{\text{lactate}}, \text{mM}$
wild-type	$226 \pm 11$	$1090 \pm 200$	$0.21 \pm 0.04$
Y254F	$6.6 \pm 0.4$	$37 \pm 5$	$0.18 \pm 0.03$

\*Conditions: 100 mM potassium phosphate, 1 mM EDTA, pH 7.5, 25°C.

*Viscosity Effects.* Since the solution viscosity is higher in D<sub>2</sub>O than in H<sub>2</sub>O, the effects of viscosity on the kinetic parameters were determined. For the wild-type enzyme in solutions of higher viscosity there is an increase in the  $V/K_{\text{lactate}}$  value. For the Y254F enzyme, the  $V/K_{\text{lactate}}$  value also increases as the solution viscosity increases. Unlike wild-type Flb<sub>2</sub>, for Y254F enzyme the  $V_{\text{max}}$  value is not sensitive to the changes in solution viscosity (Figure 7).

*Rapid Reaction Kinetics.* Measurement of the rate of FMN reduction for the Y254F enzyme was not possible since the mutation decreases the rate of FMN reduction such that this step is in competition with reoxidation by a slow electron transfer between prosthetic groups in the tetrameric enzyme (data not shown)(56). Instead the rate of heme reduction was measured in the stopped-flow spectrophotometer. For both the wild-type and Y254F enzymes the heme reduction follow a biphasic increase in absorbance at 557 nm, with slow and fast phases where only the fast phase is substrate dependent (Figure 8). The  $k_{\text{red}}$  and the  $k_{\text{red}}/K_{\text{d}}$  values are very close to the  $V_{\text{max}}$  and  $V/K_{\text{lac}}$  values (Table 8). The values for the wild-type enzyme are consisted with previously reported values (45).

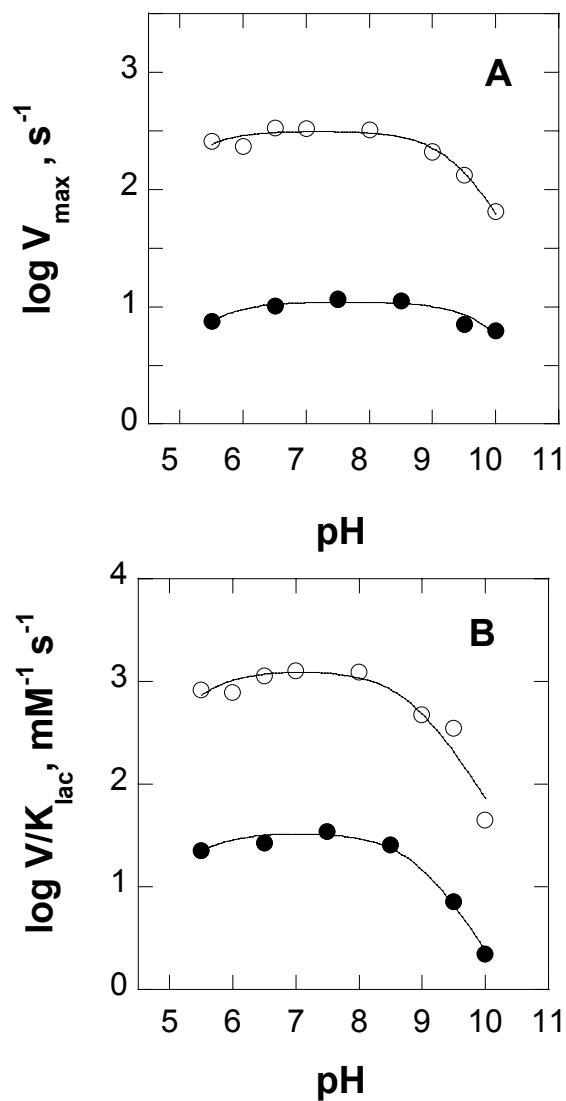


FIGURE 6. pH dependence of wild-type and Y254F flavocytochromes b<sub>2</sub>. Initial rates were determined with ferricyanide as the electron acceptor as described in Experimental Procedures. Panel A shows the  $V_{\max}$  profile and panel B the  $V/K_{\text{lactate}}$  profile for the wild type (O) and for the Y254F enzyme (●) enzymes. The lines are fits of the data to equation 5. Wild-type values are from reference (70).

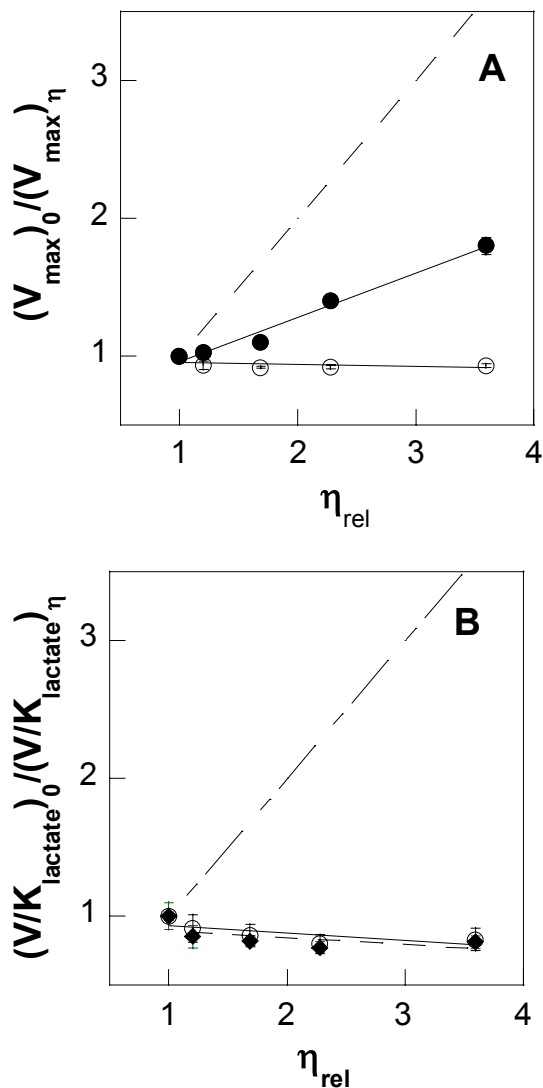


FIGURE 7. Effects of viscosity on the steady state kinetic parameters for wild-type flavocytochrome  $b_2$  (●) and the Y254F enzyme (○). Panel A shows the effect on the  $V_{max}$  value and panel B the effect on the  $V/K_{lactate}$  value when the viscosity is increased with glycerol. The dashed line has a slope of one and indicates the expected results for a fully diffusion limited reaction. Wild-type values are from reference (70).

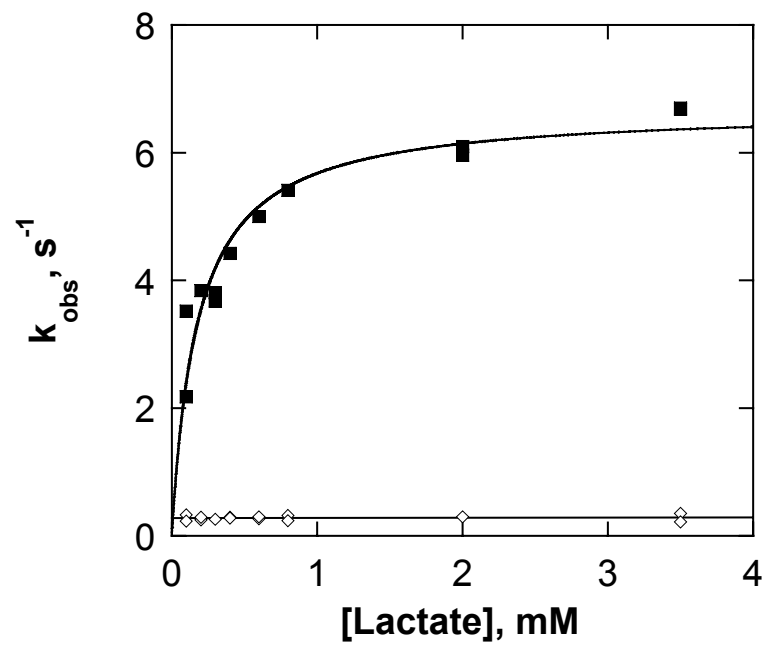


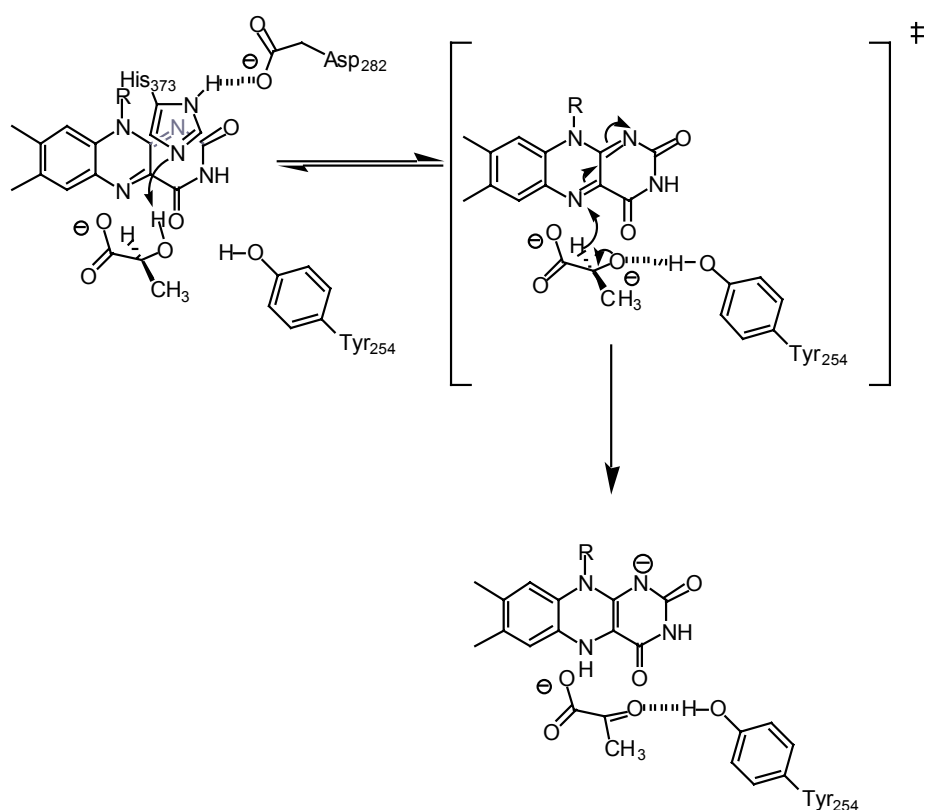
FIGURE 8. Rate of heme reduction for the Y254F enzyme as a function of lactate concentration. The rate of the fast phase is shown in solid squares and the rate of the slow phase in open diamonds.

## DISCUSSION

The chemical mechanism of Flb<sub>2</sub> has been a subject of investigation by several research groups (12, 46, 70). The mechanism of Flb<sub>2</sub> has been assumed to be similar to the mechanism of the flavoenzyme D-amino acid oxidase (DAAO), a flavoenzyme that oxidizes D-amino acids to the corresponding keto acids (2, 74). CH bond cleavage in DAAO was thought to occur via a carbanion mechanism (4, 75) until the three dimensional structure of the pig kidney enzyme was solved. The active site of DAAO does not contain an amino acid residue to act as base to abstract the proton at the  $\alpha$ -position to form the proposed carbanion intermediate (9, 76). The discrepancy between the experimental and structural data has motivated the reevaluation of the mechanism of DAAO and related enzymes. Recent reports have provided evidence that is consistent with a mechanism involving the direct hydride transfer of the  $\alpha$ -H to the flavin in DAAO (10). The mechanism of Flb<sub>2</sub> has been probed previously with primary and solvent deuterium isotope effects using the wild-type and mutant enzymes (70). The results were inconsistent with a concerted hydride transfer mechanism; instead a stepwise hydride transfer mechanism was proposed, in which abstraction of the hydroxyl proton of lactate by His373 is coupled to a conformational change prior to hydride transfer to the flavin (Scheme 16). A carbanion mechanism in which Tyr254 acts as a base requires this residue to be ionized for catalysis (Scheme 15a). Comparison of the  $V_{\max}$  and  $V/K_{\text{lactate}}$  pH rate profiles for wild-type and Y254F clearly show that Tyr254 is not the residue responsible for the observed  $pK_a$ s (Table 5 and Figure 6). This suggest that for Tyr254 to be ionized in the wild-type enzyme its  $pK_a$  value must be less than 5. If instead Tyr254 is in the neutral form its  $pK_a$  value must be greater than 10, a much smaller perturbation. For abstraction of the OH proton a base will be needed to be

deprotonated Tyr254. Although there are no residues in close proximity to Tyr254 to act as base, a water molecule might play this role.

Scheme 16



Scheme 16 presents the proposed stepwise hydride transfer mechanism of lactate oxidation in flavocytochrome  $b_2$ . The active site His<sub>373</sub> abstracts the proton from the hydroxyl group of lactate forming the alkoxide intermediate which is stabilized by hydrogen bonding with Tyr<sub>254</sub>.



The inverse  $^{D_2O}(V/K_{\text{lactate}})$  value for the wild-type has been proposed to arise from an isomerization step that is favored in deuterium oxide and is coupled to OH bond cleavage (Scheme 16) (70). In the mutant enzyme the precision for the  $^{D_2O}(V/K_{\text{lactate}})$  value is too low to permit confident analyses. The  $^{D_2O}V_{\text{max}}$  value in the wild-type arises from a step after flavin reduction, possibly in the electron transfer step (70). The  $^{D_2O}V_{\text{max}}$  value for the wild-type enzyme decreases when [2- $^2\text{H}$ ]-lactate is used as substrate. Similarly, for the Y254F enzyme the  $^{D_2O}V_{\text{max}}$  value decreases with [2- $^2\text{H}$ ]-lactate (Table 6). In both cases the results are consistent with the solvent sensitive step occurring on a different step than CH bond cleavage. In addition, the  $k_{\text{red}}$  value for the Y413F enzyme is close to the  $V_{\text{max}}$  value, indicating that CH bond cleavage limits the catalytic cycle in the mutant enzyme (Table 8). It follows then that the  $^{D_2O}V_{\text{max}}$  value arises from a step involving electron transfer to the final electron acceptor.

The  $V/K_{\text{lactate}}$  values for the wild-type and Y254F enzyme show a slight increase as the viscosity increases (Figure 7B)(70). For the wild-type enzyme this increase in the  $V/K_{\text{lactate}}$  value was proposed to arise from an isomerization step which is sensitive to solution viscosity. Since in the Y254F enzyme a similar increase in the  $V/K_{\text{lactate}}$  values is observed it is reasonable to conclude that this step has not been affected in the mutant enzyme. In the wild-type enzyme a solvent sensitive step such as product release partially limits the  $V_{\text{max}}$  value. In the mutant enzyme, since CH cleavage is more rate limiting the  $V_{\text{max}}$  value is not sensitive to solution viscosity (Figure 7A).

The stepwise hydride mechanism of Scheme 16 (70) provides a scenario for the role of Tyr254 that is consistent with all of the experimental data. The decrease in the values of the steady state kinetic parameters and the increase in the deuterium isotope effects are consistent with Tyr254 playing a role in transition state stabilization, specifically in stabilization of the alkoxide prior to hydride transfer to the flavin. The

lack of effect on the  $K_{\text{lactate}}$  value, which has been determined to be equal to the  $K_d$  (16), is consistent with this residue not interacting with lactate in the Michaelis complex (Tables 5 and 8). This is also consistent the lack of increase in the  $K_i$  values for various competitive inhibitors with the Y254F and Y254L enzymes (72).

## CHAPTER IV

### CHARACTERIZATION OF THIOLACTATE AS SUBSTRATE FOR FLAVOCYTOCHROME B<sub>2</sub>

#### INTRODUCTION

The availability of mutant enzymes where the chemical step is rate limiting has proven to be very useful in the study of enzyme mechanisms. Similarly, the use of isotopic labeling of substrates can provide valuable information about mechanisms of enzyme catalysis (77, 78). Substrates where chemistry is rate limiting or with slightly different chemical properties can also be employed to understand enzyme mechanisms in great detail.

The mechanism of oxidation of lactate to pyruvate by flavocytochrome b<sub>2</sub> (Flb<sub>2</sub>) involves cleavage of CH and OH bonds. The characterization of a substrate for Flb<sub>2</sub> with different chemical properties either in the CH or OH bond can provide information about the mechanism of this enzyme. In lactate the OH group can be replaced by SH and the chemical properties of the SH can be useful in determining the mechanism of the reaction catalyzed by Flb<sub>2</sub>. The partial characterization of thiolactate as substrate for Flb<sub>2</sub> is presented in this chapter.

#### EXPERIMENTAL PROCEDURES

*Materials.* Thiolactate (98%) was purchased from Aldrich Chemical Co. (Milwaukee, WI). Lithium L-Lactate and D,L-lactate were from Sigma (St. Louis, MO). Hydroxyapatite was from Bio-Rad Laboratories (Hercules, CA).

*Enzyme Preparation and Data Analysis.* The expression and purification of wild-type and D282N enzymes and data analysis were done as described in Chapter II.

*DNA Manipulation.* The plasmid containing the gene for the D282N enzyme was a generous gift from Dr. Florence Lerderer. Site directed mutagenesis of His373 to glutamine was performed following the procedure the QuikChange protocol (Stratagene) with the primers 5'-GGTGGTTCTATCCAATCAAGGTGGTAGACAATTAGA- 3' and 5'- TCTAATTGTCTACCACCTTGATTGGATAGAACCACC -3'. The H373Q mutation was introduced into the genes for the wild-type enzyme and the flavin domain enzyme (70).

*Assays.* Steady state kinetic assays were performed using cytochrome c as the final electron acceptor. The  $K_m$  value for cytochrome c was determined by monitoring the increase in the absorbance at 550 nm in an assay containing 100 mM potassium phosphate, 1mM EDTA, and either 5 mM L-lactate or 5 mM thiolactate at pH 7.5 and 25 °C. A path length of 0.4 cm was used, and an  $\epsilon_{550}$  value of  $20.5 \text{ mM}^{-1}\text{cm}^{-1}$  for cytochrome c (16). Steady state assays with varied concentrations of lactate and thiolactate were performed in 100 mM potassium phosphate, 1 mM EDTA, and 400  $\mu\text{M}$  cytochrome c at pH 7.5 and 25 °C. Again, a path length of 0.4 cm was used, and the reaction was monitored following the increase in absorbance of cytochrome c at 550 nm. Assays were initiated by the addition of 10  $\mu\text{L}$  of enzyme to a final concentration of 0.0135  $\mu\text{M}$  for the wild-type enzyme and 0.31  $\mu\text{M}$  for the D282N enzyme in a final volume of 1 ml. Initial rates were analyzed using the Michaelis-Menten equation.

*Rapid Reaction Kinetics.* Rapid reaction kinetic measurements were performed with a Applied Photophysics SX.18MV stopped-flow spectrophotometer. The enzyme in 100 mM potassium phosphate and 1 mM EDTA at pH 7.5 was mixed with an equal volume of the same buffer containing various amounts of thiolactate or lactate at 25 °C.

The flavin reduction was followed at 438 nm and heme reduction at 550 nm. Analysis of the stopped-flow traces and steady was done as indicated in chapter I.

## RESULTS

*Wild-Type Flavocytochrome b<sub>2</sub>*. The first challenge in this research was to determine an electron acceptor which could be used for assays of both lactate and thiolactate. Because ferricyanide has been proven to be an effective electron acceptor in steady-state analysis with lactate, ferricyanide was tried first as an electron acceptor. However, thiolactate was found to reduce ferricyanide in the absence of enzyme; therefore, another electron acceptor had to be found. Dichloroindophenol (DCIP) was also tried, and again the thiolactate reduced the DCIP in the absence of the enzyme. Finally, cytochrome *c* was tried as an electron acceptor and was found to have minimal background activity with thiolactate alone. Therefore it was chosen as the electron acceptor in the kinetic assays. The  $K_M$  value for cytochrome *c* was determined for the wild-type enzyme at 5 mM lactate or thiolactate. The  $K_{\text{cytochrome } c}$  value with thiolactate is about one third that with lactate (Table 9).

With cytochrome *c* as electron acceptor the steady state kinetic parameters of both substrates were determined. The  $V_{\text{max}}$  and  $V/K$  values are shown in Table 10. Comparing the values of thiolactate to those of lactate suggest that thiolactate is a reasonably good substrate for the wild-type enzyme.

As an alternative approach, a stopped-flow spectrophotometer was used to measure the rates of reduction of the prosthetic groups in the wild-type enzyme. At low concentrations of thiolactate after reduction of the flavin or heme, reoxidation of the cofactor was observed. This was diminished at higher concentration of thiolactate. In order to obtain the rate of reduction only the first 2 s of the traces were analyzed (the fast phase is over in less than one second). The rate of flavin reduction was monitored at 438 nm with both lactate and thiolactate in the absence of cytochrome c. The  $k_{\text{red}}$  and  $k_{\text{red}}/K_d$  values for thiolactate indicate that it is a good substrate for wild-type Flb<sub>2</sub> (Table 11). The rate of heme reduction was monitored at 550 nm. The results of this experiment can be found in Table 12. Again, comparing the values found for thiolactate to those for lactate further support the conclusion of thiolactate being a good substrate for Flb<sub>2</sub>.

*D282N Flavocytochrome b<sub>2</sub>*. The results from the steady state kinetic assays with the D282N enzyme are shown in Table 10. In agreement with values found in previous work, the  $V_{\text{max}}$  and  $V/K$  values for lactate are reduced significantly compared to the wild-type values (17, 70). The  $V_{\text{max}}$  and  $V/K$  values with thiolactate as a substrate are also reduced as compared to wild-type values. In addition, the rate of heme reduction was measured by stopped flow with 5 mM lactate or thiolactate. The  $k_{\text{red}}$  value for lactate is close to that for thiolactate.

Table 9. Wild-type Flavocytochrome  $b_2$  Steady-State Kinetic Parameters for Cytochrome  $c$

Substrate	$V, s^{-1}$	$V/K_{\text{cytochrome } c}, \mu\text{M}^{-1}\text{s}^{-1}$	$K_{\text{cytochrome } c}, \mu\text{M}$
Lactate	$163 \pm 16$	$0.79 \pm 0.09$	$207 \pm 45$
Thiolactate	$30 \pm 2.0$	$0.39 \pm 0.05$	$78 \pm 15$

Conditions: 100 mM potassium phosphate, 1 mM EDTA, 5 mM lactate or thiolactate, concentration of cytochrome  $c$  varied from 30  $\mu\text{M}$  to 400  $\mu\text{M}$  at pH 7.5 and 25 °C.

Table 10. Steady-State Kinetic Parameters for the Oxidation of Lactate and Thiolactate by Wild-type and the Mutant D282N Flavocytochromes b<sub>2</sub>

enzyme	Lactate			Thiolactate		
	V (s <sup>-1</sup> )	V/ K <sub>lactate</sub> , mM <sup>-1</sup> s <sup>-1</sup>	K <sub>lactate</sub> , mM	V, s <sup>-1</sup>	V/ K <sub>thiolactate</sub> , mM <sup>-1</sup> s <sup>-1</sup>	K <sub>thiolactate</sub> , mM
wild-type	81 ± 5	258 ± 46	0.31 ± 0.07	32 ± 4	39 ± 11	0.90 ± 0.04
D282N	3.1 ± 0.2	8.8 ± 1.5	0.35 ± 0.07	1.3 ± 0.1	9 ± 2	0.15 ± 0.05

Conditions: 100 mM potassium phosphate, 1 mM EDTA, and 400 μM cytochrome c, and varying concentrations of lactate and thiolactate from 0.1 mM to 6.0 mM at pH 7.5 and 25 °C.



Table 11. Rapid Reaction Kinetic Parameters for the Oxidation of Lactate and Thiolactate by Wild-type Flavocytochrome  $b_2$  measured at 438 nm

Substrate	$k_{\text{red}}, \text{s}^{-1}$	$k_{\text{red}} / K_{\text{d}},$ $\text{mM}^{-1}\text{s}^{-1}$	$K_{\text{d}},$ $\text{mM}$
Lactate <sup>a</sup>	$520 \pm 19$	$1100 \pm 78$	$0.47 \pm 0.05$
Thiolactate <sup>b</sup>	$156 \pm 19$	$53 \pm 8$	$2.9 \pm 0.7$

<sup>a</sup> From reference (70).

<sup>b</sup> 100 mM potassium phosphate and 1 mM EDTA, varying concentration of lactate and thiolactate from 0.3 mM to 5.0 mM at pH 7.5 and 25 °C.

Table 12. Rapid Reaction Kinetic Parameters for the Oxidation of Lactate and Thiolactate by Wild-type and the Mutant D282N Flavocytochromes  $b_2$  Measured at 550 nm

Parameters	wild-type	D282N
Lactate		
$k_{\text{red}}, \text{s}^{-1}$	$226 \pm 11$	$4.8 \pm 0.4^{\text{a}}$
$k_{\text{red}} / K_{\text{lactate}}, \text{mM}^{-1}\text{s}^{-1}$	$1089 \pm 199$	ND <sup>b</sup>
$K_{\text{lactate}}, \text{mM}$	$0.21 \pm 0.05$	ND <sup>b</sup>
Thiolactate		
$k_{\text{red}}, \text{s}^{-1}$	$84 \pm 8$	$3.1 \pm 0.06^{\text{a}}$
$k_{\text{red}} / K_{\text{thiolactate}}, \text{mM}^{-1}\text{s}^{-1}$	$33 \pm 4$	ND <sup>b</sup>
$K_{\text{thiolactate}}, \text{mM}$	$2.5 \pm 0.5$	ND <sup>b</sup>

Conditions: 100 mM potassium phosphate and 1 mM EDTA, varying concentration of lactate and thiolactate from 0.3 mM to 5.0 mM at pH 7.5 and 25 °C.

<sup>a</sup>Assays were done at 5 mM of substrate.

<sup>b</sup>Not determined.

## DISCUSSION

The reaction of Flb<sub>2</sub> involves the cleavage of CH and OH bonds. In previous studies the relative rates of these bonds have been probed by labeling the compound with deuterium instead of hydrogen. CH bond cleavage has been determined to be partially rate limiting for the wild-type enzyme and more rate limiting for several mutant enzymes (45,70,18,72).

In order to gain insight into the chemical mechanism of flavocytochrome b<sub>2</sub>, the use of thiolactate as an alternative substrate can be a useful tool, since the SH group has a lower pK<sub>a</sub> than the OH in lactate. This different chemical property in combination with pH effects can potentially allow to probe the ionization of the SH group and thus of the OH in the transition state of Flb<sub>2</sub>. In the work described here, thiolactate was characterized as a substrate for the wild-type enzyme. The V<sub>max</sub> value with thiolactate is within 5 fold of the value for lactate, while the V/K value is 6 fold lower with this substrate. The rate of reduction of the flavin and heme groups are only 3 and 7 fold lower than with lactate, while the (k<sub>red</sub>/K) values with thiolactate for flavin and heme reduction are 20 and 33 fold lower. The steady state and rapid reaction kinetic results indicate that thiolactate is a good substrate for wild-type Flb<sub>2</sub>.

In the active site of Flb<sub>2</sub> Asp282 is proposed to orient His373 in the proper position for proton abstraction (18). In the D282N enzyme the CH bond cleavage becomes totally rate limiting, indicating that the interaction between Asp282 and His373 is important for catalysis. With this mutant enzyme the values for the kinetic parameters with thiolactate are almost identical to those with lactate. Additionally, with thiolactate as substrate the mutation of Asp282 to asparagine has a decreased effect on the V/K value (Figure 9). This result suggests that with the weaker SH bond it is easier for the D282N enzyme to catalyze the reaction. Mechanistically this indicates that the His373

abstracts the proton at the OH position. Characterization of the H373Q enzyme will provide further information.

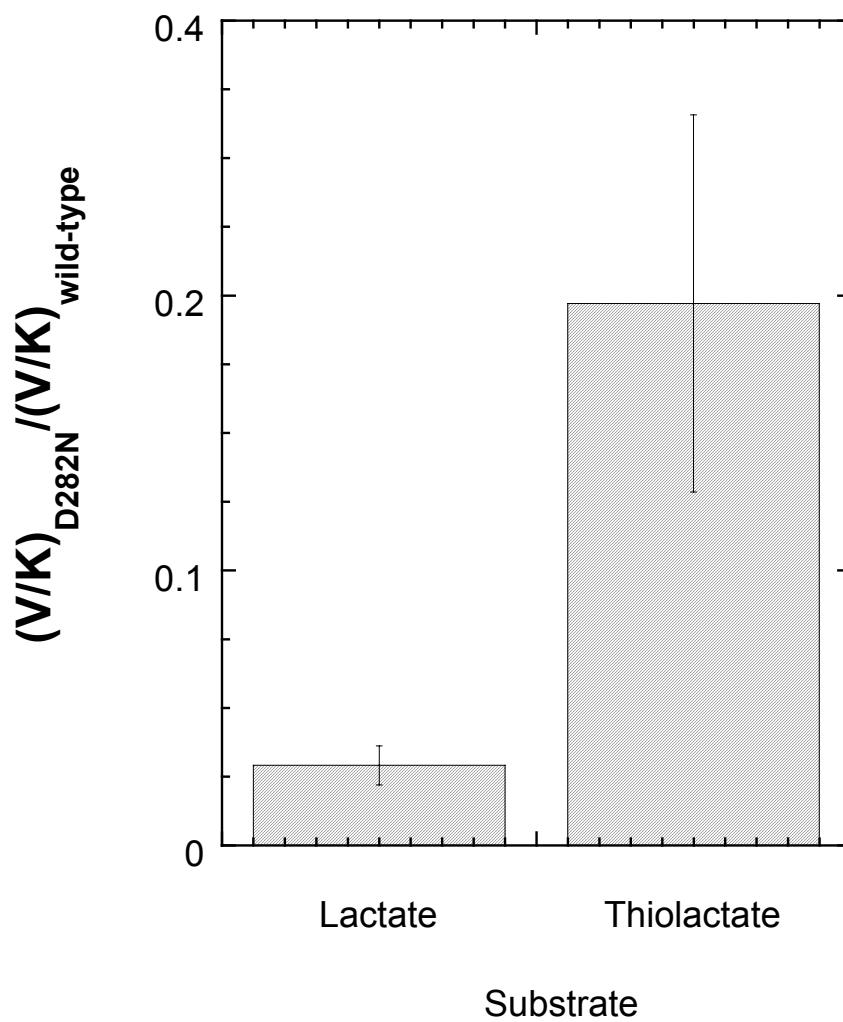


FIGURE 9. Ratio of the activities of D282N and wild-type enzymes with thiolactate and lactate.

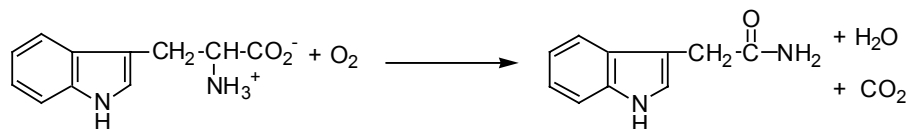
## CHAPTER V

### ANALYSIS OF THE ROLES OF AMINO ACID RESIDUES IN THE FLAVOPROTEIN TRYPTOPHAN 2-MONOOXYGENASE MODIFIED BY 2- OXO-3-PENTINOATE: CHARACTERIZATION OF HIS338, CYS339, AND CYS511 MUTANT ENZYMES

#### INTRODUCTION

Tryptophan 2-monooxygenase (TMO) [E.C. 1.13.12.3] from *Pseudomonas savastanoi* catalyzes the oxidative decarboxylation of tryptophan to indoleacetamide, carbon dioxide, and water (Scheme 17). This reaction is the first of two steps in the bacterial pathway for synthesis of the plant hormone indoleacetic acid (79). Localized high levels of indoleacetic acid at sites of infection result in the formations of knots or galls on the infected plants (80).

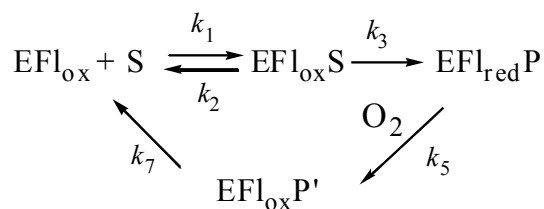
Scheme 17



TMO is a member of a family of generally poorly characterized flavoproteins which catalyze the oxidative decarboxylation of amino acids (30, 81). The kinetic mechanism of TMO has been determined with tryptophan as substrate (Scheme 18). In the reductive half-reaction the substrate binds to the enzyme forming the imino acid bound to the reduced flavin. In the oxidative half-reaction, oxygen reacts with the reduced enzyme-imino acid complex to produce indoleacetamide and the oxidized FAD

(29). Kinetic isotope effects have shown that CH bond cleavage is only partially rate limiting with tryptophan as substrate, with product release limiting turnover. Studies of the effects of pH on activity have shown that an amino acid residue in the free enzyme

Scheme 18



with a  $\text{pK}_a$  value of 6 must be deprotonated and a second group with a  $\text{pK}_a$  value of about 10 must be protonated for activity. The temperature dependence of the  $\text{pK}_a$  value for indoleacetamide binding is consistent with a histidine residue being the ionizable group with the  $\text{pK}_a$  value of 6 (82).

Chemical modification studies of TMO using several reagents have indicated the presence of histidine and cysteine residues at or near the active site (83). Recently, Gadda *et al.* (84) characterized 2-oxo-3-pentynoate as an active site directed inactivator of TMO; the sites of modification by 2-oxo-3-pentynoate were identified as the conserved residues Cys339 and Cys511. In these studies, it was also noted that His338 was conserved in all the TMO's described to date. Based on this conservation and the results from kinetic analyses, it was hypothesized that H338 was also in the active site (84). Site directed mutagenesis was used to investigate the roles of His338, Cys339 and Cys511 in catalysis by TMO. The results of these studies are described in this chapter.

## EXPERIMENTAL PROCEDURES

*Materials.* L-Tryptophan and L-methionine were purchased from USB

(Cleveland, OH); indoleacetamide was from Sigma (St. Louis, MO); DEAE-Sephacel and Phenyl-Sepharose were from Amersham Pharmacia (Uppsala, Sweden); and *E. coli* M15 (pREP4) was from Qiagen (Valencia, CA).

*DNA Manipulation.* Plasmids containing the genes for the mutant proteins H338N, C339A, and C511A enzymes in the expression plasmid pQE51 (Qiagen) were generous gifts from Dr. Angelo Spina of the University of Verona. Mutagenesis of Cys511 to serine was performed using the QuikChange protocol (Stratagene). The protein coding regions for all the plasmids were sequenced to ensure that no unwanted mutations were incorporated during the polymerase chain reaction. Plasmids were transformed into *E. coli* M15.

*Protein Expression and Purification.* Wild-type and mutant enzymes were expressed by inoculating six 1.5 L flasks of LB broth containing 100 µg/ml ampicillin and 25 µg/ml kanamycin with 10 ml of an overnight culture. These were incubated at 37°C until the  $A_{600}$  value reached 0.2-0.4. At this point isopropyl β-D-thiogalactopyranoside was added to a final concentration of 500 µM. After an additional 8 h at 30 °C, cells were collected by centrifugation. The cell paste was resuspended in 250 ml 100 mM Tris-HCl, 1 mM EDTA, 50 µM indoleacetamide, 0.5 mM dithiothreitol, 0.5 mM phenylmethylsulfonyl fluoride, 0.2 mg/ml lysozyme, pH 8.3. The resuspended cells were lysed by sonication for eight cycles of 30 s each. The lysate was centrifuged for 20 min at 20,000xg, the pellet was discarded, and the supernatant was brought to 0.55% (w/v) with polyethyleneimine, using a 0.1 g/ml stock solution in 100 mM Tris-HCl, pH 8.3. After centrifugation for 20 min at 20,000xg, solid ammonium sulfate was added to the supernatant to yield 60% saturation. The sample was stirred for 20 min; the precipitate collected by centrifugation for 20 min at 20,000xg was dissolved in the appropriate buffer for the subsequent column.

The chromatographic steps for purification of the wild-type and mutant C511S enzymes were as described previously (83). For purification of the C339A and H338N enzymes, the 60% ammonium sulfate pellets were suspended in 20 mL of 50 mM Tris-HCl, 1 mM EDTA, 0.5 mM dithiothreitol, 50  $\mu$ M indoleacetamide, 10% glycerol, pH 8.3, and dialyzed for 8 h against 2 L of the same buffer with two buffer changes. The sample was centrifuged for 20 min at 20,000xg and then loaded onto a DEAE-Sepharose column (3x15 cm) equilibrated with the same buffer. The enzyme was eluted with a 600 ml gradient from 0 to 300 mM NaCl in the same buffer; the enzyme eluted in the middle of the gradient at  $\sim$ 150 mM NaCl. Fractions containing TMO were pooled, brought to 60% ammonium sulfate saturation, and centrifuged for 20 min at 20,000xg. The pellet was resuspended in 25 ml of 350 mM ammonium sulfate, 1 mM EDTA, 0.5 mM dithiothreitol, 50  $\mu$ M indoleacetamide, pH 8.3, clarified by centrifugation, and loaded onto a Phenyl-Sepharose column (3x15 cm) equilibrated with the same buffer. The enzyme was eluted with a 400 ml gradient of 350 mM to 0 mM ammonium sulfate; the enzyme eluted one third through the gradient. Protein concentrations for the wild type and mutant enzymes were calculated from the absorbances at 466 nm using an extinction coefficient of 11.4 mM<sup>-1</sup> cm<sup>-1</sup> (83).

*Enzyme Assays.* Enzyme activity was routinely measured in air-saturated 50 mM Tris-HCl, 1 mM EDTA, 0.5 mM dithiothreitol, pH 8.3, at 25 °C, by monitoring the rate of oxygen consumption in a computer-interfaced Hansatech oxygen monitoring system. Different oxygen concentrations were obtained by bubbling appropriate mixtures of O<sub>2</sub>/N<sub>2</sub> into the assay mixture until saturation was reached.

*Data Analysis.* Kinetic data were fit using the programs Kaleidagraph (Adelbeck Software, Reading, PA) and Igor (Wavemetrics, Lake Oswego, OR). Initial rate measurements were fit to the Michaelis-Menten equation. Isotope effects were calculated



using equation 2, which describes separate isotope effects on the  $V_{\max}$  and  $V/K_{aa}$  values;  $F_i$  is the fraction of heavy atom substitution in the substrate,  $E_v$  is the isotope effect on  $V_{\max}$  minus 1, and  $E_{VK}$  is the isotope effect on the  $V/K_{aa}$  value minus 1 (85). Inhibition constants for indoleacetamide were calculated by fitting the data to equation 10. This equation depicts the behavior of a competitive inhibitor where  $K_i$  is the inhibition constant for that inhibitor.

$$v = \frac{VA}{K_m(1 + F_i(E_{vk})) + A(1 + F_i(E_v))} \quad (2)$$

$$v = \frac{VA}{K_m \left(1 + \frac{I}{K_i}\right) + A} \quad (10)$$

## RESULTS

*Protein Expression.* To probe the roles of His338, Cys339, and Cys511 in catalysis, the H338N, C339A, and C511A enzymes were constructed and expressed in *E. coli*. While both the H338N and the C339A enzymes were readily expressed at levels comparable to the wild type enzyme, their behavior during purification was different, suggesting changes in the conformation of these enzymes. Specifically, these enzymes did not bind to Phenyl-Sepharose in 350 mM potassium phosphate buffer. The purification protocol was modified to account for this difference. Both enzymes would bind to Phenyl-Sepharose in the presence of 350 mM ammonium sulfate after prior purification by DEAE-Sepharose chromatography, thereby allowing their purification.

In contrast, it was not possible to obtain pure C511A enzyme in the active form. The enzyme was expressed well and could be purified to homogeneity following the protocol for the C339A and H338N enzymes. However, the resulting protein contained no FAD and was inactive. All attempts to reincorporate the FAD into the mutant were

unsuccessful. As an alternative approach, the C511S enzyme was constructed. This enzyme proved to be better behaved and could be expressed and purified following the protocol for the wild-type enzyme. The visible absorbance spectra of the three active mutant proteins were not distinguishable from that of the wild type enzyme.

*Steady State Kinetics.* Steady state kinetic parameters were determined for the mutant enzymes with tryptophan and methionine as the amino acid substrates (Table 13). Neither the H338N nor the C339A mutation has a drastic effect on the kinetic parameters with tryptophan as substrate. The  $V/K_{\text{trp}}$  value decreases about 7 fold with the H338N enzyme and about 3.5 fold for the C339A enzyme, compared to the wild type values. The  $V_{\text{trp}}$  value shows smaller effects. The  $V/K_{\text{O}_2}$  value decreases 4 and 2 fold for the H338N and the C339A enzymes, respectively. The  $K_{\text{O}_2}$  values for the H338N and C339A enzymes are similar to the wild-type value. The  $V_{\text{max}}$  and  $V/K$  values for methionine are also very close to the wild type values.

The steady state kinetic parameters with both amino acid substrates are altered much more by the C511S substitution (Table 13). The  $V_{\text{max}}$  value with tryptophan as substrate only decreases about 2.6 fold, but the  $V/K_{\text{trp}}$  value decreases close to 20 fold. With methionine as substrate, the  $V_{\text{max}}$  value decreases about 10 fold while the  $V/K_{\text{met}}$  value remains close to the wild-type value. The effects of this mutation on the oxidative half reaction are similar to the effects of the C339A and H338N mutations. The  $V/K_{\text{O}_2}$  value decreases approximately 5-fold and the  $K_{\text{O}_2}$  value remains close to the wild-type value.

*Inhibition by Indoleacetamide.* In order to examine the effect of the mutations on binding, the inhibition constant for the competitive inhibitor indoleacetamide was determined for all three mutant enzymes (Table 13). The  $K_i$  values for the C339A and H338N enzymes are not significantly different from the  $K_i$  value for the wild-type

enzyme. In the case of the C511S enzyme the  $K_i$  value for indoleacetamide increases 4-fold. These results are consistent with the steady state results with tryptophan as substrate, where only the C511S enzyme exhibits a significant change in the kinetic parameters.

*Kinetic Isotope Effects.* Primary deuterium kinetic isotope effects with 2-<sup>2</sup>H-tryptophan and 2-<sup>2</sup>H-methionine were measured for all three mutant enzymes (Table 14). For the wild-type enzyme, both the  $^D V_{\text{trp}}$  value and the  $^D(V/K_{\text{trp}})$  value are small, consistent with C-H bond cleavage being only partially rate limiting with this substrate due to its high commitment to catalysis and rate-limiting product release (82). With the H338N and C339A enzymes, the  $^D V_{\text{trp}}$  and  $^D(V/K_{\text{trp}})$  values are very close to those for the wild-type enzyme. These results indicate that the relative rates of chemical steps are not greatly affected by these mutations. With the C511S enzyme the  $^D V_{\text{trp}}$  value is not significantly different from the wild type value, while the  $^D(V/K_{\text{trp}})$  value increases. In the case of the C511S mutant, the results suggest that substitution of this residue by serine makes chemical steps more rate limiting.

With methionine as substrate for the wild-type enzyme, C-H bond cleavage is more rate limiting (82). For the H338N and C339A enzymes, the values of the isotope effects with methionine are very close to the values for the wild-type enzyme. In contrast, both the  $^D V$  and the  $^D(V/K_{\text{met}})$  values are higher for the C511S enzyme (Table 14).

## DISCUSSION

Tryptophan monooxygenase is one of several flavoenzymes which catalyze the oxidative deamination of  $\alpha$ -amino acids to form amides. Others are lysine monooxygenase (81, 86) and phenylalanine oxidase (30). Unlike the case with these latter two enzymes, the catalytic mechanism of TMO has been analyzed by a range of approaches, so that a detailed kinetic mechanism of the enzyme is available (29, 82). Several active site-directed reagents have been used to identify catalytically important residues. Both thiol and imidazole-directed reagents inactivate the enzyme in a manner consistent with modification of active site residues, suggesting that cysteinyl and histidinyl residues play critical roles (83). Cys338 and Cys511 were recently identified as residues modified when TMO is inactivated by 2-oxo-3-pentynoate (84). Both modification and inactivation are blocked by indoleacetamide, a reversible inhibitor (84), suggesting that these residues are in the active site. Consistent with an important role of these two residues, they are conserved in the several TMO sequences which are available. The adjacent residue His338 is also conserved; its proximity to a residue modified by 2-oxo-3-pentynoate and the inactivation of TMO seen upon treatment with diethylpyrocarbonate (83) suggested that this residue may also be in the active site (84). The results described here rule out a critical catalytic role for either Cys339 or His338, but do suggest that Cys511 may play an important role. In the case of the C339A enzyme, there are only small changes in the kinetic parameters. The  $V_{\max}$  value and the  $V/K$  values for both substrates decrease 2- to 3-fold. With methionine as substrate there

Table 13. Steady State Kinetic Parameters of Tryptophan Monooxygenase Mutant Proteins

kinetic parameter	Enzyme			
	wild-type	H338N	C339A	C511S
$V_{\text{trp}}, \text{s}^{-1}$	$13.2 \pm 0.67$	$4.0 \pm 0.2$	$10 \pm 0.5$	$5 \pm 0.2$
$K_{\text{trp}}, \text{mM}$	$0.036 \pm 0.004$	$0.083 \pm 0.016$	$0.097 \pm 0.015$	$0.25 \pm 0.05$
$V/K_{\text{trp}}, \text{mM}^{-1}\text{s}^{-1}$	$360 \pm 37$	$50 \pm 8$	$105 \pm 13$	$19 \pm 2$
$K_{\text{O}_2(\text{trp})}, \text{mM}$	$0.09 \pm 0.01$	$0.11 \pm 0.03$	$0.15 \pm 0.08$	$0.28 \pm 0.17$
$V/K_{\text{O}_2(\text{trp})}, \text{mM}^{-1}\text{s}^{-1}$	$140 \pm 18$	$33 \pm 6$	$65 \pm 28$	$30 \pm 13$
$V_{\text{met}}, \text{s}^{-1}$	$5.6 \pm 0.23$	$4.8 \pm 0.2$	$6.1 \pm 0.42$	$0.70 \pm 0.01$
$K_{\text{met}}, \text{mM}$	$22.4 \pm 1.4$	$11 \pm 1$	$14 \pm 3$	$2.0 \pm 0.16$
$V/K_{\text{met}}, \text{mM}^{-1}\text{s}^{-1}$	$0.25 \pm 0.012$	$0.44 \pm 0.06$	$0.42 \pm 0.06$	$0.33 \pm 0.02$
$K_{\text{indoleacetamide}}, \mu\text{M}$	$16 \pm 0.8$	$13 \pm 3$	$28 \pm 6$	$68 \pm 8$

Conditions: 50 mM Tris, 1 mM EDTA, 0.5 mM dithiothreitol, pH 8.3, 25 °C.

is no significant change in any kinetic parameter for the C339A enzyme. There is also no change in any of the isotope effects with either substrate, consistent with chemical and other steps being decreased by comparable amounts. These results are most consistent with a subtle change in the overall structure of the protein which results in a slightly less active conformation. The lack of an effect on the parameters with methionine as substrate suggests that the conformational change results in a restricted active site which binds indolic compounds less well, but still can bind smaller substrates effectively. Mutagenesis of His338 to asparagine has a somewhat larger effect, but qualitatively the effect of the mutation is the same as that of the C339A mutation. The decreases in the  $V/K$  and  $V_{\max}$  values with tryptophan are about twice those seen upon mutation of the adjacent residue, but those with methionine are unchanged. In addition, the isotope effects with this enzyme are very close to those seen with both the wild type and the C339A enzymes. Thus, His338 is likely to be involved in maintaining an active conformation but is not directly involved in catalysis or binding. These results resemble the effects of mutating the conserved histidine in D-amino acid oxidase. This residue, His307 in the pig enzyme, forms an ion pair with an aspartate residue on the surface of the protein near a loop which closes over the active site when substrate is bound (9). Mutagenesis of this residue to serine decreases the rates of all steady state kinetic parameters by about five fold (87).

Only in the case of C511S TMO do the kinetic parameters with both methionine and tryptophan decrease significantly. Cys511 is clearly important for maintaining the protein structure, since the C511A enzyme proved too unstable to survive purification. Still, the very conservative replacement of the cysteine with serine provides a stable enzyme, so that a thiol at this position is not essential. The kinetic parameters given in Tables 1 and 2 can be used to determine the effect of the C511S.

Table 14. Primary Deuterium Isotope Effects for Tryptophan Monooxygenase Mutant Proteins

kinetic parameter	wild-type	H338N	C339A	C511S
$^D V_{\text{trp}}$	$1.22 \pm 0.07$	$1.11 \pm 0.07$	$1.05 \pm 0.05$	$1.23 \pm 0.06$
$^D(V/K_{\text{trp}})$	$1.16 \pm 0.25$	$1.26 \pm 0.15$	$1.20 \pm 0.08$	$1.92 \pm 0.22$
$^D V_{\text{met}}$	$2.43 \pm 0.15$	$2.50 \pm 0.25$	$2.62 \pm 0.05$	$2.90 \pm 0.06$
$^D(V/K_{\text{met}})$	$1.8 \pm 0.3$	$2.20 \pm 0.4$	$2.33 \pm 0.08$	$2.70 \pm 0.30$

Conditions: 50 mM Tris, 1 mM EDTA, 0.5 mM dithiothreitol, pH 8.3, 25 °C.

mutation on the intrinsic rate constants of Scheme 18. The relationships between the intrinsic rate constants and the steady state kinetic parameters are given by equations 11-15 (88). Here,  $^Dk_3$  is the intrinsic deuterium kinetic isotope effect on the rate constant for the chemical step,  $k_3$ . This has previously been determined with tryptophan and methionine as substrates for wild type tryptophan monooxygenase to be 2.4 and 5.3, respectively (29, 82). If it is assumed that the intrinsic isotope effects for the C511S enzyme are unchanged from these values, equations 3-7 describe the five intrinsic rate constants in terms of five measurable steady state kinetic parameters. Table 15 gives the values of  $k_1 - k_7$  calculated from the data of Tables 1 and 2 using equations 3-7.

$$\left(\frac{V}{K}\right)_{aa} = \frac{k_1 k_3}{k_2 + k_3} \quad (11)$$

$$\left(\frac{V}{K}\right)_{O_2} = k_5 \quad (12)$$

$$V_{\max} = \frac{k_3 k_7}{k_3 + k_7} \quad (13)$$

$$^D\left(\frac{V}{K}\right)_{aa} = \frac{^Dk_3 + \frac{k_3}{k_2}}{1 + \frac{k_3}{k_3}} \quad (14)$$

$$^D V_{\max} = \frac{^Dk_3 + \frac{k_3}{k_7}}{1 + \frac{k_3}{k_7}} \quad (15)$$



Table 15. Calculated Intrinsic Rate Constants for C511S Tryptophan Monooxygenase

Kinetic Parameter	tryptophan			methionine		
	Wild type enzyme	C511S	$\Delta\Delta G^\ddagger$	Wild type enzyme	C511S	$\Delta\Delta G^\ddagger$
$c_f$	(~8) <sup>a</sup>	0.52 ± 0.25		4.4 ± 1.7	1.53 ± 0.32	
$c_{vf}$	5.4 ± 1.7	5.1 ± 1.4		2.0 ± 0.24	1.26 ± 0.05	
$k_1, \text{mM}^{-1}\text{s}^{-1}$	(~400) <sup>a</sup>	55 ± 26	1.2 ± 0.3	0.31 ± 0.15	0.54 ± 0.14	-0.33 ± 0.37
$k_2, \text{s}^{-1}$	(~17) <sup>a</sup>	58 ± 38	-0.7 ± 0.5	3.8 ± 1.6	1.04 ± 0.36	0.77 ± 0.36
$k_3, \text{s}^{-1}$	84 ± 44	30 ± 13	0.61 ± 0.49	17 ± 3.2	1.59 ± 0.43	1.4 ± 0.2
$k_5, \text{mM}^{-1}\text{s}^{-1}$	(139 ± 4) <sup>a</sup>		0.91 ± 0.28			
	140 ± 18	30 ± 13	0.92 ± 0.29			
$k_7, \text{s}^{-1}$	16 ± 6.6	6.0 ± 2.1	0.58 ± 0.36	8.4 ± 1.2	1.3 ± 0.34	1.1 ± 0.2

<sup>a</sup>Values from references (29) and (82).

With tryptophan as substrate, the values of  $k_1$  and  $k_2$  for the wild type enzyme cannot be determined with any reasonable degree of precision. This is due to the large value of  $k_3/k_2$ , which is between 7 and 15 (82). As a result the isotope effect on the  $V/K_{\text{trp}}$  value is too close to one to use equation 6 in the analysis of the data. Even with that caveat the data of Table 15 indicate that binding of tryptophan is affected, with the rate of association,  $k_1$ , decreasing 5-fold or more. The rate of dissociation,  $k_2$ , may in fact be increased by the mutation, but the precision of the data and the uncertainty in the value of  $k_2$  for the wild type enzyme make this less than certain. The several fold increase in the  $K_d$  value for indoleacetamide is consistent with the association rate constant decreasing more than the dissociation rate constant for that compound. This decrease in affinity for the amino acid is not seen with methionine as substrate, suggesting that it is the binding of the indole ring of tryptophan which is altered. Indeed, there is a decrease in the  $K_d$  value for methionine in the C511S enzyme. The effects on the rate of the chemical step are not significantly different with the two amino acid substrates, with an average decrease of about six fold in  $k_3$ . The rate constants for steps in the oxidative half reaction,  $k_5$  and  $k_7$ , also decrease 5 fold on average with both substrates in the C511S enzyme. Thus, the changes in the steady state kinetic parameters seen in the C511S enzyme are due to changes in a number of kinetic parameters. In no case does a single rate constant decrease by more than an order of magnitude, establishing that the thiol of Cys511 is not involved in catalytic steps as either an acid/base catalyst or a nucleophile. A reasonable conclusion from these data is that Cys511 is required to maintain the proper structure of the active site, but is not involved in the actual chemistry.

Interpretation of the effects of these mutations and identification of active site residues of TMO is clearly made more difficult by the absence of direct information on

the three-dimensional structure of the protein. To identify possible homologous proteins with known structure to aid in this analysis, a PSI-BLAST (89) search was made using the *P. savastanoi* TMO sequence. This identified the flavoenzyme L-amino acid oxidase as the most closely related enzyme, with e values of  $10^{-8}$  to  $10^{-12}$ . The LAAO with the most significant score is that from *Calloselasma rhodostoma*. This LAAO and *P. savastanoi* TMO are 24% identical and 40% similar, well above the levels expected solely from random chance. The similarity of the reactions catalyzed by TMO and LAAO supports the identification of these enzymes as homologous. The reductive half reactions of LAAO and TMO are the same, the oxidation of an L-amino acid with transfer of a hydride equivalent to the FAD (90). The enzymes differ in the oxidative half reactions, in that LAAO does not catalyze a subsequent oxidative decarboxylation to form an amide. A sequence alignment of LAAO and TMO is shown in Figure 10. Cys339, His338, and Cys511 are not conserved between the two enzymes, suggesting that they are not required for the common catalytic reactions of the two enzymes.

The crystal structure of *C. rhodostoma* LAAO has been solved at 2.0 Å resolution (27). Surprisingly, LAAO has the same fold as monoamine oxidase B (91). When the program 3D-PSSM (92) is used to thread the sequence of TMO onto proteins of known structure, a highly significant match is obtained with the structure of monoamine oxidase B and an only slightly less significant match with LAAO. The differences in the structural models of TMO built using MAO or LAAO are mostly in the position of surface loops. The FAD binding domain of LAAO consists of three discontinuous regions which correspond to residues 41-69, 276-346, and 496-536 in TMO and thus includes the three residues analyzed here. Figure 11A shows the locations of His338, Cys339, and Cys511 of TMO in a structure modeled on LAAO. His338 and Cys339 are on a loop on the surface of the protein, adjacent to the adenosine portion of

the FAD. Binding of indoleacetamide to the wild type enzyme results in changes in the FAD spectrum (83), suggesting that there is a conformational change in the region of the protein surrounding the flavin when the inhibitor binds. The decreased reactivity of Cys338 with 2-oxo-3-pentynoate when indoleacetamide is bound (84) can be attributed to propagation of the conformational change upon inhibitor binding to the loop containing this residue, located as it is near the FAD. Conversely, mutagenesis of either His338 or Cys339 could have subtle effects on the interactions of the protein with the FAD, leading to the small and generalized changes in the kinetic parameters described here. The differences in behavior during chromatography of these proteins are also consistent with subtle changes in the protein surface.

TMO Cys511 corresponds to Glu457 in LAAO (Figure 10). A carboxylate oxygen of this residue forms a hydrogen bond with a ribitol hydroxyl of the FAD in the latter enzyme (27). Modeling shows that the thiol of a cysteine in the same position would be within hydrogen bonding distance (2.7 Å) of the same flavin hydroxyl (Figure 11B). LAAO Glu457 is on one end of a loop which ends with Gly464, Trp465, and Ile466. The first two of these residues form hydrogen bonds with the FAD, at N(1) and the C(2) oxygen of the isoalloxazine ring, respectively. Gly464 and Trp465 also form part of the binding site for the amino acid substrate. These three residues correspond to Gly500, Trp501, and Ile502 in TMO and are also conserved in that enzyme (Figure 10). The conservation of these residues in both TMO and LAAO suggests that they play similar roles in both enzymes. We attribute the properties of the C511S protein to a distortion of the interactions of the protein with the FAD and a loss of flexibility of the active site due to the propinquity of Cys/Glu457 to residues critical for amino acid binding. Replacement of this residue with alanine would be expected to weaken flavin binding, consistent with the formation of inactive apoenzyme observed in attempts to

purify C511A TMO. The more conservative C511S mutation would be able to form the hydrogen bond to the flavin, but the much stronger interaction of oxygen relative to sulfur could alter the dynamics of this region of the protein. Given the propinquity of Cys511/Glu457 to these three conserved active site residues, a change in dynamics or structure of the peptide backbone around Cys511 could be reflected in the binding site for substrates. The effects of the mutation on the individual catalytic steps are consistent with such a model.

In conclusion, characterization of the effects of mutagenesis of His338, Cys339, and Cys511 rule out critical catalytic roles such as acid/base catalysis for these residues. All three mutations result in changes in the rates of multiple steps in catalysis and binding, with the C511S enzyme showing the greatest change. The structural effects of the mutations can be interpreted upon identification of tryptophan monooxygenase and L-amino acid oxidase as homologous proteins.

```

TMO      1                               MYDHFNSPSIDILYDYGPFLLKCEMTGGIGSYSAG 35
LAAO   -18                             MNVFFMFSLFLAALGSCADDNPLAECFQENDYEEFLEIARGLKA 29

TMO:    36  TPTPR-VAIVGAGISGLVAATELLRAGVKDVLVLESSRDRIGGRVWSQVFDQTRPRYIAEM 94
LAAO    30  TSNPKHVIVGAGMAGLSAAYVLAGAGHQVTVL-EASERPGGRV--RTYRNEEAGWYANL 86

TMO     95  GAMRFPPSATGLFHYLKKFGISTSTTFDPDGVVDTELHY-RGKRYHWPAGKKPELFRRV 153
LAAO    87  GPMRLPEKHRIVREYIRKFDLRLNEFSQEN---DNAWYFIKNIRKKVGEVKKDPGLLKYP 143

TMO    154  YEGWQSLLESEGYLLEG--GSLVAPLDITAMLKSGRLEEAIAWQWLNVFRDCSFYNAIV 211
LAAO   144  VKPSEAGKSSAGQLYEESLGKVVEELKRT-----NCSYILNKY 180

TMO    212  CIFTGRHPPGGDRWARPEDFELFSGLSGIGSGGFLPVFQAGFTEILRM-VINGYQSDQRLI 270
LAAO   181  DTYSTKEYLIKEGDLSPGAVDMIGDLLNEDSGY----VSFIESLKHDDIFAYEKRFDEI 236

TMO    271  PDGISSLAARLADQSFDGKALRDRVCF-SRVGRISREAEKIIIQTEAGEQR----VFDRV 325
LAAO   237  VDGMDKLPTAMY-----RDIQDKVHFNAQVIKIQQNDQKVTVVYETLSKETPSVTADYV 290

TMO    326  IVTSSNRAMQMIHCLTDSESFLSRDVARAVRETHLTGSSKLFILTRTKFWIKNKLPTTIQ 385
LAAO   291  IVCTTSRAVRLIKF---NPLLPKK-AHALRSVHYRSGTKIFLTCTTKFW-----E 337

TMO    386  SDGLVRGVYCLD-----YQDPEPEGHGV-VLLSYTWEDDAQKMLLAMPDKKTRCQVLVDD 438
LAAO   338  DDGIHGGKSTDLPSRFIYPNHNFTNGVGVIIAYGIGDDANFQAL-DFKDCADIVFND 396

TMO    439  LAAIH----PTFASYLLPVDGDYERYVLHHDWLTDPHSAGAFKLNYPGEDVYSQRLFFQP 494
LAAO   397  LSLIHQLPKKDIQSFCYP-----SVIQKWSLDKYAMGGITTFTP----YQFQHFSDP 444

TMO    495  MTANSPNKDTGLYLAGCSCSFAGGWIEGAVQTALNSA----CAVLRSTGGQLSKGNPL 548
LAAO   445  LTASQGR----IYFAGEYTAQAHGWIDSTIKSGLRAARDVNLASENPSGIHLSNDNEL 498

```

FIGURE 10. Alignment of *P. savastanoi* tryptophan monooxygenase and *C. rhodostoma* L-amino acid oxidase. The alignment was generated with the program PSI-BLAST, using the TMO sequence as the probe. Residues conserved in both TMO and LAAO are in bold. The asterisks indicate His338, Cys339, and Cys511 of TMO.

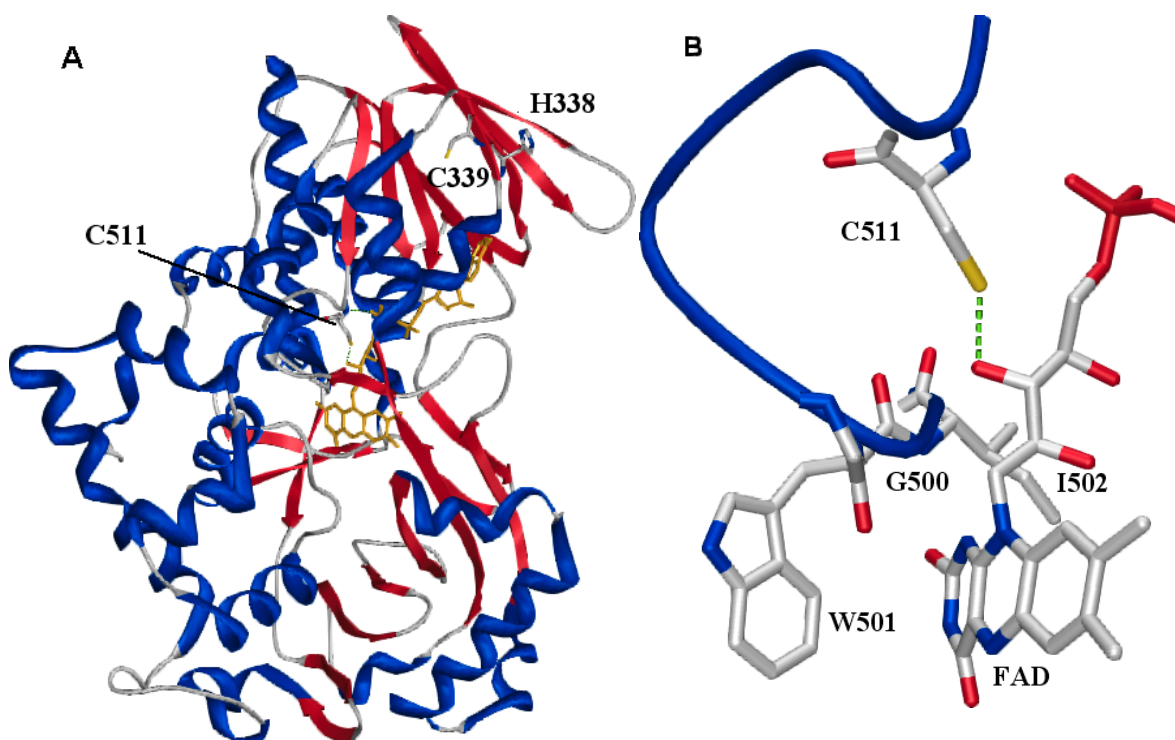


FIGURE 11. Modeling of tryptophan monooxygenase using the L-amino acid oxidase structure. A. Location of His338, Cys339, and Cys511. B. Proposed interaction between Cys511 and the FAD in tryptophan monooxygenase. The structures were drawn using the program SwisPDBViewer, the PDB file 1F8S, and the alignment of Figure 10.

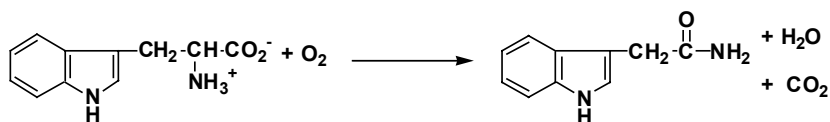
## CHAPTER VI

**TYROSINE 413 IN TRYPTOPHAN 2-MONOOXYGENASE, A MEMBER OF  
THE L-AMINO ACID OXIDASE FAMILY, IS IMPORTANT FOR CATALYSIS  
AND PROPER CONFORMATION OF THE ENZYME-INTERMEDIATE  
COMPLEX**

**INTRODUCTION**

The flavin containing enzyme tryptophan 2-monooxygenase (TMO; E.C. 1.13.12) catalyzes the oxidation of tryptophan to indoleacetamide, carbon dioxide and water (Scheme 19) (93). TMO from *Pseudomonas savastanoi* contains one tightly bound FAD cofactor per polypeptide of 61 kDa. The TMO gene in *P. savastanoi* is present on a plasmid which also contains the gene for the enzyme indoleacetamide hydrolase (79, 94). The presence of this plasmid and similar genes in *Agrobacterium tumefaciens* allow these pathogenic bacteria to produce high levels of indoleacetic acid from tryptophan at the site of infection. The indoleacetic acid induces the formation of plant tumors known as galls. Crown gall diseases caused by *A. tumefaciens* in perennial fruits and ornamental crops and olive knot diseases produced by *P. savastanoi* in olive plants lower productivity and increase susceptibility of the infected plants to pathogens and environmental stress (95).

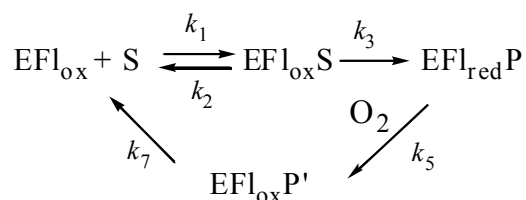
Scheme 19





TMO belongs to a group of flavoenzymes that catalyzes the oxidative decarboxylation of amino acids. Other members of this group are L-phenylalanine oxidase (30), L-arginine 2-monooxygenase (31), and L-lysine 2-monooxygenase (32, 86). TMO is the only enzyme in this group for which both the kinetic and chemical mechanisms have been studied in detail. Scheme 20 shows the kinetic mechanism for TMO determined with tryptophan as substrate (29). Although the kinetic mechanism of TMO is well understood, structural information about this and related flavoenzymes is lacking. We have identified the flavoenzyme L-amino acid oxidase (LAAO) as a homologue of TMO (96). Although the amino acid sequences of TMO and LAAO are only 24 % identical, both enzymes oxidize L-amino acids to form imino acid

Scheme 20



intermediates in their respective reductive half-reactions (27, 82). TMO differs from LAAO in catalyzing the decarboxylation of this intermediate in the oxidative half-reaction. The structure of *Calloselasma rhodostoma* LAAO with the inhibitor *o*-aminobenzoate bound has been solved at 2.0 Å resolution (27). The carboxylate of the inhibitor and by implication the amino acid substrate is bound to Arg90 and Tyr372 (Figure 12). The identification of Tyr413 as the residue corresponding to Try372 of LAAO and the use of site directed mutagenesis to analyze the role of this residue in catalysis is described in this chapter.

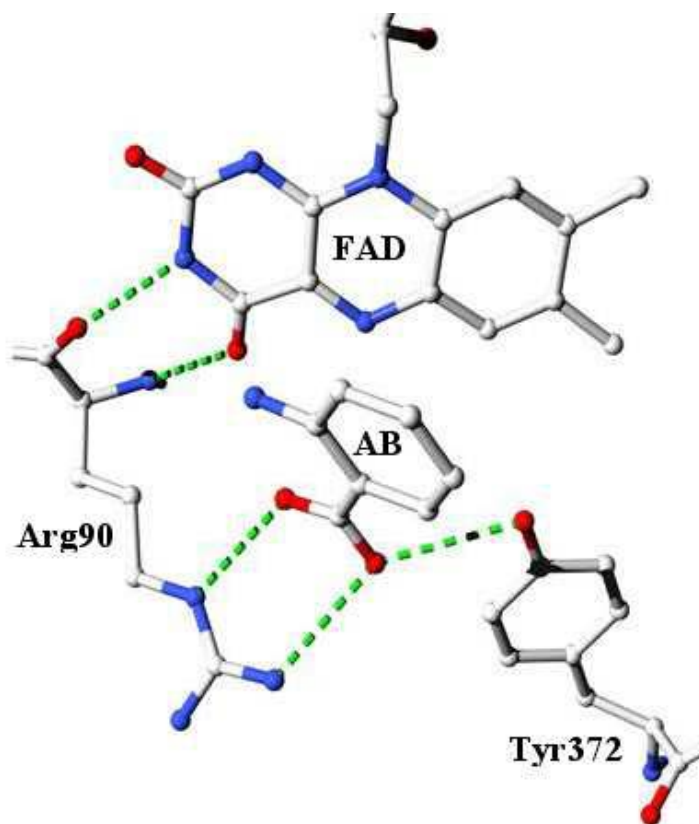


FIGURE 12. Active site of L-amino acid oxidase with aminobenzoate (AB) bound showing the interactions with Arg90 and Tyr372. The figure was made using SwissPDBViewer and the PDB file 1F8S.

## EXPERIMENTAL PROCEDURES

*Materials.* L-Tryptophan was purchased from USB (Cleveland, OH). Indoleacetamide and glucose oxidase were from Sigma (St. Louis, MO). DEAE-Sepharcel and phenyl-Sepharose were from Amersham Pharmacia (Uppsala, Sweden). *E. coli* M15 (pREP4) was from Qiagen (Valencia, CA) and catalase from Roche (Basel, Switzerland). [ $\alpha$ - $^2$ H]-L-Tryptophan was synthesized by the method of Kiick and Phillips (97).

*Methods.* UV-Visible spectra were taken on a Hewlett-Packard Model 8458A diode array spectrophotometer. The HPLC apparatus consisted of Waters 2475 pumps with a Waters automated gradient maker, a Waters 625 scanning fluorescence detector, and a Millenium software package. Rapid reaction kinetic measurements were performed on an Applied Photophysics SX.18MV stopped-flow spectrophotometer.

*DNA Manipulation.* The plasmid pQE51 (Qiagen, Valencia, CA) was used for expression of all proteins described here (96). Site directed mutagenesis was performed using the QuikChange protocol (Stratagene). Plasmids were first transformed into XL1Blue cells for selection and plasmid preparations. Plasmid purification was performed using standard kits from Qiagen.

*Protein Expression and Purification.* Wild-type and mutant enzymes were expressed in M15 *E. coli* cells. All Luria-Bertani (LB) broth and agar plates contained 100  $\mu$ g/ml ampicillin and 25  $\mu$ g/ml kanamycin. For each cell growth, the relevant permanent stock was streaked onto a LB agar plate. A 60 ml LB broth culture was inoculated with a single colony from this plate and incubated overnight at 37 °C. The next day six flasks containing 1 L of LB broth were each inoculated with 10 ml of the overnight culture. These cultures were incubated at 37 °C until the  $A_{600}$  reached a value between 0.6-0.8. At that time isopropyl- $\beta$ -D-thiogluconopyranoside was added to a final

concentration of 0.5 mM, and the temperature was decreased to 28 °C. After 6-8 hrs, cells were collected by centrifugation, and the resulting cell pellets were combined and resuspended in 250 ml of 50 mM Tris, 1 mM EDTA, 0.5 mM dithiothreitol, 0.5 mM phenylmethylsulfonyl fluoride, 50 µM indoleacetamine, 0.2 mg/ml lysozyme, pH 8.3. Following lysis by sonication the lysate was spun at 20,000xg for 30 min. The supernatant was brought to 0.5 % (w/v) polyethylenimine, using a 0.1 g/ml stock solution in 100 mM Tris-HCl, pH 8.3. After centrifugation at 20,000xg for 20 min, the supernatant was brought to 60% ammonium sulfate saturation by adding solid ammonium sulfate. The solution was stirred for 20 min at 4 °C and spun for 30 min at 20,000xg. The resulting precipitant was resuspended in the appropriate buffer for subsequent chromatographic steps.

The remainder of the purification of the wild-type TMO followed the procedure of Emanuele *et al.* (83). For purification of the mutant enzymes, the 60% ammonium sulfate pellet was resuspended in 25 ml of 50 mM Tris, 1 mM EDTA, 0.5 mM dithiothreitol, 50 µM indoleacetamide, 10% glycerol, pH 8.3, and dialyzed against 2 L of the same buffer overnight. After a buffer change and further dialysis for 6 h, the sample was subject to centrifugation for 20 min at 20,000xg. The supernatant was loaded onto a DEAE-Sephacel column (3x10 cm) previously equilibrated with the same buffer. The enzyme was eluted from the column with a 600 ml gradient from 0-200 mM NaCl in the same buffer. Fractions containing TMO were identified by polyacrylamide gel electrophoresis in the presence of sodium dodecyl sulphate. Fractions containing TMO were pooled, brought to 60% ammonium sulfate saturation, and precipitated by centrifugation at 20,000xg for 20 min. The resulting pellet was resuspended in 50 mM Tris, 1 mM EDTA, 50 µM indoleacetamide, 0.5 mM dithiothreitol, 10% glycerol, pH 8.3, dialyzed against the same buffer, and spun at 20,000xg for 20 min. Purified enzymes

were stored at  $-80\text{ }^{\circ}\text{C}$  at a concentration greater than  $50\text{ }\mu\text{M}$ . Using this method 50-90 mg of enzyme were normally obtained. The concentrations of the wild-type and mutant enzymes were calculated from the absorbance at 466 nm using an extinction coefficient of  $11.4\text{ mM}^{-1}\text{ cm}^{-1}$  (83).

*Indoleacetamide Removal.* A saturated solution of ammonium sulfate in 50 mM Tris, 1 mM EDTA, 1 mM dithiothrietol, pH 8.3, was added to an equal volume of purified wild-type or mutant enzyme ( $\sim 15\text{ mg}$ ) and incubated at  $4\text{ }^{\circ}\text{C}$  for 20 min. After centrifugation at 20,000xg for 20 min, the resulting pellet was resuspended in 10 ml of 100 mM phenylalanine, 50 mM Tris, 1 mM EDTA, 1 mM dithiothrietol, pH 8.3, and incubated on ice for 20 min. An equal volume of a saturated solution of ammonium sulfate in the same buffer was added, and the mixture was incubated on ice for another 20 min. After centrifugation at 20,000xg for 20 min, the resulting supernatant was discarded. The procedure was repeated three times. The final pellet was resuspended in 5 ml of 100 mM phenylalanine, 50 mM Tris, 1 mM EDTA, 1 mM dithiothrietol, pH 8.3, and dialyzed against 2 changes of 1 L of 50 mM Tris, 1 mM EDTA, 0.5 mM dithiothreitil, 10% glycerol, pH 8.3, at  $4\text{ }^{\circ}\text{C}$ . After this treatment no trace of indoleacetamide could be detected in the protein samples by HPLC analysis. The wild-type enzyme in the absence of indoleacetamide is stable if stored at  $-80\text{ }^{\circ}\text{C}$  for several months. This is not true for the Y413A and Y413F enzymes. The Y413A enzyme loses activity after several days at  $-80\text{ }^{\circ}\text{C}$  and thus was used immediately after removal of indoleacetamide. The Y413F enzyme lost all activity in the absence of indoleacetamide.

*Enzyme Assays.* TMO activity was routinely measured in 2.5 mM tryptophan,  $250\text{ }\mu\text{M}$  oxygen, 1 mM EDTA, 0.5 mM dithithreitil, 50 mM Tris pH 8.3, at  $25\text{ }^{\circ}\text{C}$ , by monitoring the rate of oxygen consumption in a computer interfaced Hansatech oxygen

monitoring system (Norfolk, UK) or in a Yellow Spring Instrument model 5300 oxygen electrode (Yellow Springs, OH) with a Servogor 124 (Leeds, UK) chart recorder. For the Y413A and Y413F enzymes 20 mM tryptophan was used. For pH studies, the buffer was 52 mM Tris, 52 mM ethanolamine, and 100 mM ACES. Anaerobic conditions for stopped-flow experiments were obtained by filling the system with a solution of 1 mM EDTA, 0.5 mM dithiothreitol, 1 mM glucose, 50 mM Tris pH 8.3, containing 0.6  $\mu$ M glucose oxidase the night before the experiment was performed. Buffer and enzyme solutions were made anaerobic by cycles of vacuum and flushing with oxygen free argon. Hydrogen peroxide formation was determined by measuring the decrease in the rate of oxygen consumption in the presence of 0.01 mg/ml catalase in a 1 ml assay containing 17 mM L-tryptophan, 1 mM EDTA, 0.5 mM dithiothreitol, 50 mM Tris, pH 8.3, at 25 °C.

*Data Analysis.* The kinetic data were analyzed using the programs Kaleidagraph (Adelbeck Software, Reading, PA) and Igor (Wavemetrics, Lake Oswego, OR). Initial rate data were fit to the Michaelis-Menten equation. Isotope effects were calculated using equation 2. This equation describes separate isotope effects on  $V_{\max}$  and  $V/K_{\text{trp}}$ ;  $F_i$  is the fraction of heavy atom substitution in the substrate,  $E_V$  is the isotope effect on the  $V_{\max}$  value minus 1, and  $E_{VK}$  is the isotope effect on the  $V/K_{\text{trp}}$  value minus 1. Inhibition constants were obtained by fitting the data to equation 10 which describes the behavior of a competitive inhibitor where  $K_i$  is the inhibition constant. The  $\text{pK}_a$  values were calculated using equations 5 and 16. Equation 5 describes a pH profile that is bell-shaped and has two  $\text{pK}_a$  values, where  $K_1$  and  $K_2$  are the dissociation constants for the ionizable groups and  $C$  is the pH-independent value of the kinetic parameter. Equation 16 is similar to equation 5 but with only one ionizable group which must be unprotonated. Stopped-flow traces were fit to equation 9 which describes a biphasic exponential decay;

A is the measured absorbance,  $\lambda_1$  and  $\lambda_2$  are the first order rate constants for the two phases,  $A_1$  and  $A_2$  are the absorbances of species A and B at time t, and  $A_\infty$  is the final absorbance. The rates of flavin reduction as a function of amino acid concentration were fit to equation 8, where  $k_{\text{red}}$  is the maximum rate of flavin reduction and  $K_d$  is the apparent dissociation constant for the substrate.

$$v = \frac{VA}{K_m(1 + F_i(E_{vk})) + A(1 + F_i(E_v))} \quad (2)$$

$$v = \frac{VA}{K_m\left(1 + \frac{I}{K_i}\right) + A} \quad (10)$$

$$\log Y = \log \frac{C}{1 + \frac{H}{K_1} + \frac{K_2}{H}} \quad (5)$$

$$\log Y = \log \frac{C}{1 + \frac{H}{K_1}} \quad (16)$$

$$A = A_\infty + A_1 e^{-\lambda_1 t} + A_2 e^{-\lambda_2 t} \quad (9)$$

$$k_{\text{obs}} = \frac{k_{\text{red}}A}{K_d + A} \quad (8)$$

## RESULTS

*Phenylalanine Scanning.* In the crystal structure of LAAO with aminobenzoate bound, Tyr372 hydrogen bonds to the carboxylate of the inhibitor in the active site. The homology of TMO and LAAO suggests the presence of a similar tyrosine residue in the active site of TMO. Although the N-terminal FAD binding domains (residues 36-100 in TMO) are 44% identical, the C-terminal three quarters of the enzymes are only 24%

identical (Figure 13). This low identity makes it difficult to confidently identify a tyrosine residue in the C-terminal half of TMO as corresponding to Tyr372 in LAAO. Ten tyrosines are conserved in the TMO sequences available in the data base. In order to identify the tyrosine important for catalysis in TMO, each conserved tyrosine was mutated to phenylalanine, and the mutant enzymes were expressed, purified and the steady state kinetic parameters determined with tryptophan as substrate. Only mutation of Tyr413 decreases the  $V_{\max}$  and  $V/K_{\text{tp}}$  values more than four fold (Figure 14). This result identifies Tyr413 as the most critical tyrosine residue in TMO and supports the alignment of Figure 13 in which this residue aligns with Tyr372 of LAAO.

*Steady State Kinetics of Y413F and Y413A TMO.* Since the scanning mutagenesis suggested that Tyr413 enzyme is important for catalysis, the steady state kinetics of the Y413F enzyme was further characterized. In addition, the Y413A enzyme was expressed and characterized. The results of the kinetic analyses are given in Table 16. The most pronounced effect is on the  $V/K_{\text{tp}}$  values which decrease at least two orders of magnitude for both enzymes. Both mutations cause a decrease in the  $V_{\max}$  values, with a greater effect on the Y413A enzyme. Smaller changes were seen in the  $V/K_{\text{O}_2}$  values. The inhibition constants for the competitive inhibitors indoleacetamide and indolepyruvate were also measured. The  $K_i$  values for both inhibitors increase for both mutant proteins, with larger effects for the Y413F enzyme. The  $K_i$  value for indolepyruvate shows a larger increase than the  $K_i$  value for indoleacetamide with both enzymes.

*Primary Kinetic Isotope Effects.* In order to obtain information about the effects of mutation of Tyr413 on the rate of CH bond cleavage, the primary deuterium kinetic



TMO	1		MYDHFNSPSIDILYDYGPFLLKCKEMTGGIGSYSAG	35
LAAO	-18		MNVFFMFSLFLAALGSCADDRNPLAECFQENDYEEFLEIARNGLKA	29
TMO:	36	<b>TPTPR-VAIVGAGISGLVAATELLRAGVKDVLVYESRDRIGGRVWSQVFDQTRPRYIAEM</b>		94
LAAO	30	<b>TSNPKHVIVGAGMAGLSAAVYLAGAGHQVTVL-EASERPGGRV--RTRYNEEAGWYANL</b>		86
TMO	95	<b>GAMRFPPSATGLFHYLKKFGISTSTTFDPGVDTELHY-RGKRYHWPAGKKPPELFRRV</b>		153
LAAO	87	<b>GPMRLPEKHRIVREYIRKFDLRLNEFSQEN---DNAWYFIKNI RKKVGEVKKDPGLLKYP</b>		143
TMO	154	YEGWQSLLSEGYLLEG--GSLVAPLDITAMLSKGRLEEAIAWQGLNVFRDCSFYNAIV		211
LAAO	144	VKPSEAGKSAGQLYEESLGKVVVEELKRT-----NCSYILNKY		180
TMO	212	CIFTGRHPPGGDRWARPEDFELFGLSGLIGSGGF LPVFQAGFTEILRM-VINGYQSDQRLI		270
LAAO	181	DTYSTKEYLIKEGDLSPGAVDMI GDLLNEDSGYY----VSFIESLKHDDIFAYEKRFDEI		236
TMO	271	PDGISSLAARLADQSF DGKALRDRVCF-SRVGRISREA EKII IQTEAGEQR----VFDRV		325
LAAO	237	VDGMDKLP TAMY-----RDIQDKVHFNAQVIKIQQNDQKVTVVYETLSKETPSVTADYV		290
TMO	326	IVTSSNRAMQMIHCLTDES EFLSRDVARAVRETHLTGSSKLFILTRTKFWIKNKLPTTIQ		385
LAAO	291	IVCTTSRAVRLIKF---NPPLL PPK-AHALRSVHYRSGTKIFLTCTTKFW-----E		337
TMO	386	SDGLVRGVYCLD-----YQPDEPEGHGV-VLLSYTWEDDAQKMLAMPDKKTRCQVLVDD		438
LAAO	338	DDGIHGKSTTDLPSRFIYYPNHNFTNGVGVIIAMGIGDDANFFQAL-DFKDCADIVFND		396
TMO	439	LAAIH----PTFASYLLPVDGDYERYVLHHDWLTDPHSAGAFKLNYPGEDVYSQRLFFQP		494
LAAO	397	LSLIHQLPKKDIQSFCYP-----SVIQWSLDKYAMGGITFTFP----YQFQHFSDP		444
TMO	495	MTANSPNKDTGLYLAGCSCSFAGGWIEGAVQTALNSA----CAVLRSTGGQLSKGNPL		548
LAAO	445	LTASQGR----IYFAGEYTAQAHGWIDSTIKSGLRAARDVNLA SENPSGIHLSNDNEL		498

FIGURE 13. Amino acid sequence alignment of *P. savastanoi* tryptophan 2-monooxygenase and *C. rhodostoma* L-amino acid oxidase. The alignment was generated with the program PSI-Blast using the amino acid sequence of TMO as a probe. The numbering for LAAO is that used in reference (27). The residues shown in *italics* were not used in the alignment. The conserved amino acids are in bold. Tyr372 of LAAO and Tyr413 of TMO are shown in white letters.

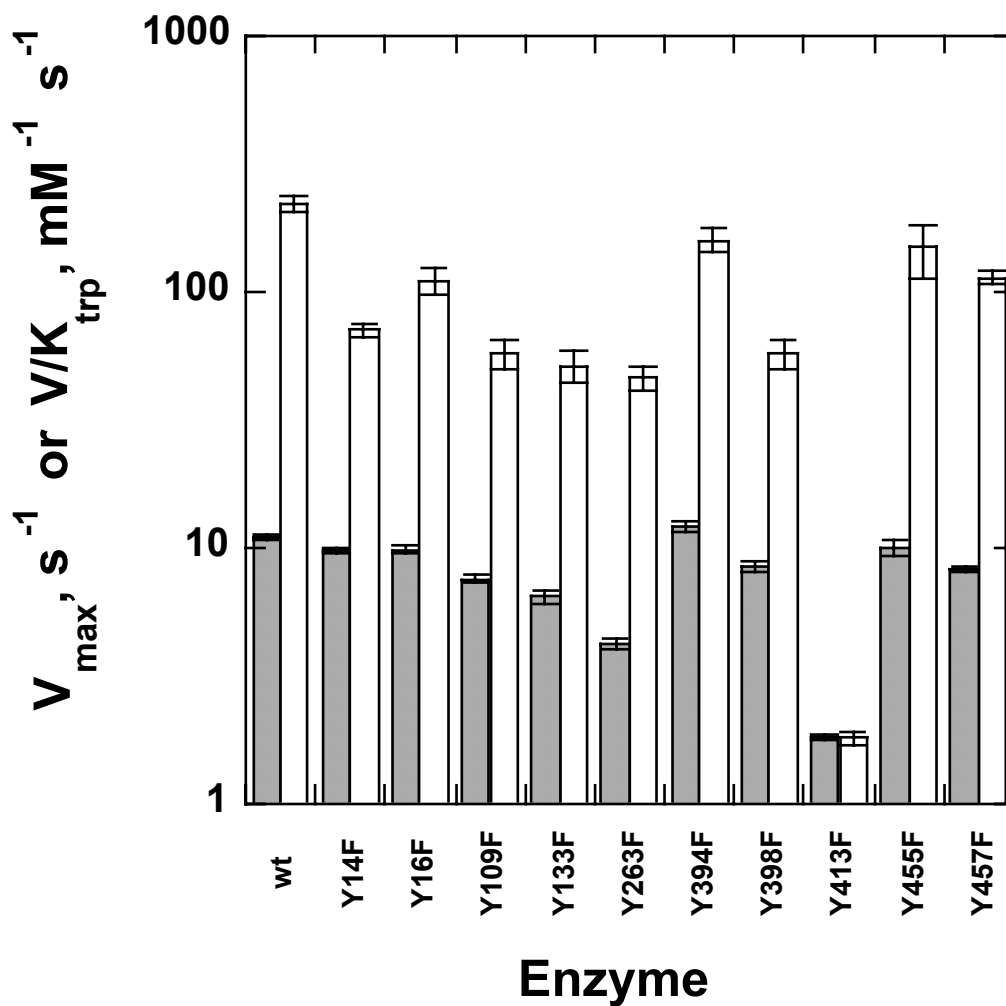


FIGURE 14. Results of phenylalanine scanning mutagenesis of TMO. Apparent steady state  $V_{\max}$  (gray bars) and  $V/K_{\text{trp}}$  (clear bars) values for wild-type and mutant TMO were determined as described in Experimental Procedures.

isotope effects with tryptophan as substrate were measured. In the wild-type enzyme the  $^D V_{\max}$  and  $^D(V/K_{\text{trp}})$  values are very close to unity, indicating that CH bond cleavage is not rate limiting (Table 16) (29). For the Y413F enzyme the  $^D V_{\max}$  and  $^D(V/K_{\text{trp}})$  values both increase to about 2. With the Y413A enzyme both isotope effects increase further to a value of about 4 (Table 16).

*Spectral Changes During Flavin Reduction.* When wild-type TMO is mixed with tryptophan in the absence of oxygen the absorbance between 350 and 520 decreases and that above 520 increases (Figure 15) (29). These changes in absorbance are very rapid and are followed by a slow decrease in absorbance at all wavelengths until the fully reduced enzyme spectrum is formed. The long wavelength absorbance is due to the reduced enzyme imino acid intermediate (29). With the wild-type enzyme in absence of oxygen this intermediate dissociates at a rate of  $0.0080 \pm 0.003 \text{ s}^{-1}$  to produce the free reduced enzyme. In the reduction of the Y413A and Y413F enzymes the rapid decrease in absorbance between 320 and 520 nm is also observed, but the spectrum of the reduced flavin is obtained at a rate of  $0.015 \pm 0.004 \text{ s}^{-1}$ . Neither mutant enzyme showed any absorbance at long wavelengths (Figure 15). The reduction of Y413A enzyme was also monitored in the stopped-flow spectrophotometer with a diode-array detector and no long wavelength absorbance was detected (data not shown).

*Rapid Reaction Kinetics.* The rate of flavin reduction by tryptophan was measured directly by monitoring the decrease in the absorbance at 466 nm in the stopped-flow apparatus under anaerobic conditions. This was only possible for the Y413A enzyme. The mutant enzymes are purified with indoleacetamide bound, as is the wild-type enzyme (83). The indoleacetamide must be removed for rapid reaction kinetic analyses. When this was done by the method developed for the wild-type enzyme, which involves dialysis against methanol, both mutant proteins lost all activity. An alternative

method was developed in which the indoleacetamide complexed enzyme was reduced several times with excess phenylalanine to displace the indoleacetamide. With this method it was possible to obtain the fully active Y413A enzyme without indoleacetamide. However, this enzyme was unstable in the absence of indoleacetamide and had to be used immediately for stopped-flow experiments. Even with the modified protocol, the Y413F enzyme had no activity once the indoleacetamide was removed, so that rapid reaction analyses could be not carried out with this mutant protein.

With Y413A TMO as with the wild-type enzyme, flavin reduction is biphasic; only the rate of the fast phase is substrate dependent (29). The rate of the fast phase as a function of tryptophan concentration could be fit to equation 6 to yield the limiting rate of reduction,  $k_{red}$ , and the  $K_d$  value for tryptophan. The  $k_{red}$  value for Y413A TMO is 195 fold less than the wild-type value, and the  $K_d$  value 13 fold higher than the wild-type value (Table 17). The  $^Dk_{red}$  value is greater for the mutant enzyme than for the wild-type enzyme.

*Hydrogen Peroxide Formation.* The amounts of hydrogen peroxide formed in the reactions catalyzed by Y413F and Y413A TMO were determined by measuring the decrease in the rate of oxygen consumption in the presence of catalase. For the wild-type enzyme with tryptophan as a substrate, catalase has no effect on the rate of oxygen consumption, indicating no hydrogen peroxide is produced (83). With the Y413F and Y413A enzymes the rates decrease in the presence of catalase. The magnitude of the change in the rate of oxygen consumption was used to calculate the amount of hydrogen peroxide released per oxidized tryptophan during catalysis. The Y413F enzyme produced  $0.75 \pm 0.01$  mol of hydrogen peroxide per tryptophan consumed, while  $0.95 \pm 0.025$  mol of  $H_2O_2$  were produced by the Y413A enzyme.

Table 16. Steady State Kinetic Parameters for Wild-type and Mutant Tryptophan 2-Monooxygenases\*

Parameters	Wild-type <sup>d</sup>	Y413F	Y413A
$V_{\max}$ , s <sup>-1a</sup>	13.2 ± 0.7	4.0 ± 0.3	0.69 ± 0.03
$V/K_{\text{trp}}$ , mM <sup>-1</sup> s <sup>-1b</sup>	360 ± 37	1.8 ± 0.1	0.35 ± 0.02
$K_{\text{trp}}$ , mM <sup>b</sup>	0.04 ± 0.005	1.0 ± 0.1	1.48 ± 0.14
$V/K_{\text{O}_2}$ , mM <sup>-1</sup> s <sup>-1a</sup>	140 ± 18	18 ± 3	6 ± 1
$K_{\text{O}_2}$ , mM <sup>a</sup>	0.09 ± 0.01	0.22 ± 0.05	0.12 ± 0.02
<sup>D</sup> $V_{\max}$ <sup>c</sup>	1.22 ± 0.07	1.9 ± 0.1	4.4 ± 0.3
<sup>D</sup> ( $V/K_{\text{trp}}$ ) <sup>b</sup>	1.16 ± 0.25	2.1 ± 0.1	4.0 ± 0.4
$K_{\text{indoleacetamide}}$ , μM <sup>b</sup>	16 ± 2	76 ± 6	47 ± 5
$K_{\text{indolepyruvate}}$ , μM <sup>b</sup>	40 ± 9 <sup>c</sup>	388 ± 50	216 ± 35

\*Standard conditions: 50 mM Tris, 1 mM EDTA, 0.5 mM dithiothreitol, pH 8.3, at 25 °C.

<sup>a</sup> Measured by varying the concentration of oxygen at 2.5 mM or 20 mM tryptophan for the wild-type and mutant enzymes, respectively.

<sup>b</sup> Measured by varying the tryptophan concentration at 230 μM oxygen.

<sup>c</sup> Determined by comparing the rates with 10 mM [ $\alpha$ -H] and 10 mM [ $\alpha$ -<sup>2</sup>H]tryptophan at 1.2 mM oxygen.

<sup>d</sup> From reference (29).

<sup>e</sup> This work.

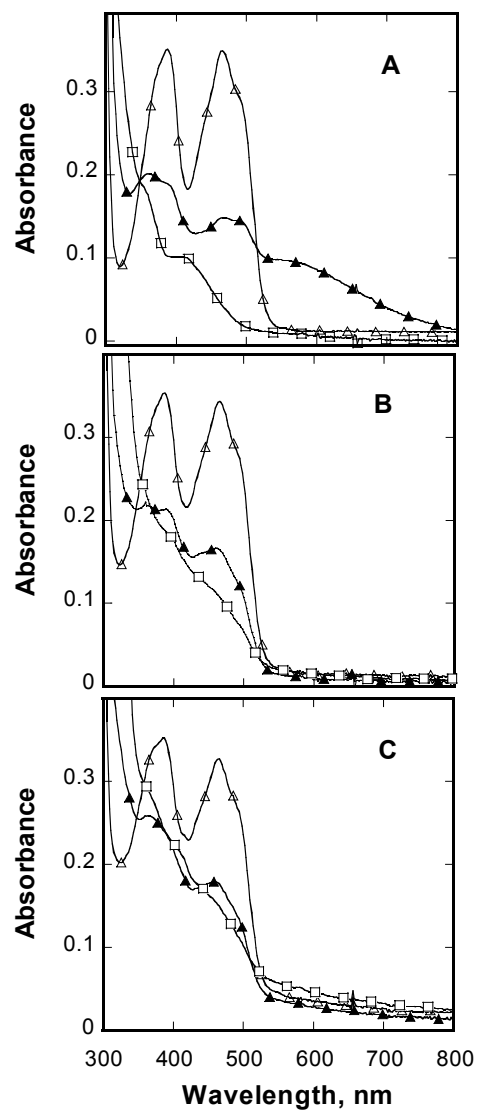


FIGURE 15. Spectral changes during reduction of TMO by tryptophan. A, the reduction of the wild-type enzyme in the absence of oxygen before ( $\Delta$ ), 20 sec ( $\blacktriangle$ ) and 30 min ( $\square$ ) after addition of 1 mM tryptophan. For the Y413A (B) and Y413F (C) enzymes the spectra were taken before ( $\Delta$ ), 15 sec ( $\blacktriangle$ ) and 10 min ( $\square$ ) after addition of 3 mM tryptophan. The conditions were 50 mM Tris, 1 mM EDTA, 0.5 mM dithiothreitol, pH 8.3, 25 °C.

Table 17. Rapid Reaction Kinetic Parameters for Wild-type and Y413A Tryptophan 2-Monooxygenases\*

Enzymes	$k_{\text{red}}, \text{s}^{-1}$	$K_{\text{d}}, \text{mM}$	${}^{\text{D}}k_{\text{red}}$
wild-type <sup>a</sup>	$139 \pm 4$	$0.11 \pm 0.015$	$2.4 \pm 0.06$
Y413A	$0.71 \pm 0.02$	$1.2 \pm 0.1$	$4.2 \pm 1.2^{\text{b}}$

\* Conditions: 50 mM Tris, 1 mM EDTA, 0.5 mM dithiothrietol, pH 8.3, 25 °C.

<sup>a</sup> From reference (29)

<sup>b</sup> Determined by comparing the rates of flavin reduction at 10 mM [ $\alpha$ -H] and 10 mM [ $\alpha$ -<sup>2</sup>H]tryptophan.

*pH Studies.* The effect of pH on the  $V/K_{\text{trp}}$  value was determined for both mutant enzymes. The wild-type  $V/K_{\text{trp}}$  pH profile is bell-shaped, consistent with the involvement of two ionizable groups, one with an apparent  $\text{pK}_a$  value of 5.3 and the other with an apparent  $\text{pK}_a$  value of 9.9 (82). The  $V/K_{\text{trp}}$  pH profiles of both the Y413F and the Y413A enzymes show a single  $\text{pK}_a$  with a value close to 6 for a group that must be deprotonated for activity (Table 18 and Figure 16).

## DISCUSSION

An important part of the study of any enzyme mechanism is the identification of residues involved in catalysis. For the flavoenzymes that catalyze the oxidative decarboxylation of amino acids such structural information is lagging more mechanistic studies. There is no available amino acid sequence for L-arginine 2-monooxygenase or L-lysine 2-monooxygenase, while only the first 90 residues of L-phenylalanine oxidase has been sequenced (98). In contrast complete amino acid sequences of TMO from several organisms are available. No three dimensional structural information is available for any of these enzymes, including TMO. We have identified LAAO as a homologue of TMO (96). LAAO and TMO both act on L-amino acids, prefer phenylalanine and tryptophan as substrates, and have identical reductive half reactions in which the  $\alpha$  CH bond of the amino acid is cleaved and an imino acid intermediate is formed (74, 83). The identification of LAAO as a homologue is especially important since the crystal structure of the enzyme from *Calloselasma rhodostoma* has been solved (27). The active site of LAAO shows that Arg90 and Tyr372 are critical for binding the amino acid substrate. The results of mutagenesis of the conserved tyrosine residues in TMO shown in Figure 14 identify Tyr413 as the residue homologous to Tyr372 of LAAO. This result



Table 18. pK<sub>a</sub> Values for Wild-type and Tyr413 Mutant Tryptophan 2-Monooxygenases\*

Enzyme	pK <sub>a</sub>	pK <sub>b</sub>	Equation
wild-type	5.34 ± 0.05	9.89 ± 0.05	3
Y413F	6.20 ± 0.06		4
Y413A	6.12 ± 0.06		4

\*Conditions: 250 μM O<sub>2</sub>, 100 mM ACES, 52 mM Tris, 52 mM ethanolamine, 25 °C.

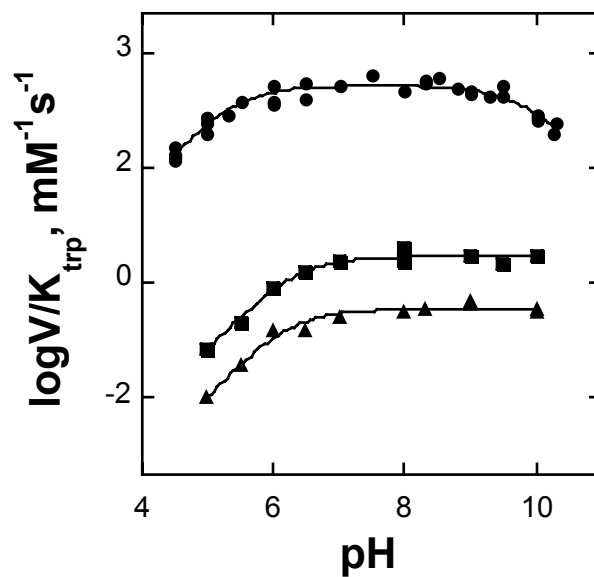


FIGURE 16.  $V/K_{\text{trp}}$  pH dependence of the wild-type (●), Y413A (■) and Y413F (▲) enzymes. The lines are fits of the data to equation 5 for the wild-type enzyme and to equation 16 for the mutant enzymes.

validates the sequence alignment shown in Figure 13 and further supports the homology between LAAO and TMO.

The detailed characterization of the effects of mutagenesis of Tyr413 confirm its importance for catalysis and provide insight into the role of this residue and of Tyr372 in LAAO. The effect of the mutation on the inhibition constants can be used as a measure of the contribution of Tyr413 to binding. The  $K_{\text{indolepyruvate}}$  values increase more than 5-10 fold for both mutant enzymes, while the  $K_{\text{indoleacetamide}}$  value increases by half as much. The greater increase in the  $K_{\text{indolepyruvate}}$  values is consistent with Tyr413 interacting with the carboxylate of the inhibitor and thus of the substrate. The increase in the  $K_{\text{indoleacetamide}}$  suggests that Tyr413 has a weak interaction with the carbonyl oxygen of indoleacetamide or that the binding of the indole ring has been affected by the mutations. The changes in binding energies for indolepyruvate are  $-1.3$  and  $-1.0$  kcal mol<sup>-1</sup> for the Y413F and Y413A enzymes, respectively. Using the  $K_d$  value obtained in the stopped-flow for the Y413A enzyme, a change in the binding energy for the substrate of  $-1.4$  kcal mol<sup>-1</sup> can be calculated (Table 19). These values are close to the values expected for the elimination of a hydrogen bond (99).

If Tyr413 is to form a hydrogen bond with a carboxylate oxygen, the phenolic oxygen must be protonated. The pH dependences of the  $V/K_{\text{trp}}$  value for both the Y413F and the Y413A enzyme show only one  $\text{pK}_a$  value of 6.0 for a residue that must be deprotonated for activity. This is different from the wild-type pH profile where two  $\text{pK}_a$ 's are observed, one for a group that must be deprotonated for activity with a  $\text{pK}_a$  value of 5.3, and another for a group that must be protonated for activity with a  $\text{pK}_a$  value of 9.9. The lack of the second  $\text{pK}_a$  in the alkaline region of the pH profiles of the mutant enzymes suggests that Tyr413 is the residue responsible for that  $\text{pK}_a$ .

Table 19. Differences in Binding Energies and Activation Energies Between Wild-type and Tyr413 Mutant Tryptophan 2-Monooxygenases\*

Enzymes	$\Delta\Delta G_s$ (kcal/mol)	$\Delta\Delta G_{red}^\ddagger$ (kcal/mol)	$\Delta\Delta G^\ddagger$ (kcal/mol)	$\Delta\Delta G_I$ (kcal/mol)
Y413F	nd <sup>a</sup>	2.0	3.1	-1.3
Y413A	-1.4	3.0	4.0	-1.0

\*The difference in binding energies ( $\Delta\Delta G_s$ ) were calculated by using the equation  $\Delta\Delta G_s = RT \ln [K_{wt}/K_{mutant}]$ . For the binding energies of inhibitors ( $\Delta\Delta G_I$ ) the  $K_i$  values for indolepyruvate were used, and for the activation energies ( $\Delta\Delta G^\ddagger$ ) the  $V/K_{trp}$  values were used. The change in the activation energies for flavin reduction ( $\Delta\Delta G_{red}$ ) were calculated using the  $k_{red}$  value measured for the Y413A and the value for  $V_{max}$  for the Y413F enzyme.

<sup>a</sup>nd, not determined.

The deletion of the hydroxyl or phenol moiety at position 413 of TMO produces a decrease in the  $V_{\max}$  value and has a more pronounced effect on the  $V/K_{\text{trp}}$  value. These effects suggest that this residue is involved in catalysis. In the mechanism of Scheme 20 the step with rate constant  $k_3$  includes the chemical step where CH bond cleavage occurs. In TMO the value of  $k_3$  can be directly determined by measuring the rate of flavin reduction (29). For the Y413A enzyme the  $k_3$  value decreases 195 fold as compared to the wild-type value. The  $k_3$  value in Y413A TMO is very close to the value of  $V_{\max}$ ; this indicates that catalysis in the Y413A enzyme is totally limited by the rate of flavin reduction. No stopped-flow data are available for the Y413F enzyme due to the total loss of activity in the absence of indoleacetamide. For the wild-type TMO, the intrinsic  $\text{pK}_a$  for a group in the free enzyme which must be deprotonated for catalysis is  $6.0 \pm 0.2$  (82). The  $\text{pK}_a$  value of 6.1-6.2 in the  $V/K_{\text{trp}}$  pH profiles for the Tyr413 mutant enzymes is consistent with a decrease in the forward commitment to catalysis ( $k_3/k_2$ ) to a value less than 0.5 such that the  $\text{pK}_a$  observed in the  $V/K_{\text{trp}}$  profiles for both mutant proteins is within 0.2 units of the intrinsic  $\text{pK}_a$  value. If the intrinsic kinetic isotope effect on  $k_3$  for Y413F is similar to the intrinsic isotope effect of 2.4 for the wild-type enzyme using equation 8; the value of  $k_3/k_7$  can be calculated as  $0.5 \pm 0.4$ . This result suggest that the  $k_3$  value must be very close to the observed  $V_{\max}$  value of  $4 \text{ s}^{-1}$  and that  $k_7$  must be 2 fold higher than  $k_3$  for Y413F enzyme. Thus, this mutation decreases the rate of flavin reduction by 35 fold for the Y413F enzyme. For the Y413A enzyme the value of  $k_7$  must be at least 10 times greater than  $k_3$  since this is the limiting value on  $V_{\max}$  (Table 20).

With the  $k_3$  values for both Y413F and Y413A enzymes the effects of the mutation on the chemical step can be calculated. The changes in the activation energies for flavin reduction ( $\Delta\Delta G_{\text{red}}^\ddagger$ ) are  $2.0 \text{ kcal mol}^{-1}$  and  $3.0 \text{ kcal mol}^{-1}$  for the Y413F and

Y413A enzymes, respectively (Table 19). This indicates that the main function of Tyr413 is on the chemical steps leading to CH and flavin reduction.

For Y413A TMO both the  $^D V_{\max}$  and the  $^D(V/K_{\text{trp}})$  values are around 4.2. This value is larger than the intrinsic isotope effect measured with tryptophan for the wild-type enzyme (29). This suggests that in the Y413A enzyme the transition state is more symmetric with this substrate. A similar isotope effect was measured with alanine and methionine as substrates for wild type TMO (82). It is possible that the Y413A mutation has changed the transition state with tryptophan to a transition state more similar to that of alanine and methionine. Changes in the intrinsic isotope effect values are also observed with the pig kidney D-amino acid oxidase where the values vary from 3 to 5.7 depending on the amino acid substrate (100).

The reaction of the reduced enzyme with oxygen is affected in both mutant enzymes, as seen by their reduced  $V/K_{\text{O}_2}$  values (Table 16). In the wild-type enzyme oxygen reacts with the reduced enzyme imino acid complex and decarboxylation of the imino acid occurs in this step (Scheme 20). In the mutant enzymes the long wavelength charge-transfer absorbance band is not observed and the imino acid-enzyme complexed dissociates at a faster rate than in the wild-type enzyme (Figure 15) (29). This result suggests that the mutation affects the binding of the imino acid intermediate and the orientation of the indole ring with respect to the isoalloxazine ring of the FAD. In the wild-type enzyme the  $V/K_{\text{O}_2}$  value with methionine is lower than the  $V/K_{\text{O}_2}$  value with tryptophan (29). It has been suggested that the active site with of TMO with methionine is more solvent exposed since hydrogen peroxide is released during catalysis with this substrate (29). A different conformation of the enzyme-tryptophan complex must be present in the mutants during catalysis since hydrogen peroxide is released and the charge transfer absorbance of the imino acid enzyme complex is not observed. The

decrease in oxygen reactivity in the Tyr413 mutants might arise from a more open solvent exposed active site that is not optimized for reaction with molecular oxygen. This is in line with the results in glucose oxidase where changes in the electrostatic environment of the active site decrease the  $V/K_{O_2}$  value several orders of magnitude (101).

In summary the detailed characterization of Tyr413 mutant enzymes identifies this residue as the active site residue in TMO corresponding to Tyr372 of LAAO. From comparison of the rate constants for the steps in the catalytic cycle of TMO it can be concluded that Tyr413 is involved in binding but the main role is in stabilization of the transition state for CH bond cleavage and flavin reduction (Table 20).

Table 20. Intrinsic Rate Constants for Wild-type and Tyr413 Mutant Tryptophan Monooxygenases.

Kinetic Parameter	Wild-type enzyme <sup>a</sup>	Y413F	Y413A
$K_d$ , mM	$0.11 \pm 0.05$	$1.0 \pm 0.1^b$	$1.2 \pm 0.1^c$
$k_3$ , $s^{-1}$	$139 \pm 4$	$4 \pm 0.3$	$0.71 \pm 0.02^c$
$k_5$ , $mM^{-1}s^{-1}$ <sup>e</sup>	$140 \pm 18$	$18 \pm 3$	$6 \pm 1$
$k_7$ , $s^{-1}$	14	> 8	>7

<sup>a</sup> Values from references (29).

<sup>b</sup> For the mutant enzymes the  $K_m = K_d$  since there are no commitments.

<sup>c</sup> Values measured in the stopped-flow spectrophotometer.

<sup>e</sup> Values corresponding to the  $V/K_{O_2}$  values.



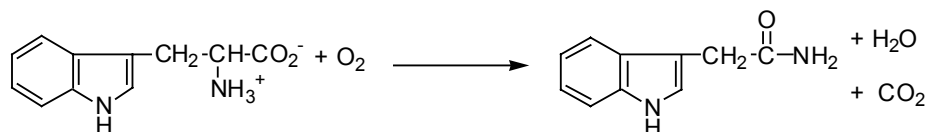
## CHAPTER VII

**ARG98 IS IMPORTANT FOR SUBSTRATE BINDING AND TRANSITION  
STATE STABILIZATION IN THE REACTION CATALYZED BY  
TRYPTOPHAN 2-MONOOXYGENASE**

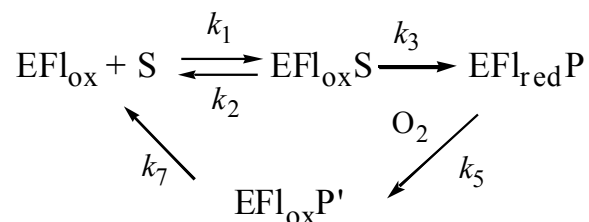
**INTRODUCTION**

The biosynthesis of the plant hormone indoleacetic acid (IAA) by plasmid encoded enzymes from plant pathogens such as *Agrobacterium tumefaciens* and *Pseudomonas savastanoi* induces the formation of tumor like structures at the site of infection (79, 95). The biosynthesis of IAA by these bacteria involves a two step reaction in which tryptophan is converted to indoleacetic acid by tryptophan 2-monooxygenase and indoleacetamide hydrolase (94). Tryptophan 2-monooxygenase (TMO) is an FAD containing enzyme that catalyzes the oxidative decarboxylation of tryptophan to indoleacetamide (Scheme 21). TMO can also oxidize other L-amino acids such as phenylalanine, methionine and alanine with decreased activity as the size of the substrate decreases (29, 83). The kinetic mechanism of TMO has been determined with tryptophan as substrate and can be divided into two half-reactions (Scheme 22). In the

Scheme 21



Scheme 22



reductive half-reaction the  $\alpha$ -CH bond of the amino acid is broken and a hydride equivalent is transferred to the FAD prosthetic group, forming the reduced enzyme and the imino acid. In the oxidative half-reaction the reduced enzyme-imino acid complex reacts with molecular oxygen forming oxidized FAD and the amide product (29).

No three-dimensional structural information is available for the flavoenzymes that catalyze the oxidative decarboxylation of amino acids, TMO, phenylalanine oxidase (30), lysine monooxygenase (32) and L-arginine 2-monooxygenase (31). Previously we have identified the flavoprotein L-amino acid oxidase as a structural homologue of TMO (96). LAAO and TMO show high identity in the region corresponding to the FAD binding domain in LAAO (Figure 17). This region is predicted to be the FAD binding region in TMO since it contains the dinucleotide binding motif (102). Additionally, the GG motif identified in the LAAO family of enzymes as important for FAD binding is also found in the TMO enzymes. This GG motif is also found in monoamine oxidase and other flavoenzymes families, suggesting that they share common ancestry (103). In the crystal structure of LAAO, the carboxylate of the competitive inhibitor *o*-aminobenzoate ion pairs with Arg90 (Figure 18). This residue corresponds to Arg98 in TMO (Figure 17).

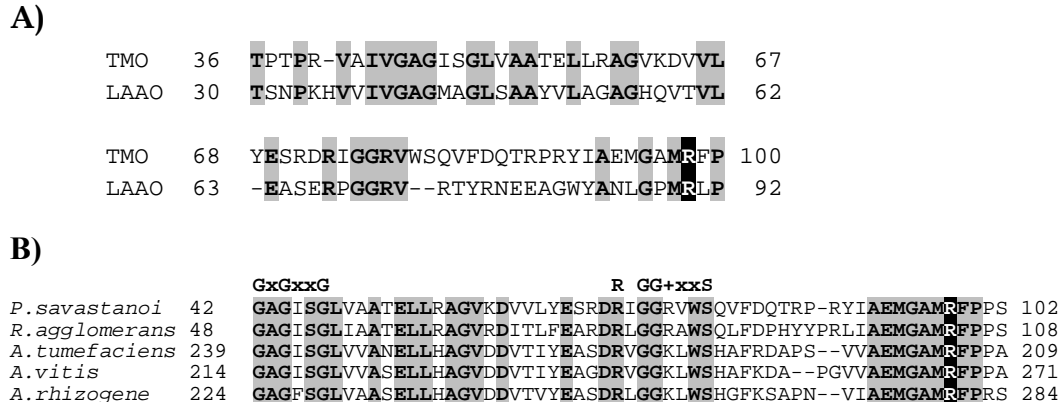


FIGURE 17. A) Amino acid sequence alignment of *P. savastanoi* tryptophan 2-monooxygenase with the FAD binding domain of *C. rhodostoma* L-amino acid oxidase. The alignment was generated with the program PSI-Blast using the amino acid sequence of TMO as a probe. The numbering for LAAO is that used in reference (27). B) Sequence of putative FAD binding domain of tryptophan 2-monooxygenases. The GxGxxG motif of the putative nucleotide binding region and the GG motif of the family of L-amino oxidases are indicated (103). The conserved amino acids are highlighted. The conserved arginine residue is shown in white letters.

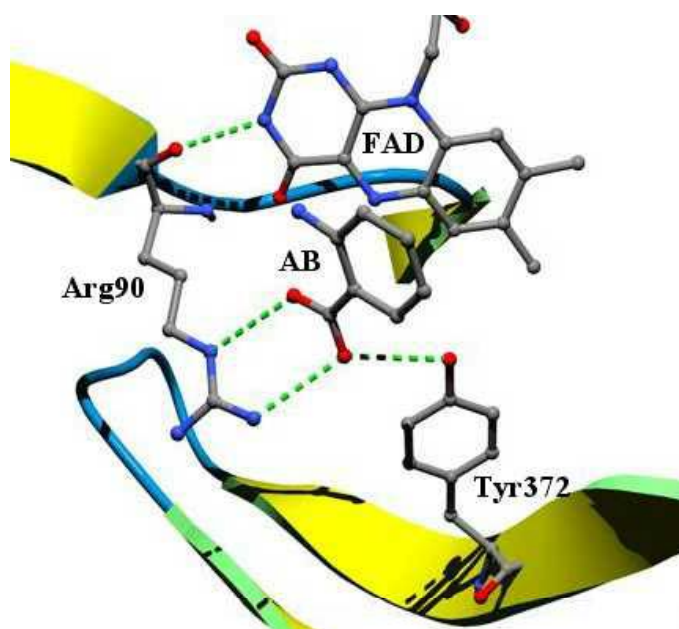


FIGURE 18. Active site of *Calloselasma rhodostoma* L-amino acid oxidase with aminobenzoate (AB) bound showing the interactions with Arg90 and Tyr372. The figure was made using SwissPDBViewer and the PDB file 1F8S.

## EXPERIMENTAL PROCEDURES

*Materials.* L-Tryptophan was purchased from USB (Cleveland, OH). Indoleacetamide, indolepyruvic acid and glucose oxidase were from Sigma (St. Louis, MO). DEAE-Sephacel and phenyl-Sepharose were from Amersham Pharmacia (Uppsala, Sweden), *Escherichia coli* M15 (pREP4) was from Qiagen (Valencia, CA) and catalase from Roche (Basel, Switzerland). [ $\alpha$ - $^2$ H]-L-Tryptophan was synthesized by method of Kiick and Phillips (97).

*Methods.* Enzyme activity assays were performed on a Hansatech oxygen monitoring system (Norfolk, UK) with a computer interfaced graphical mode and on a Yellow Springs Instrument model 5300 oxygen electrode (Yellow Springs, OH) with a Servogor 124 (Leeds, UK) chart recorder. UV-Visible spectra were taken on a Hewlett-Packard Model 8458A diode array spectrophotometer. The HPLC apparatus consisted of Waters 2475 pumps with a Waters automated gradient maker, a Waters 625 scanning fluorescence detector, and Millennium software for data processing. Rapid reaction kinetic measurements were performed on an Applied Photophysics SX.18MV stopped-flow spectrophotometer. The stopped-flow spectrophotometer was made anaerobic by filling the system with a solution of 1 mM EDTA, 1 mM glucose, 50 mM Tris pH 8.5, containing 0.03  $\mu$ M glucose oxidase the night before the experiment was performed. Substrate and enzyme solutions were made anaerobic by cycles of vacuum and flushing with oxygen free argon.

*DNA Manipulation.* The expression of wild-type TMO using the pQE51 plasmid has previously been described (96). This was used as the template for construction of plasmids expressing the mutant enzymes. The primers for the R98A mutagenesis were 5'-CATTGCAGAAATGGGTGCGATGGCGTTTCCTCCCAGTGCAACTGGC-3' and 5'-GCCAGTTGCACTGG GAGGAAACGCCCATCGCACCCATTTCTGCAATG-3'.

For the R98K mutagenesis the primers were 5'-CATTGCAGAAATGGGTGCGATGAAATTTCCTCCCAGTGCAACTGGC-3' and 5'-GCCAGTTGCACTGGGAGGAAATTTTCATCGCACCCATTTCTGCAATG-3' (the nucleotides changed are underlined). Site directed mutagenesis was performed using the QuikChange protocol (Stratagene). The protein coding regions for all the plasmids were sequenced to ensure that no unwanted mutations were incorporated during the polymerase chain reaction.

*Enzyme Assays.* Standard enzyme assays were in 50 mM Tris, 250  $\mu$ M oxygen, 1 mM EDTA, 0.5 mM dithiothreitol, pH 8.3, at 25 °C, at different concentrations of [ $\alpha$ -H]-tryptophan or [ $\alpha$ -<sup>2</sup>H]-tryptophan. Different oxygen concentrations were obtained by bubbling the assay mixture with the appropriate O<sub>2</sub>/N<sub>2</sub> gas mixtures. Enzyme activity as a function of pH was measured in 52 mM Tris, 52 mM ethanolamine, 100 mM ACES. The formation of hydrogen peroxide was determined by measuring the decrease in the oxygen consumption upon addition of catalase (0.01 mg/ml) at 17 mM tryptophan.

*Protein Expression and Purification.* For growth of the wild-type and Arg98 mutant enzymes a single colony of *Escherichia coli* M15 (pREP4) containing the appropriate plasmid was used to inoculate an 60 ml culture of LB (100  $\mu$ g/ml ampicillin, 25  $\mu$ g/ml kanamycin). After overnight growth at 37 °C, 6 flasks containing 1.5 L of LB (100  $\mu$ g/ml ampicillin, 25  $\mu$ g/ml kanamycin) were inoculated with 10 ml of the overnight culture. The cultures were incubated at 37 °C until the Abs<sub>600</sub> reached a value of 0.6-0.8. At this point 1.5 ml of 0.5 M isopropyl- $\beta$ -D-thiogluconopyranoside was added to each flask and the temperature was decreased to 28°C. After incubation for an additional 6-8 hr, the cells were harvested by centrifugation at 5000xg for 30 min at 4 °C. Purification of the wild-type enzyme was performed as described in reference (83). For purification of the Arg98 mutant enzymes the cell pellets were resuspended in 250

ml of 50 mM Tris, 1 mM EDTA, 0.5 mM dithiothreitol, 50  $\mu$ M indoleacetamide, 0.5 mM phenylmethylsulfonyl fluoride, 0.2 mg/ml lysozyme, pH 8.3. After stirring the cell suspension for 30 min at 4 °C, the cells were lysed by sonication. Cell debris and insoluble proteins were precipitated by centrifugation at 20,000xg for 30 min at 4 °C. The resulting supernatant was brought to 0.5 % (w/v) polyethyleneimine, using a 0.1 g/ml stock solution in 50 mM Tris, 1 mM EDTA, 0.5 mM dithiothreitol, pH 8.3. After centrifugation at 20,000xg for 30 min at 4 °C, the supernatant was brought to 60% saturation of ammonium sulfate. The solution was stirred at 4 °C for 20 min, and the protein was precipitated by centrifugation at 20,000xg for 30 min at 4 °C. The resulting pellets were resuspended in 20 ml of 50 mM Tris, 1 mM EDTA, 0.5 mM dithiothreitol, 50  $\mu$ M indoleacetamide, 10% glycerol, pH 8.3, and dialyzed against 2 changes of 2 L of the same buffer. After centrifugation at 20,000xg for 20 min at 4 °C, the protein sample was loaded onto a DEAE-Sephacel column (3x20 cm) previously equilibrated with the same buffer. The mutant enzymes were eluted with a linear gradient of 0-200 mM NaCl. Both enzymes eluted around 150 mM NaCl.

*Indoleacetamide Removal.* To 5 ml of purified enzyme (~30-60  $\mu$ M) an equal volume of a saturated solution of ammonium sulfate in 50 mM Tris, 1 mM EDTA, pH 8.3, was added. After 20 min at 4 °C, the protein was precipitated by centrifugation at 20,000xg for 20 min. The enzyme was resuspended in 5 ml of 100 mM phenylalanine, 50 mM Tris, 1 mM EDTA, pH 8.3, and incubated at 4 °C for 20 min during which the protein solution went from bright yellow to light yellow. The enzyme was then precipitated by centrifugation for 20 min at 20,000xg. This procedure was repeated twice. The final pellet was suspended in 5 ml of 100 mM phenylalanine, 50 mM Tris, 1 mM EDTA, pH 8.3, and dialyzed against two buffer changes of 1 L of 50 mM Tris, 1 mM EDTA, 0.5 mM dithiothreitol, 10 % glycerol, pH 8.3. The presence of

indoleacetamide was monitored by HPLC with fluorescence detection; no traces of the compound were detected in the final enzyme samples.

*Data Analysis.* The kinetic data were analyzed using the programs Kaleidagraph (Adelbeck Software, Reading, PA) and Igor (Wavemetrics, Lake Oswego, OR). Initial rate data were fit to the Michaelis-Menten equation. Isotope effect values were obtained from fits of the data to equation 2. This equation describes separate isotope effects on  $V_{\max}$  and  $V/K_{\text{trp}}$ ;  $F_i$  is the fraction of the heavy atom,  $E_{V/K}$  is the isotope effect on  $V/K$  minus 1, and  $E_V$  is the isotope effect on  $V_{\max}$  minus 1. The inhibition constants for the wild-type and R98K enzyme were obtained using equation 10, which describes the behavior of a competitive inhibitor where  $K_i$  is the inhibition constant. The  $K_i$  values for the R98A enzyme were obtained by analyzing the effect of different inhibitor concentrations at 2.0 mM tryptophan ( $K_m = 3.3$  mM) by the method of Dixon (104). The  $V/K_{\text{trp}}$  values at different pH values for the wild-type were fit to equation 5 where  $K_1$  and  $K_2$  are the dissociation constant for the ionizable groups and  $C$  is the pH independent  $V/K_{\text{trp}}$  value. The  $V_{\max}$  value for the wild-type enzyme and the  $V_{\max}$  and  $V/K_{\text{trp}}$  values for the Arg98 mutant enzymes as a function of pH were fit to equation 17, where  $K_1$  is the dissociation constant for the ionizable group,  $Y_L$  is the activity at low pH and  $Y_H$  is the activity at high pH. Stopped-flow traces were fit to equation 9 which describes a biphasic exponential decay;  $\lambda_1$  and  $\lambda_2$  are the first order rate constants for each phase;  $A_1$  and  $A_2$  are the absorbance of each species at time  $t$  and  $A_\infty$  is the final absorbance. The



rate of the rapid phase at different concentration of tryptophan was analyzed using equation 8; here  $k_3$  is the maximum rate of flavin reduction and  $K_d$  is the apparent dissociation constant for the substrate.

$$v = \frac{VA}{K_m(1 + F_i(E_{vk})) + A(1 + F_i(E_v))} \quad (2)$$

$$v = \frac{VA}{K_m\left(1 + \frac{I}{K_i}\right) + A} \quad (10)$$

$$\log Y = \log \frac{C}{1 + \frac{H}{K_1} + \frac{K_2}{H}} \quad (5)$$

$$\log Y = \log \frac{Y_L + \frac{Y_H K_1}{H}}{1 + \frac{K_1}{H}} \quad (17)$$

$$A = A_\infty + A_1 e^{-\lambda_1 t} + A_2 e^{-\lambda_2 t} \quad (9)$$

$$k_{\text{obs}} = \frac{k_{\text{red}}A}{K_d + A} \quad (8)$$

## RESULTS

*Steady State Kinetic Parameters.* We have previously identified the enzyme LAAO as a homologue of TMO (96). The most highly conserved region corresponds to the FAD binding domain of LAAO, residues 30-92 (Figure 17). Arg90 of LAAO aligns with Arg98 in TMO; this residue is conserved in all available TMO sequences. To test the role of Arg98 in TMO this residue was changed to lysine and alanine. The steady state kinetic parameters the mutant enzymes are given in Table 21. In the R98K enzyme the  $V_{\text{max}}$  and  $V/K_{\text{trp}}$  values decrease by one and two orders of magnitude, respectively. In

the case of the R98A enzyme these values decrease even more substantially. The reactivity of the reduced enzyme with molecular oxygen was also affected in the mutant enzymes. The  $V/K_{O_2}$  values decrease 18 and 44 fold for the R98K and R98A enzymes, respectively. These results strongly suggest that the presence of an arginine at position 98 is essential for efficient catalysis in TMO.

The  $K_i$  values for indoleacetamide and indolepyruvate were also determined for the R98K and R98A enzymes. The  $K_{\text{indoleacetamide}}$  value remains unchanged for the R98K enzyme, but increases around two fold for the R98A enzyme. In contrast, the  $K_{\text{indolepyruvate}}$  value increases only slightly for the R98K enzyme while that for the R98A enzyme increases by an order of magnitude (Table 21). These results are consistent with a positive charge at position 98 being important for binding of carboxylate containing ligands in the active site of TMO.

The effect of mutation of Arg98 on the rate of CH bond cleavage was determined by measuring deuterium kinetic isotope effects. In the wild-type enzyme the rate of CH bond cleavage is only partially rate limiting on  $V_{\text{max}}$  and  $V/K_{\text{trp}}$  as indicated by the small isotope effect values on these kinetic parameters (Table 21)(82). The conservative substitution of Arg98 to lysine increases both the  $^D V_{\text{max}}$  and the  $^D(V/K_{\text{trp}})$  value significantly, while the R98A mutation increases them further (Table 21).

*Formation of Hydrogen Peroxide.* The formation of hydrogen peroxide was determined by measuring the decrease in the rate of oxygen consumption in the presence of catalase. For the wild-type enzyme with tryptophan addition of catalase has no effect on the rate of oxygen consumption, indicating that no hydrogen peroxide is formed (83). In contrast, the rate of oxygen consumption for both Arg98 mutant enzymes decreases in the presence of catalase. The decrease in the rate of oxygen consumption was used to

Table 21. Steady State Kinetic Parameters for Wild-type and Arg98 Mutant Enzymes\*

Parameters	Wild-type <sup>d</sup>	R98K	R98A
$V_{\max}$ , $S^{-1a}$	$13.2 \pm 0.7$	$1.05 \pm 0.05$	$0.21 \pm 0.003$
$V/K_{\text{trp}}$ , $\text{mM}^{-1}\text{s}^{-1b}$	$360 \pm 37$	$1.5 \pm 0.15$	$0.042 \pm 0.006$
$K_{\text{trp}}$ , $\text{mM}^b$	$0.04 \pm 0.005$	$0.30 \pm 0.04$	$3.3 \pm 0.7$
$V/K_{\text{O}_2}$ , $\text{mM}^{-1}\text{s}^{-1a}$	$140 \pm 18$	$7.5 \pm 2$	$3.2 \pm 0.2$
$K_{\text{O}_2}$ , $\text{mM}^a$	$0.09 \pm 0.01$	$0.14 \pm 0.05$	$0.067 \pm 0.005$
$^D V_{\max}^c$	$1.22 \pm 0.07$	$3.1 \pm 0.2$	$4.3 \pm 0.2$
$^D(V/K_{\text{trp}})^b$	$1.16 \pm 0.25$	$1.8 \pm 0.3$	$5.7 \pm 1.5$
$K_{\text{indoleacetamide}}$ , $\mu\text{M}^b$	$16 \pm 2$	$20 \pm 2$	$45 \pm 15$
$K_{\text{indolepyruvate}}$ , $\mu\text{M}^b$	$40 \pm 9^e$	$71 \pm 11$	$670 \pm 150$

\*Standard conditions: 50 mM Tris, 1 mM EDTA, 0.5 mM dithiothreitol, pH 8.3, at 25 °C.

<sup>a</sup> Measured by varying the concentration of oxygen at 2.5 mM or 20 mM tryptophan for the wild-type and mutant enzymes, respectively.

<sup>b</sup> Measured by varying the tryptophan concentration at 230  $\mu\text{M}$  oxygen.

<sup>c</sup> Determined by comparing the rates with 10 mM [ $\alpha$ -H] and 10 mM [ $\alpha$ -<sup>2</sup>H] tryptophan at 1.2 mM oxygen.

<sup>d</sup> From reference (27).

<sup>e</sup> This work.

calculate the amount of hydrogen peroxide produced during catalysis for these enzymes. For the R98K enzyme,  $0.90 \pm 0.06$  mol of hydrogen peroxide were formed per oxidized tryptophan, while for the R98A enzyme,  $0.97 \pm 0.03$  mol of hydrogen peroxide were produced.

*Spectral Changes During Anaerobic Reduction.* The changes in the spectra of the wild-type and Arg98 mutant enzymes during reduction by tryptophan under anaerobic conditions were determined. The spectral changes for the wild-type enzyme have been previously characterized (29). The absorbance of the flavin decreases rapidly between 350 and 520 nm and increases above 520 nm. These changes are followed by a slow decrease at all wavelengths until the spectrum of the reduced enzyme is obtained (Figure 19)(29). The long wavelength absorbance is due to a charge transfer interaction between the imino acid intermediate and the reduced flavin in the active site (29). For the Arg98 mutant enzymes the decrease in absorbance between 350 and 520 nm was observed but no increase in absorbance above 520 nm was detected. The spectra of the reduced mutant enzymes were obtained more quickly than with the wild-type enzyme (Figure 19).

*Rapid Reaction Kinetics.* The rate of flavin reduction in the absence of oxygen ( $k_3$  in Scheme 22) was measured in the stopped-flow spectrophotometer. In the absence of oxygen equal volumes of enzyme and substrate were mixed and the absorbance at 466 nm was recorded. For the wild-type and Arg98 mutant enzymes the decrease in absorbance was biphasic with only the fast phase being substrate depended. The rate of flavin reduction for the R98K enzyme decreased close to 200 fold and for the R98A enzyme almost 1000 fold compared to the wild-type enzyme (Table 22). The rate of the slow phase for the wild-type enzyme is  $0.008 \pm 0.0003 \text{ s}^{-1}$  (29), increasing to  $0.016 \pm 0.005 \text{ s}^{-1}$  and  $0.026 \pm 0.007 \text{ s}^{-1}$  for the R98K and R98A enzymes, respectively.

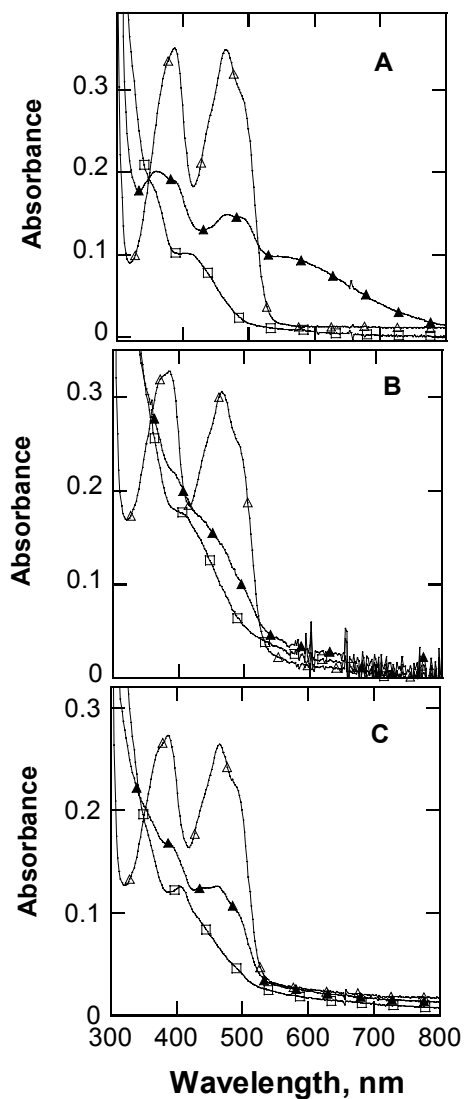


FIGURE 19. Spectral changes during reduction of wild-type and Arg98 mutant enzymes by tryptophan. (A) Reduction of the wild-type enzyme before ( $\Delta$ ), 20 sec ( $\blacktriangle$ ) and 30 min ( $\square$ ) after addition of 1 mM tryptophan. For the R98A (B) enzyme the spectra were taken before ( $\Delta$ ), 30 sec ( $\blacktriangle$ ) and 180 sec ( $\square$ ) after addition of 10 mM tryptophan. For the R98K (C) enzyme the spectra were taken before ( $\Delta$ ), 40 sec ( $\blacktriangle$ ) and 280 sec ( $\square$ ) after addition of 1.25 mM tryptophan. The conditions were 50 mM Tris, 1 mM EDTA, 0.5 mM dithiothreitol, pH 8.3, 25 °C.

Table 22. Rapid Reaction Kinetic Parameters for Tryptophan 2-Monooxygenase Enzymes.

Enzymes	$k_3, s^{-1}$	$K_d, mM$
wild-type <sup>a</sup>	$139 \pm 4$	$0.11 \pm 0.015$
R98K	$0.77 \pm 0.02$	$0.085 \pm 0.011$
R98A	$0.16 \pm 0.01$	$3.4 \pm 0.8$

<sup>a</sup>Values from reference (29).

*pH Effects.* The  $V_{\max}$  pH rate profiles for the wild-type and both mutant enzymes all show high and low activities plateaus with a single  $pK_a$  for a group that must be unprotonated for maximal activity (Figure 20 A). For the R98K and R98A enzymes the  $pK_a$  value is about 9.2, significantly higher than the wild-type enzyme the  $pK_a$  value (Table 23). The  $V/K_{\text{tp}}$  pH profile for the wild-type enzyme is bell-shaped, consistent with the presence of two ionizable groups. One group must be unprotonated for catalysis with a  $pK_a$  value of 5.3 and another group must be protonated for activity with a  $pK_a$  value of 9.9. In contrast the  $V/K_{\text{tp}}$  pH profiles for the mutant enzymes display low and high activity plateaus with single  $pK_a$  values for a group that must be unprotonated of 9.5 and 9.9 for the R98K and R98A enzymes, respectively (Figure 20 and Table 23).

## DISCUSSION

The identification of TMO as a member of the LAAO family of enzymes has opened the possibility of obtaining information about the role of active site residues of a member of this family of proteins for the first time. To date, there has been no reports of expression of a recombinant LAAO. The conservation of Arg98 in all TMOs and the conservation of Arg90 in LAAO suggest that these residue plays similar roles in the two enzymes. The steady state kinetic parameters for the R98K and R98A enzymes show that Arg98 is important for activity in TMO.

The role of this residue in the catalytic cycle of TMO can be determined by calculating the effect of the mutations on the rate constant for each step shown in Scheme 22 (Table 24)(29). The  $K_d$  value and the flavin reduction ( $k_3$ ) can be directly measured in the stopped-flow spectrophotometer, the value for  $k_5$  corresponds to the  $V/K_{O_2}$  value, and  $k_7$  can be calculated. The  $K_d$  value does not change for the R98K

Table 23. pK<sub>a</sub> Values for Wild-type and Mutant Tryptophan 2-Monooxygenases.

Enzyme	Parameter	pK <sub>1</sub>	pK <sub>2</sub>	Equation
wild-type <sup>a</sup>	V	6.20 ± 0.13		4
	V/ K <sub>trp</sub>	5.34 ± 0.05	9.89 ± 0.05	3
R98K	V	9.07 ± 0.13		4
	V/ K <sub>trp</sub>	9.50 ± 0.19		4
R98A	V	9.30 ± 0.19		4
	V/ K <sub>trp</sub>	9.86 ± 0.17		4

<sup>a</sup>Values from reference (82)



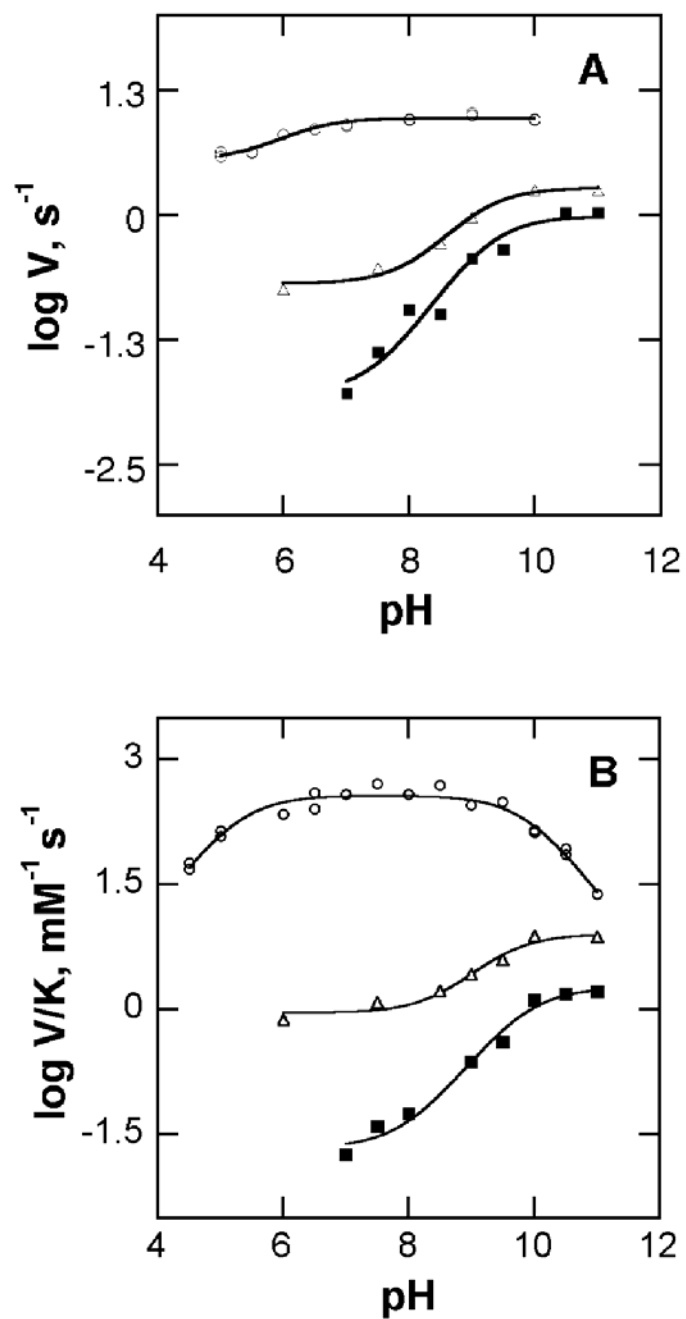


FIGURE 20.  $V/K_{trp}$  (A) and  $V_{max}$  (B) pH dependence of the wild-type (O), R98K ( $\Delta$ ) and R98A ( $\blacksquare$ ) enzymes.

enzyme while it increases close 30 fold for the R98A enzyme. This clearly indicates that the conservation of a positive charge at position 98 is essential for effective binding of tryptophan in TMO. The change in the inhibition constants for indoleacetamide and indolepyruvate support this observation and in addition demonstrate that Arg98 interact specifically with the carboxylate group. The  $K_i$  value for indoleacetamide does not change significantly for either mutant enzyme. This is the expected result since indoleacetamide does not contain a carboxylate group. In contrast the  $K_i$  value for indolepyruvate for the R98A enzyme increases 17 fold and for the R98K enzyme only slightly. The effect of removing this positive charge produces a change in the activation energy for binding tryptophan and indolepyruvate of  $\sim 2.0$  and  $1.6 \text{ kcal mol}^{-1}$ , respectively (Table 24).

The value of  $k_3$  decreases dramatically for both mutant enzymes (Table 22). Although the conservation of a positive charge in the R98K enzyme is sufficient to enable effective binding of tryptophan, the flavin reduction step is significantly affected. The values for  $k_3$  for the mutant enzymes indicate that the steps leading to flavin reduction are totally limiting in the mutant enzymes, since these values are close to the  $V_{\max}$  values. For the R98K enzyme the change in transition state activation energy for CH bond cleavage is  $3.0 \text{ kcal mol}^{-1}$  and it is equal to the change in the activation energy for flavin reduction (Table 24). This is consistent with the proposal that the positive charge of lysine is sufficient for binding but not to afford effective flavin reduction. For the R98A enzyme addition of the effects on binding and flavin reduction closely match to the observed change on the activation energy for the transition state of  $5.2 \text{ kcal mol}^{-1}$  (Table 24). The  $V/K_{O_2}$  value is reduced close to 20 and 50 fold for the R98K and R98A enzymes, respectively. The values for  $k_7$  were not measured directly for the mutant

Table 24. Differences in Binding Energies and Activation Energies Between Wild-type and Mutants Tryptophan 2-Monooxygenases\*

Enzymes	$\Delta\Delta G_s$ (kcal/mol)	$\Delta\Delta G^\ddagger$ (kcal/mol)	$\Delta\Delta G_3^\ddagger$ (kcal/mol)	$\Delta\Delta G_I$ (kcal/mol)
R98K	~0	3.2	3.0	0.3
R98A	2.0	5.2	3.9	1.6

\*The difference in binding energies ( $\Delta\Delta G_s$ ) were calculated by using the equation  $\Delta\Delta G_s = RT \ln [K_{wt}/K_{mutant}]$ . For the binding energies of inhibitors ( $\Delta\Delta G_I$ ) the  $K_i$  values for indolepyruvate were used, and for the activation energies ( $\Delta\Delta G^\ddagger$ ) the  $V/K_{trp}$  values were used. The changes in the activation energies for flavin reduction ( $\Delta\Delta G_{red}$ ) were calculated using the  $k_3$  values.

Table 25. Intrinsic Rate Constants for Wild-type and Mutant Tryptophan 2-

## Monooxygenases

Kinetic Parameter	Wild-type enzyme <sup>a</sup>	R98K	R98A
$K_d$ , mM	$0.11 \pm 0.05$	$0.08 \pm 0.011^b$	$3.4 \pm 0.8^b$
$k_3$ , s <sup>-1</sup>	$139 \pm 4$	$0.77 \pm 0.02^b$	$0.16 \pm 0.01^b$
$k_5$ , mM <sup>-1</sup> s <sup>-1</sup> , <sup>c</sup>	$140 \pm 18$	$7.5 \pm 2$	$3.2 \pm 0.2$
$k_7$ , s <sup>-1</sup>	14	$>10^d$	$>2^d$

<sup>a</sup> From reference (29).

<sup>b</sup> Measured in the stopped-flow spectrophotometer.

<sup>c</sup> Values corresponding to the  $V/K_{O_2}$  values.

<sup>d</sup> See discussion.

enzymes but it can be estimated that  $k_7$  is at least 10 times the value of  $k_3$ , such that  $V_{\max} \approx k_3$  for both mutant enzymes (Table 25).

A possible role for Arg98 is to position the transition state intermediate in the correct orientation for effective electron transfer to the flavin. Evidence for this comes from two experimental data, one the abolishment of the long wavelength absorbance corresponding to the charge transfer complex between the reduced enzyme and the imino acid complex, and the second the formation of hydrogen peroxide by both mutant enzymes. A different binding mode that makes the active site more solvent exposed is also consistent with the decrease  $V/K_{O_2}$  values for the mutant enzymes. In the wild-type enzyme with tryptophan the low intrinsic isotope value suggest an early the transition state with this substrate. In contrast with that with a slow substrate such as alanine the intrinsic isotope effect increases to a value close to 5, suggesting a later transition state (82). In the R98A enzyme the large isotope effect is consistent with a later transition state with tryptophan for this enzyme.

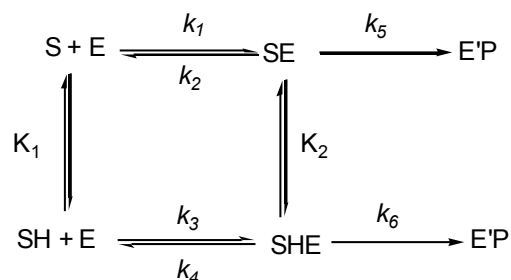
In the yeast *Rhodotorula gracilis* D-amino acid oxidase (RgDAAO) mutation of Arg285, which is proposed to bind the carboxylate of the amino acid substrate has similar effects to those seen here for TMO. The  $V_{\max}$  and  $k_3$  values decrease ~400 fold with alanine as substrate for the R285K and an order of magnitude more for the R285A enzyme. Also the long wavelength species is not observed in the RgDAAO Arg285 mutants (105). This is consistent with the importance of an arginine residue in binding and flavin reduction in these related flavoproteins.

The shapes of  $V/K_{trp}$  pH profiles are different from the wild-type profile for both mutant enzymes. The  $V/K_{trp}$  value for the mutant enzymes increases as the pH of the solution increases and shows a single  $pK_a$  value for a group that must be unprotonated for activity. In the wild-type a bell-shaped profile is observed for the  $V/K_{trp}$  profile,

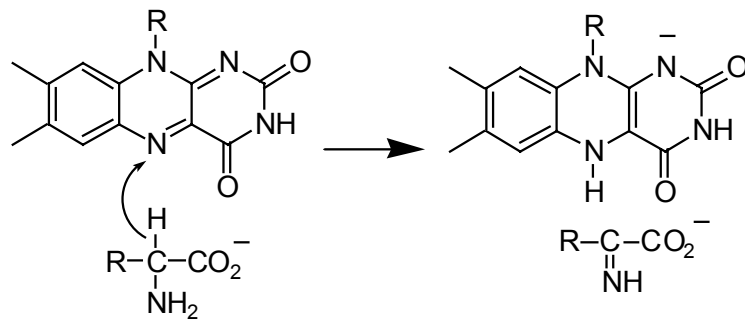
consistent with a group that must be unprotonated for activity and another group that needs to be protonated (82). The observed  $pK_a$  values for both mutant enzymes are very close to the  $pK_a$  value for the amino group of tryptophan. These results are consistent with Scheme 23 where the enzyme binds to both the protonated and unprotonated form of the substrate but only the unprotonated form is the reactive species. In the wild-type the  $pK_a$  value of the amino group for tryptophan or phenylalanine does not show but it is observed with methionine, similar to the Arg98 mutants (82).

The shape of the  $V_{max}$  pH profile is similar for the wild-type and mutant enzymes with low and high plateaus with a single  $pK_a$  value (82). The  $pK_a$  value is shifted  $\sim 3$  pH units and is close to the  $pK_a$  value of the amino group. The fact that the  $pK_a$  of the amino group shows in the  $V_{max}$  profiles can be explained if the wrong protonation form of the substrate acts as an inhibitor (Scheme 23). These results suggest that the mechanism of CH bond cleavage in TMO occurs as shown in Scheme 24. The unprotonated form of the substrate binds and a direct hydride transfer to the flavin takes place. This is consistent with a recent report on DAAO which suggests that this enzyme catalyzes the oxidation of D-amino acids with the same mechanism (10). In summary, the results presented here show that the positive charge at position 98 affords adequate binding but it is not sufficient to stabilize the transition state for effective flavin reduction.

Scheme 23



Scheme 24



## CHAPTER VIII

### SUMMARY

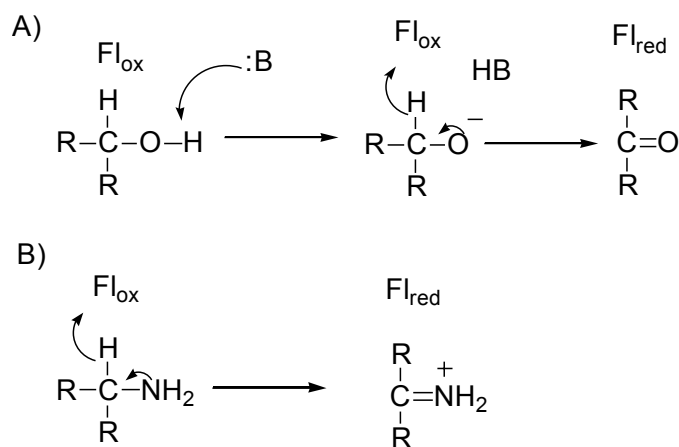
In the preceding chapters I presented an examination of the chemical mechanisms of two flavoproteins that catalyze the oxidation of CH bond at the alpha position of amino acids or hydroxy acids. The mechanism of oxidation by flavocytochrome b<sub>2</sub> was proposed to occur via a stepwise mechanism where the OH proton is abstracted prior to hydride transfer from the  $\alpha$ -CH. The effects of mutation of Tyr254 to phenylalanine can be explained by the role of this residue in stabilization of the intermediate after OH bond cleavage (Chapter III, Scheme 13). The enhanced activity of the D282N enzyme with thiolactate compared to the activity with lactate is also consistent with the proposed mechanism. The work presented here on Flb<sub>2</sub> is applicable to the other members of the  $\alpha$ -hydroxy acid oxidases family of enzymes which have the same active site architecture and catalyzed the same chemical reaction.

This work also identified the enzyme tryptophan 2-monooxygenase as a homologue of L-amino oxidase and elucidated the roles of Tyr413 and Arg98 in TMO. Tyr413 needs to be protonated for binding and the positive charge at position 98 is essential for adequate binding. The slow rate of the chemical steps in the Arg98 mutant enzymes allowed the identification of the protonated state of the amino acid substrate during catalysis. The results on TMO clearly show the structural homology to LAAO and suggest that mechanistically TMO uses the same chemical mechanism as D-amino acid oxidase, where the unprotonated form of the substrate is the active form for catalysis and a hydride is transferred to the FAD from the CH position without the action of a base during this process.



In summary the results suggest that in the mechanism of flavoenzymes that catalyze the oxidation of CH bond adjacent to either a hydroxyl or amino groups first the amide or hydroxyl group is deprotonated and then the CH bond is cleaved via a direct hydride transfer to the flavin cofactor. The mechanistic difference between these two groups of enzymes is in the deprotonation of the amino and hydroxyl groups (Scheme 25). In the  $\alpha$ -hydroxy acid oxidases an active site base is necessary to cleave the strong OH bond ( $pK_a \sim 15$ ), while in the amino acid oxidases the relatively weaker NH bond of the amino groups ( $pK_a \sim 9$ ) is deprotonated prior to binding. The binding of the substrates in the active site involves an interaction with an arginine and a tyrosine residue in both families of enzymes.

Scheme 25



Scheme 25 shows the (A) proposed mechanism of oxidation of  $\alpha$ -hydroxy acids in which an active site base is needed for abstraction of the hydroxyl proton prior to hydride transfer. (B) Proposed mechanism of oxidation of amino acids, where the unprotonated form of the substrate is the active form for catalysis and no active site base is necessary.

## REFERENCES

1. Massey, V. (2000) *Biochem. Soc. Trans.* 28, 283-296.
2. Fitzpatrick, P.F. (2001) *Acc. Chem. Res.* 34, 299-307.
3. Ghisla, S. (1982) in *Flavins and Flavoproteins* (Massey, V. and Williams, C.H. Jr., Eds.) pp 133-142, Elsevier, New York.
4. Walsh, C.T., Schonbrunn, A., and Abeles, R.H. (1971) *J. Biol Chem.* 246, 6855-6866.
5. Urban, P. and Lederer, F. (1984) *Eur.J. Biochem.* 144, 345-351.
6. Walsh, C., Schonbrunn, A., Massey, V., and Abeles, R. (1972) *J. Biol. Chem.* 247, 6004-6006.
7. Marcotte, P. and Walsh, C. (1976) *Biochemistry* 15, 3070-3076.
8. Pompon, D. and Lederer, F. (1985) *Eur. J. Biochem.* 148, 145-154.
9. Mattevi, A., Vanoni, M.A., Todone, F., Rizzi, M., Teplyakov, A., Coda, A., Bolognesi, M., and Curti, B. (1996) *Proc. Natl. Acad. Sci. USA* 93, 7496-7501.
10. Kurtz, K.A., Rishavy, M.A., Cleland, W.W., and Fitzpatrick, P.F. (2000) *J. Am. Chem. Soc.* 122, 12896-12897.
11. Diêp Lê, K.H. and Lederer, F. (1991) *J. Biol. Chem.* 266, 20877-20881.
12. Labeyrie, F., Baudras, A., and Lederer, F. (1978) *Methods Enzymol.* 53, 238-256.
13. Lederer, F. (1991) Flavocytochrome  $b_2$ . (Muller, F., Ed.) *Chemistry and Biochemistry of Flavoenzymes*, Vol. II. pp 153-242. CRC Press, Boca Raton, FL.
14. Xia, Z. and Mathews, F.S. (1990) *J. Mol. Biol.* 212, 837-863.
15. Reid, G.A., White, S., Black, M.T., Lederer, F., Mathews, F.S., and Chapman, S.K. (1988) *Eur. J. Biochem.* 178, 329-333.
16. Rouviere-Fourmy, N., Capeillere-Blandin, C., and Lederer, F. (1994) *Biochemistry* 33, 798-806.

17. Gaume, B., Sharp, R.E., Manson, F.D.C., Chapman, S.K., Reid, G.A., and Lederer, F. (1995) *Biochimie* 77, 621-630.
18. Gondry, M. and Lederer, F. (1996) *Biochemistry* 35, 8587-8594.
19. Müh, U., Williams, C.H. Jr., and Massey, V. (1994) *J. Biol. Chem.* 269, 7989-7993.
20. Müh, U., Massey, V., and Williams, C.H. Jr. (1994) *J. Biol. Chem.* 269, 7982-7988.
21. Müh, U., Williams, C.H. Jr., and Massey, V. (1994) *J. Biol. Chem.* 269, 7994-8000.
22. Sanders, S.A., Williams, C.H. Jr., and Massey, V. (1999) *J. Biol. Chem.* 274, 22289-22295.
23. Lehoux, I.E. and Mitra, B. (2000) *Biochemistry* 39, 10055-10065.
24. Dubois, J., Chapman, S.K., Mathews, F.S., Reid, G.A., and Lederer, F. (1990) *Biochemistry* 29, 6393-6400.
25. Massey, V. and Curti, B. (1967) in *Flavins and Flavoproteins* (Yagi, K., Ed.) pp 226-234, Walter de Gruyter, Berlin.
26. Du, X.Y. and Clemetson, K.J. (2002) *Toxicon* 40, 659-665.
27. Pawelek, P.D., Cheah, J., Coulombe, R., Macheroux, P., Ghisla, S., and Vrielink, A. (2000) *EMBO J.* 19, 4204-4215.
28. Kosuge, T., Heskett, M.G., and Wilson, E.E. (1966) *J. Biol. Chem.* 241, 3738-3744.
29. Emanuele, J.J. Jr. and Fitzpatrick, P.F. (1995) *Biochemistry* 34, 3710-3715.
30. Koyama, H. (1982) *J. Biochem.* 92, 1235-1240.
31. Flashner, M.S. and Massey, V. (1974) in *Mol. Mech. Oxygen Activation*. (Hayaishi, O., Ed.) pp 245-283, Academic Press, New York.
32. Takeda, H., Yamamoto, S., Kojima, Y., and Hayaishi, O. (1969) *J. Biol. Chem.* 244, 2935-2941.
33. Sherry, B. and Abeles, R.H. (1985) *Biochemistry* 24, 2594-2605.
34. McCann, A.E. and Sampson, N.S. (2000) *J. Am. Chem. Soc.* 122, 35-39.

35. Menon, V., Hsieh, C.-T., and Fitzpatrick, P.F. (1995) *Bioorganic Chem.* 23, 42-53.
36. Silverman, R.B. (1995) *Acc. Chem. Res.* 28, 335-342.
37. Walker, M.C. and Edmondson, D.E. (1994) *Biochemistry* 33, 7088-7098.
38. Brown, L.E. and Hamilton, G.A. (1970) *J. Am. Chem. Soc.* 92, 7225-7227.
39. Urban, P., Chirat, I., and Lederer, F. (1988) *Biochemistry.* 27, 7365-7371.
40. Giegel, D.A., Williams, C.H.Jr., and Massey, V. (1990) *J. Biol. Chem.* 265, 6626-6632.
41. Tsou, A.Y., Ransom, S.C., Gerlt, J.A., Buechter, D.D., Babbitt, P.C., and Kenyon, G.L. (1990) *Biochemistry* 29, 9856-9862.
42. Yorita, K., Aki, K., Ohkuma-Soyejima, T., Kokubo, T., Misaki, H., and Massey, V. (1996) *J. Biol. Chem.* 271, 28300-28305.
43. Bright, H.J. and Appleby, M. (1969) *J. Biol. Chem.* 244, 3625-3634.
44. Capeillere-Blandin, C., Bray, R.C., Iwatsubo, M., and Labeyrie, F. (1975) *Eur. J. Biochem.* 54, 549-566.
45. Pompon, D., Iwatsubo, M., and Lederer, F. (1980) *Eur. J. Biochem.* 104, 479-488.
46. Daff, S., Ingledeu, W.J., Reid, G.A., and Chapman, S.K. (1996) *Biochemistry* 35, 6345-6350.
47. Xia, Z.-X., Shamala, N., Bethge, P.H., Lim, L.W., Bellamy, H.D., Xuong, N.H., Lederer, F., and Mathews, F.S. (1987) *Proc. Natl. Acad. Sci. USA* 84, 2629-2633.
48. Lederer, F. and Mathews, F.S. (1987) in *Flavins and Flavoproteins* (Edmondson, D.E. and McCormick, D.B., Eds.) pp 133-142, Walter de Gruyter, Berlin.
49. Lindqvist, Y. and Brändèn, C.-I. (1989) *J. Biol. Chem.* 264, 3624-3628.
50. Black, M.T., White, S.A., Reid, G.A., and Chapman, S.K. (1989) *Biochem. J.* 258, 255-259.
51. Lederer, F. (1996) in *Flavins and Flavoproteins* (Stevenson, K.J., Massey, V., and Williams, C.H., Eds.) pp 545-553, University of Calgary Press, Calgary, Alberta, Canada.

52. Stenberg, K., Clausen, T., Lindqvist, Y., and Macheroux, P. (1995) *Eur. J. Biochem.* 228 , 408-416.
53. Yorita, K., Janko, K., Aki, K., Ghisla, S., Palfey, B.A., and Massey, V. (1997) *Proc. Natl. Acad. Sci. USA* 94, 9590-9595.
54. Kunkel, T.A., Roberts, J.D., and Zakour, R.A. (1987) *Methods Enzymol.* 154, 367-380.
55. Balme, A., Brunt, C.E., Pallister, R.L., Chapman, S.K., and Reid, G.A. (1995) *Biochem. J.* 309, 601-605.
56. Gondry, M., Diêp Lê, K.H., Manson, F.D.C., Chapman, S.K., Mathews, F.S., Reid, G.A., and Lederer, F. (1995) *Prot. Sci.* 4, 925-935.
57. Iwatsubo, I., Mevel-Ninio, M., and Labeyrie, F. (1977) *Biochemistry* 16, 3558-3566.
58. Schowen, K.B. and Schowen, R.L. (1982) *Methods Enzymol.* 89, 551-606.
59. Weast, R.C. (1981) in *CRC Handbook of Chemistry and Physics*, (Weast, R.C. Ed.), CRC Press Inc., p D-239, Boca Raton, FL.
60. Suzuki, H. and Ogura, Y. (1970) *J. Biochem.* 67, 291-295.
61. Hinkson, J.W. and Mahler, H.R. (1963) *Biochemistry* 2, 216-220.
62. Hermes, J.D., Roeske, C.A., O'Leary, M.H., and Cleland, W.W. (1982) *Biochemistry* 21, 5106-5114.
63. Quinn, D.M. and Sutton, L.D. (1991) in *Enzyme Mechanism from Isotope Effects* (Cook, P.F., Ed.) pp 73-126, CRC Press, Boca Raton, FL.
64. Urban, P. and Lederer, F. (1985) *J. Biol. Chem.* 260, 11115-11122.
65. Illias, R.M., Sinclair, R., Robertson, D., Neu, A., Chapman, S.K., and Reid, G.A. (1998) *Biochem. J.* 333, 107-115.
66. Makhatazde, G.I., Clore, G.M., and Gronenborn, A.M. (1995) *Nature Structural Biology* 2, 852-855.
67. Gekko, K. and Timasheff, S.N. (1981) *Biochemistry* 20, 4667-4676.
68. Karsten, W.E., Lai, C.-J., and Cook, P.F. (1995) *J. Am. Chem. Soc.* 117, 5914-5918.

69. Xie, M., Seravalli, J., Huskey, W.P., Schowen, K.B., and Schowen, R.L. (1994) *Bioorganic and Medicinal Chemistry Letters* 2, 691-695.
70. Sobrado, P., Daubner, S.C., and Fitzpatrick, P.F. (2001) *Biochemistry* 40, 994-1001.
71. Tegoni, M. and Cambillau, C. (1994) *Protein Sci* 3, 303-313.
72. Gondry, M., Dubois, J., Terrier, M., and Lederer, F. (2001) *Eur. J. Biochem.* 268, 4918-4927.
73. Oruga, Y.O. (1966) *J. Biochem.* 66, 63-71.
74. Bright, H.J. and Porter, D.J.T. (1975) in *The Enzymes*, 3rd Ed., Vol. XII (Boyer, P., Ed.) pp 421-505, Academic Press, New York.
75. Porter, D.J.T., Voet, J.G., and Bright, H.J. (1973) *J. Biol. Chem.* 248, 4400-4416.
76. Mizutani, H., Miyahara, I., Hirotsu, K., Nishina, Y., Shiga, K., Setoyama, C., and Miura, R. (1996) *J. Biochem.* 120, 14-17.
77. Cleland, W.W. (1982) *Methods Enzymol.* 87, 625-641.
78. Kraut, D.A., Carroll, K.S., and Herschlag, D. (2003) *Annu. Rev. Biochem.* 72, 517-571.
79. Comai, L. and Kosuge, T. (1980) *J. Bacteriology* 143, 950-957.
80. Magie, A.R., Wilson, E.E., and Kosuge, T. (1963) *Science* 141, 1281-1282.
81. Flashner, M.I.S. and Massey, V. (1974) *J. Biol. Chem.* 249, 2579-2586.
82. Emanuele, J.J.Jr. and Fitzpatrick, P.F. (1995) *Biochemistry* 34, 3716-3723.
83. Emanuele, J.J.Jr., Heasley, C.J., and Fitzpatrick, P.F. (1995) *Arch. Biochem. Biophys.* 316, 241-248.
84. Gadda, G., Dangott, L.J., Johnson Jr., W.H., Whitman, C.P., and Fitzpatrick, P.F. (1999) *Biochemistry* 38, 5822-5828.
85. Cleland, W.W. (1979) *Methods Enzymol.* 63, 103-138.
86. Flashner, M.I.S. and Massey, V. (1974) *J. Biol. Chem.* 249, 2587-2592.
87. Kurtz, K. (2000) M.S. Thesis, Texas A&M University, College Station, TX.

88. Cleland, W.W. (1986) in *Investigation of Rates and Mechanism*, 4th Ed., Vol. 6, Part I (Bernasconi, C.F., Ed.) pp 791-870, John Wiley and Sons, New York.
89. S. F. Altschul, T.L. Madden, A.A. Schäffer, J. Zhang, Z. Zhang, W. Miller, and D.J. Lipman (1997) *Nucleic Acids Research* 25, 3389-3402.
90. Curti, B., Ronchi, S., and Simonetta, M.P. (1991) in *Chemistry and Biochemistry of Flavoenzymes*, Vol III (Müller, F., Ed.) pp 69-94, CRC Press, Boca Raton, FL.
91. Binda, C., Newton-Vinson, P., Hubalek, F., Edmondson, D.E., and Mattevi, A. (2002) *Nature Structural Biology* 9, 22-26.
92. Kelley, L.A., MacCallum, R.M., and Sternberg, M.J.E. (2000) *J. Mol. Biol.* 299, 499-520.
93. Comai, L. and Kosuge, T. (1982) *J. Bacteriology* 149, 40-46.
94. Thomashow, M.F., Hugly, S., Buchholz, W.G., and Thomashow, L.S. (1986) *Science* 231, 616-618.
95. Escobar, M.A., Civerolo, E.L., Summerfelt, K.R., and Dandekar, A.M. (2001) *Proc. Natl. Acad. Sci. USA* 98, 13437-13442.
96. Sobrado, P. and Fitzpatrick, P.F. (2002) *Arch. Biochem. Biophys.* 402, 24-30.
97. Kiick, D.M. and Phillips, R.S. (1988) *Biochemistry* 27, 7339-7344.
98. Mukoyama, E.B., Hirose, T., and Suzuki, H. (1998) *J. Biochem.* 123, 1097-1103.
99. Fersht, A.R., Shi, J.-P., Knill-Jones, J., Lowe, D.M., Wilkinson, A.J., Blow, D.M., Brick, P., Carter, P., Waye, M.M.Y., and Winter, G. (1985) *Nature* 314, 235-238.
100. Denu, J.M. and Fitzpatrick, P.F. (1994) *Biochemistry* 33, 4001-4007.
101. Roth, J.P. and Klinman, J.P. (2003) *Proc. Natl. Acad. Sci. USA* 100, 62-67.
102. Wierenga, R.K., Terpstra, P., and Hol, W.G. (1986) *J. Mol. Biol.* 187, 101-107.
103. Vallon, O. (2000) *Proteins* 38, 95-114.
104. Dixon, M. (1953) *J. Biochem.* 55, 170-171.

105. Molla, G., Porrini, D., Job, V., Motteran, L., Vegezzi, C., Campaner, S., Piloni, M.S., and Pollegioni, L. (2000) *J. Biol. Chem.* 275, 24715-24721.



## VITA

**NAME:** Pablo Sobrado

**PLACE OF BIRTH:** San Jose, Costa Rica

**ADDRESS:** Jackson 867 Torre Z Depto. 76  
Viña del Mar, Chile  
e-mail: psobrado@yahoo.com

### EDUCATIONAL BACKGROUND:

Ph.D. Texas A&M University, College Station, TX-Biochemistry, 1997-2003  
B.S. Merrimack College, North Andover, MA-Biology, 1993-1997

### HONORS AND AWARDS:

2002 NIH Travel Grant to attend the 14th International Symposium on Flavins and Flavoproteins, Cambridge University, United Kingdom.  
2002-03 Fellowship from the National Center for Technology and Scientific Investigation (CONICIT) of Costa Rica.  
2002 Biochemistry Student Association Travel Grant.  
2002 International Education Scholarship, Texas A&M University.  
2001 Biochemistry Student Association Travel Grant.  
1994-96 Dean's List, Merrimack College.

### PROFESSIONAL MEETINGS ATTENDED:

- **29<sup>th</sup> Steenbock Symposium**, June 2003, Madison, Wisconsin.  
- **Enzyme Mechanism Conference**, January 2003, Galveston Island, Texas.  
- **14<sup>th</sup> International Symposium on Flavins and Flavoproteins**, July 2002. St John's College, University of Cambridge, United Kingdom.  
- **Gordon Research Conference on Isotopes in Biological and Chemical Science**, January 2000, Ventura, California.  
- **XV Lost Pines Conference**, October 1999, Smithville, Texas.